Water Quantity and Quality of the Yahara River Chain of Lakes

By
John R Reimer

A dissertation submitted in partial fulfillment of
the requirements for the degree of

Doctor of Philosophy
(Civil and Environmental Engineering)

at the
UNIVERSITY OF WISCONSIN-MADISON
2021

Date of final oral examination: 01/18/2021

The dissertation is approved by the following members of the Final Oral Committee:

Chin H. Wu, Professor, Civil and Environmental Engineering
Daniel B. Wright, Assistant Professor, Civil and Environmental Engineering
Gregory W. Harrington, Professor, Civil and Environmental Engineering
Qunying Huang, Associate Professor, Department of Geography
Cory P. McDonald, Assistant Professor, Civil and Environmental Engineering, Michigan Technological University

Abstract

The Yahara River Chain of Lakes (RCL), located in central Dane County, WI recently have experienced flooding (water quantity) and eutrophication (water quality), resulting in negative outcomes. The objective of this dissertation is to address water quantity, such as appropriate water levels and flood risk, and water quality at beaches and streams in the Yahara RCL. The results of this dissertation are intended to increase our understanding of one of the world's well-known lake systems - Yahara River Chain of Lakes. Furthermore, better understanding of how to manage and improve the Yahara RCL with broader impacts in application to other lake systems throughout the world is considered.

In Chapter 2, the state of the art Integrated Nowcast and Forecast Operation System (INFOS) is developed to provide water information for the Yahara RCL. The system infrastructure consists of a web portal to retrieve and display observations that are used to drive models under a high-performance computing server. Water level and flow information are obtained from a suite of models that directly simulates the RCL system. INFOS reliably and effectively models real-time reverse flows due to sustained wind forcings or seiches, and flow choking due to channel constriction. Water level planning scenarios provide insight for lake management to reduce floods under extreme rainfall events. Overall, INFOS provides reliable and timely water information for the RCL for sharing to the public, managers, and researchers.

In Chapter 3, sustainability assessment of flood risks from environmental, social, and economic perspectives in a RCL is performed. The flood assessment framework consists of five components including compiling data, modeling, mapping, estimating loss, and estimating risk. The modeled economic impact analysis reveals that the Yahara RCL is susceptible to large loss (in USD) at high return periods and long storm durations but a large risk at low return periods and

long durations. The results of social impacts show that the risk of people displaced is of concern at a low return period (10 year) independent of storm duration. From a sustainability viewpoint, Lake Monona is most at risk than the other lakes, suggesting flood mitigation efforts to improve Lake Monona would be beneficial. Overall, this chapter illustrates the importance of conducting flood risks in a RCL which vary depending on storm duration and return period.

In Chapter 4, an innovative Water Exclosure Treatment System (WETS) is developed and installed to minimize the occurrence of beach closures due to algae and *Escherchia coli* (*E. coli*). WETS consists of an "exclosure" sub-system with a five-sided polypropylene, barrier that excludes offshore lake contaminated water from the swimming area. To determine sizing of the treatment system, evaluate efficiency of UV disinfection, and aid in the design of the inlet and outlet locations for the pump system, computational fluid dynamics modeling is employed. Flushing time and Residence time maps are developed, depicting the duration of particles within the swimming area. Since deployment of WETS, there have been no beach closures issued. Overall, WETS, an innovative Water Exclosure Treatment System, provides safe, clean water inside the exclosure for minimizing beach closure.

In Chapter 5, the effect of legacy phosphorus (P) in streams on water quality before and after dredging stream sediments is assessed. Legacy P in sediments in the stream bed was discovered based on age and high concentrations of P. Laboratory microcosm and field mesocosm experiments revealed stream sediments were diffusing legacy P. Water quality response before and after dredging was evaluated from long term gage station data showing stream dredging reduced legacy P concentration from previously a source to presently a sink of upstream P. Overall, this chapter shows the important role that legacy P plays in stream sediments and how they can affect water quality outcomes and be remediated for the future.

Acknowledgments

I would like to thank many people who have supported me throughout my graduate studies at the University of Wisconsin-Madison. First, I would like to thank my advisor Dr. Chin Wu for his support. His guidance has taught me many skills to improve my abilities in research, science, and philosophy that have helped me to grow and develop in my career. Next, I would like to thank all my committee members, Drs. Dan Wright, Greg Harrington, Qunying Huang, and Cory McDonald for their advice, time, and writing suggestions of this thesis. I would also like to thank other professors that I have worked with including: Drs. Dick Lathrop, Steve Loheide, Ken Potter, John Hoopes and many others. I also benefited greatly from advice and help on hydrodynamic modeling, coding, and field measurements from the many students in the Water Resources Engineering and Environmental Fluid Mechanics program.

I am grateful to the City of Madison and Dane County that allowed me to pursue graduate studies part time while working full time. Specifically I would like to thank Larry Nelson, Rob Phillips, and Greg Fries, that provided encouragement to pursue the graduate program at UW-Madison and continued support of applying research while working at the City of Madison. I also thank Kevin Connors at Dane County that was supportive for me to finish my graduate work and for continuously promoting INFOS development for the Yahara River Chain of Lakes.

Lastly, I wish to thank support of my family. I thank my wife Anastasia and two sons John and Philip for their love and support while I was busy with research and writing of my thesis. I also wish to thank my parents for their love and support during my graduate studies.

Table of contents

1. Introduction 1

1.1 Background 1

1.2 Research objectives 5

1.3 Outline of the dissertation 6

1.4 References 8

2. Development and Application of a Nowcast and Forecast System Tool for Planning and Managing a River Chain of Lakes 12

2.1 Introduction 12

2.2 Material and methods 16

2.2.1 Study site 16

2.2.2 Nowcast and Forecast System 18

2.2.2.1 Components 18

2.2.2.2 Functions 25

2.3 Results and discussion 26

2.3.1 Flow reversal 26

2.3.2 Flow choking 31

2.3.3 Planning of water levels in the RCL 34

2.3.4 Management of RCL 37

2.4 Summary and conclusions 39

2.5 Acknowledgements 41

2.6 References 42

3. Sustainability Assessment of Flood Risks for a River Chain of Lakes 49

3.1 Introduction 49

3.2 Methods 52

3.2.1 Study site 52

3.2.2 Flood risk assessment framework 54

3.2.2.1 Data Compiling 56

3.2.2.2 Flood vulnerability modeling 58

3.2.2.3 Flood mapping 59

3.2.2.4 Flood risk calculation 60

3.2.2.5 Loss estimate 60

3.2.2.6 Sustainability assessment 61
3.3 Results 63
3.3.1 Rainfall hazards 63
3.3.2 Flood inundation impacts 66
3.3.3 Social impacts 68
3.3.4 Economic impacts 72
3.3.5 Sustainability assessment 75
3.4 Discussion 78
3.4.1 Rainfall duration 78
3.4.2 Sustainability assessment approach 79
3.4.3 Flood actions 80
3.5 Conclusions 81
3.6 Acknowledgements 82
4.7 References 83
4. Water Exclosure Treatment System (WETS): An innovative device for minimizing beach closures 93
4.1 Introduction 93
4.2 Materials and methods 96
4.2.1 Study site 96
4.2.2 Water Exclosure-Treatment System 98
4.2.2.1 Exclosure sub-system 98
4.2.2.2 Treatment sub-system 100
4.2.2.3 Measurements and analysis 101
4.2.2.4 Modeling 104
4.3 Results 107
4.3.1 Flushing time 107
4.3.2 Spatial residence time 108
4.3.3 Turbidity and E. coli 109
4.3.4 Cyanobacteria genera 112
4.4 Discussion 115
4.4.1 Beaches in the Yahara River Chain of Lakes 115
4.4.2 Economic costs and socio-economic benefits 115
4.5 Conclusions 116
4.6 Acknowledgements 118

4.7 References 119
5. Impacts of Legacy Phosphorus in Streams on Water Quality before and after Dredging 128
5.1 Introduction 128
5.2 Materials and methods 130
5.2.1 Study site 130
5.2.2 Field Measurements 132
5.2.2.1 Sediment sampling 132
5.2.2.2 Water sampling 133
5.2.2.3 Mesocosms 133
5.2.3 Laboratory experiments 134
5.2.3.1 Radionuclides 134
5.2.3.2 Microcosms 135
5.2.4 Sediment age calculation 136
5.2.5 Hydraulic dredging 136
5.3 Results 138
5.3.1 Legacy P 138
5.3.2 Microcosm P diffusion 140
5.3.3 Mesocosm P response 142
5.3.4 Stream water quality response 143
5.3.5 Hydrologic Impacts 146
5.4 Discussion 147
5.4.1 TMDL Targets 147
5.4.3 Ecological and recreational enhancements 148
5.5 Conclusions 149
5.6 Acknowledgments 150
5.7 References 151
6. Summary and Future Work 159
6.1 Summary 159
6.2 Recommendations for future work 162
6.3 References 166

List of Tables

Table 2-1. Regulatory levels for the Yahara Lakes (elevation in meters above mean sea level, NGVD29).....18

Table 2-2. Comparison of algorithm and domain approaches on number of iterations, statistical results (R^2), and computation speed. 30

Table 3-1. Cumulative rainfall (in millimeters) from 35 scenarios of various return periods and rainfall durations. 57

Table 3-2. AHP matrix judgements, criteria weights (PV), and consistency measure (CM).....62

Table 4-1. Flushing time (in days) for nine simulations comparing inlet and outlet locations. ..108

Table 4-2. One-way analysis of variance comparing site O1 (outside) to other sampling locations. 112

List of Figures

Fig 2-1. The Yahara River chain of lakes study site located in the state of Wisconsin, United States. 16

Fig 2-2. INFOS Infrastructure consisting of observations, modeling, and a high performance computing server. 19

Fig 2-3. The computational meshes of the INFOS model on the Yahara RCL and the floodplain areas (blue). I, II, and III are the three different sizes of the nested domains. 23

Fig 2-4. The time series of (a) wind field, (b) water level, and (c) discharge for the Yahara River inflow at Highway 113. The shadow zones delineate two reverse flow events. 29

Fig 2-5. (a) The specific energy diagram at the upstream (light gray line), downstream (dark gray line), and the Railroad Trestle (black line) for Q = 5.66 m^3/s; (b) The modeled water surface profile (solid line) and normal depth (dashed line) from Lake Monona at distance = 0 km to the Railroad Trestle at distance = 2.9 km; (c) Same as (a) except for 11.33 m^3/s discharge; (d) Same as (b) except for Q = 11.33 m^3/s. 34

Fig 2-6. The time series water elevations during the extreme storm events in 2008 and Lake Monona of the three planning scenarios. 36

Fig 2-7. The extreme rainfall event and water elevations (solid lines) of Lake Mendota and Lake Waubesa in June 2008, compared with those by two strategies based upon flow-through and storage management. 39

Fig 3-1. (a) The study site is located in Wisconsin, United States (left). The black bounding box represents the stochastic storm transposition domain. Colors of the symbols represent the locations of the 1 (dark green), 10 (green), 25 (light green), 50 (yellow), 100 (orange), 250 (dark orange), and 500 (red) year return periods. The 2-day (circles), 4-day (stars), 6-day (squares), 8-day (triangles), and 10-day (diamonds) storm durations are denoted (b) The Yahara River Chain of Lakes (right) shows the sub watershed boundary (gray and hydraulic model grids of water (dark red) and overland (orange). 53

Fig 3-2. Flood risk assessment framework consisting of six components including data compiling, flood scenario modeling, GIS mapping, Loss estimation, risk calculation, sustainability assessment.....55

Fig 3-3. (a) The rainfall depth-frequency curves for the Rainy Day results for 1-day to 10-day rainfall duration shown in the gray bounds. Specifically, the 4-day rainfall duration (blue solid line) and 10-day duration (red solid line) is plotted to compare with NOAA Atlas 14, 4-day (blue dashed line) and 10-day duration (red dashed line). Most recently, large rainfall occurred in 2007 in Madison (blue), 2008 in Madison (magenta), and Baraboo (green) shown by square and circle markers. (b) Cumulative rainfall is compared for 2008 Madison (magenta circles) and corresponding Rainy Day 96 year return period

results (magenta solid line). Also, 2008 Baraboo (green circles) and corresponding Rainy Day 237 year return period results (green solid line) is shown. 65

Fig 3-4. (a) Lake Monona 100 year flood inundation (light blue) and building damage locations (red) for 4-day rainfall duration in comparison to inundation (light orange) and building damage locations (red and yellow) for 10 day rainfall duration. (b) Lake Monona 500 year flood inundation (light blue) and building damage locations (red and green) for 4-day rainfall duration in comparison to inundation (light orange) and building damage locations (red) for 10 day rainfall duration. (c) Lake Mendota 100 year flood inundation (light blue) and building damage locations (red) for 4-day rainfall duration in comparison to inundation (light orange) and building damage locations (red and yellow) for 10 day rainfall duration. Shown in dark orange are building footprint locations. (d) Lake Mendota 500 year flood inundation (light blue) and building damage locations (red and green) for 4-day rainfall duration in comparison to inundation (light orange) and building damage locations (red) for 10 day rainfall duration.....67

Fig 3-5. (a) Map of flood inundation (light blue) and vulnerabilities impacted. Radar charts showing vulnerabilities by (b) land use types in hectares, (c) transportation means in kilometers, and (d) malfunction of utility services in numbers. Four cases are presented showing the 500 (red) and 100 (blue) year return periods for Madison isthmus area (dashed line) and all Yahara Lakes (solid line). 70

Fig 3-6. (a) Number of people displaced and (b) risk of people displaced versus return periods of the 10-day flood duration on Lakes Mendota (blue), Monona (red), Waubesa (orange), and Kegonsa (green). 71

Fig 3-8. Spatial distributions of expected annual damage (EAD) that are aggregated within a 1 kilometer radius in $1,000 US dollars over the 10 day storm duration of the return periods of (a) 500 year and (b) 100 year.....75

Fig 3-9. Comparison of social (light blue), economic (light orange), and environment (light green) risk for Lake Mendota (a), Monona (b), Waubesa (c) and Kegonsa (d).....76

Fig 3-10. Comparison of social, economic, and environment for Lake Mendota (blue), Monona (red), Waubesa (orange) and Kegonsa (green).....77

Fig 4-1. (a) The study site, Brittingham Beach (star on map), is located with the Yahara River Chain of Lakes, Dane County, Wisconsin, United States. WETS were also installed at other three sites (circle on map) that are Bernie's Beach, Mendota County Beach, and Goodland County Beach. (b) Aerial view of the Brittingham Beach with the exclosure system in the summer of 2011. 98

Fig 4-2. (a) The enclosure sub-system of WETs consists of five booms to separate the swimming area water from the lake proper. A treatment sub-system pumps influent water through a sand filter and ultraviolet disinfection, returning clean water to the swimming area and backwash water to the sanitary sewer. Labels O1, I1, I2, and O2 are the water sampling locations. (b) Section A-A shows the configuration of the exclosure sib-sub-system with the anchor.....99

Fig 4-3. (a) A portable trailer enclosed with the treatment sub-system. (b) A schematic of the detailed components of the strainer-filtration-ultraviolet system. Lake water influent is pumped through a strainer removing heavy debris such as aquatic plant fragments, a sand filter removing fine particles, and ultraviolet water purifiers to produce short wave radiation lethal to microorganisms. The treated effluent water is returned to the swimming area. (c) An automatic logic control uses pressure sensors to monitor performance and trigger backwashing of the sand filter to the sanitary sewer. 101

Fig 4-4. An example of unstructured meshes in the hydrodynamic model for the case of inlet at the middle and outlet at the shallow. Spatial resolution for meshes ranges from 0.3 to 1 meter. 105

Fig 4-5. The mean residence time map for nine cases with the combination of three different water intake (shallow, middle, deep) and three effluent outlet (shallow, middle, deep) locations. 109

Fig 4-6. Time series of (a) turbidity and (b) box plot at the outside sample site O1 (triangle symbol) and the inside sample site I1 (o symbol). Similarly, time series of (c) *E. coli* and (d) box plot at the outside sample site O1 (triangle symbol) and the inside sample site I1 (o symbol). 111

Fig 4-7. Three sample bottles (from left to right) show water clarity of tap water, swimming water inside the exclosure, and lake water outside the exclosure at four different times. The outside lake water is green with peak occurring on 8/16/11, suggesting high cyanobacteria concentration. Inside swimming water remains clear as compared to tap water. 113

Fig 4-8. Time series of (a) *Cylindrospermopsis* sp. and (b) box plot at the outside sample site O1 (triangle symbol) and site O2 (square symbol) and the inside sample site I1 (solid circle) and site I2 (pentagon symbol). 114

Fig 5-1. The study site is located at Dorn Creek in Dane County, Wisconsin. Circles show sampling location with colors representing P concentrations in stream sediments. Long term gage stations were installed upstream of study site at Highway Q called S1 and downstream at Highway M called S2 to measure water quality and quantity. Three slope (S) locations are shown which represent the average stream bed slope. The locations of microcosm and mesocsom experiments are shown. 131

Fig 5-2. Mesocosm experiments were conducted before dredging (left) with water sampling performed inside (green) and outside (red). After dredging (right), mesocosm were installed using water before dredging (light blue) and distilled water (blue). 134

Fig 5-3. Hydraulic dredging schematic performed between Highway Q and M as shown in blue. Hydraulic dredge transports legacy P sediment through influent pipeline (light blue) to dewatering area (red) to trap sediment and clean water is discharged back to stream through effluent pipeline (light blue). 138

Fig 5-4. (a) Sediment Age calculated from PB-210 (line) and CS-137 peak value (red circle). The error bars represent measurement uncertainty (±1σ). (b) Sediment Accumulation (black) and Cumulative Mass Rate (gray).....140

Fig 5-5. Microcosm soluble reactive phosphorus (SRP) release from surface sediments considering aerobic conditions (cyan) at site 1 (square), 7 (triangle), and 8 (circle). SRP release is also shown for subsurface sediment 0.15 m deep under anaerobic conditions (green) at site 1. Microcosms of water only without sediments under aerobic (cyan dashed line) and anaerobic (green dashed line) are shown.....141

Fig 5-6. (a) Total phosphorus and (b) SRP concentrations comparing outside stream water (green), before dredging in mesocosm (red), after dredging in mesocosm (light blue), and after dredging with stream water replaced by distilled water in mesocosm (dark blue).....143

Fig 5-7. (a) Total P Loading from upstream S1 gage (green) and downstream S2 gage (orange). (b) Difference of total P release between downstream and upstream gage stations. (c) SRP median concentrations for annual (red), growing season (green), and spring melt (blue) periods.....145

Fig 5-8. Stream discharge at upstream (purple) and downstream (orange) gage stations (a) before and (b) after dredging. Flow Ratio (c) comparing baseflow (light blue) and stormflow (dark blue) changes.....147

1. Introduction

1.1 Background

The Yahara River Chain of Lakes (RCL) is located in Dane County, Wisconsin, USA and includes five major lakes (Mendota, Monona, Wingra, Waubesa, and Kegonsa) that are fed by 1,345 km² of watershed area. The Yahara watershed land is approximately 67% agricultural but has a densely populated urban area (state capital, Madison, Wisconsin) and suburban areas. The Yahara River enters Lake Mendota, links all four lakes, and exits the chain on the western shore of Lake Kegonsa. Lake levels on Mendota are controlled by Tenney Dam where water is released into Lake Monona. Lake Monona is surrounded by an urban-dominated watershed. After leaving Lake Monona, water travels through an uncontrolled natural channel, consisting of a large wetland complex, to Upper Mud Lake before discharging to Lake Waubesa. The outlet of Lake Waubesa is at Babcock Dam and releases water through the Lower Mud Lake river-wetland corridor. The last lake in the chain is Lake Kegonsa which is controlled by the LaFollette Dam and water is released to the Yahara River which ultimately connects with the Rock River. The Yahara Lakes are central to Dane County's identity (Stedman et al., 2007), but recently high lake levels and deteriorating water quality conditions are concerning (Carpenter et al., 2006). Therefore, it is critical to understand and implement solutions to reshape and improve the Yahara RCL for current and future generations.

Flooding in the Yahara lakes has commonly occurred in recent and past years. The top ten highest water levels recorded for Lake Mendota since 1916 from high to low occurred in years 2000, 2008, 2018, 1993, 1959, 2007, 2004, 1980, 1978, and 1996. Seven of the top flood levels occurred in the past 25 of 103 years of record. Several factors are responsible for increased flow into the Yahara RCL. First, climate change has altered hydrological flows and increased the

occurrence of extreme rainfall events (Motew and Kucharik, 2013). According to the Wisconsin Initiative on Climate Change Impacts, the average annual precipitation in Dane County has increased by approximately five percent since 1950 (WICCI, 2011). Second, the extent of urbanization in the watershed has greatly increased and the amount of impervious surface such as roads, parking lots, and rooftops, reduces the amount of water that infiltrates into the ground and increases surface water runoff. Specifically, since 1970, the area of urbanized land has almost doubled from 41,000 acres to 71,000 acres. Third, over 50% of wetlands have been lost in the Yahara Watershed and drained (Lathrop et al., 1992), increasing the amount of runoff into the lakes. For delivery of water through the chain of lakes, several flow limitations are witnessed. The Yahara RCL is flat which limits delivery of water. For example, under normal conditions, the change in water levels between Lakes Monona and Waubesa is 0.4 feet over 2 miles (0.004% slope). Other flow limitations in the rivers exist such as narrow river cross sections (e.g. bridge constrictions) and sediment deposits that result in flow choking (Reimer and Wu, 2016). Also, aquatic plants cause friction and reduce water flow. In summary, flooding has commonly occured due to increased runoff into the Yahara lakes and inefficient delivery of water through the Yahara River.

Water quality conditions in the Yahara lakes have deteriorated since the early 1900s. In the late 1940s, excessive nutrient inputs (e.g., phosphorus) entered the Yahara Lakes from increased sewage discharges, fertilizer and manure application, and agricultural and urban runoff (Carpenter et al. 2006, Lathrop 2007). Large efforts have begun since the 1950s to reduce nutrient loading and eutrophication (Wardropper et al., 2015) including sewerage diversion, soil erosion control, storm water management, agriculture nutrient management plans, and wetland restoration (Lathrop 2007). Recently, several government and environmental organizations have increased

public awareness of the state of the Yahara Lake eutrophication issues and advocated for sustainable policy actions. While policy and practice implementation have been made to reduce nutrient inputs to the Yahara Lakes, elevated levels of nutrients from long-term legacies remain in the Yahara Lakes and Watershed (Betz et al., 2005; Gillon et al., 2016; Lathrop 2007).

The results of this dissertation are intended to increase our understanding of water quantity and quality of one of the world's well known studied lake systems –the Yahara River Chain of Lakes. Furthermore, better understanding of how to manage and improve the Yahara RCL and apply to other lake systems throughout the world is an important goal. Specifically, in this dissertation, knowledge gaps for improving water quantity (flooding) and quality (nutrients) in the Yahara Lakes are identified by the following questions:

i. First, *how to model water level fluctuations and flooding to provide effective and timely water information in the Yahara Lakes*? In recent years, timely water information obtained from nowcast and forecast systems have become more popular due to research, public, and management needs. Recognizing the importance of water level fluctuations, several advancements have been made in developing forecasts in the Great Lakes (Schwab and Bedford 1995), rivers (Baptista et al., 1998; Schmalz, 2011), estuaries (Lanerolle et al., 2011; Wei and Zhang, 2011), and oceans (Aikman et al. 1996). While great progress has been made in developing online systems for rivers, estuaries, or oceans, there has not been attention in literature towards online water level fluctuations and flow dynamics in a RCL system.

ii. Second, *what are the flood risks from environmental, social, and economic perspectives in the Yahara RCL*? Managing water levels in the Yahara Lakes are often debated (Isthmus, 2007). Nevertheless, achieving targeted water levels for each lake in a RCL during flooding is challenging and controversial to meet environmental, social, and economic concerns (Nyberg et al., 2014). No information is available for flood risks considering these three perspectives in the Yahara RCL.

iii. Third, *how to provide safe swimming water conditions in the event of poor water quality conditions (e.g. algae and E. coli) that threaten beaches in the Yahara Lakes*? Beaches provide well-being of local residents for swimming opportunities and boost economies from tourism (Englebert et al., 2008; Houston, 2008; Wheeler et al., 2012; Ashbullby et al., 2013). Nevertheless, poor water quality at beaches can cause health threats or illness problems along shorelines for swimmers or recreational users (Patz et al., 2008). Cyanobacteria and *E. coli* bacteria are two main causes that pose a great health risk to recreation users in the Yahara Lakes. When elevated levels are measured, the current protocol is to issue a beach closing. The beach may remain closed from 1 day to several months preventing users from swimming with little attention paid to minimize the duration of beach closures.

iv. Lastly, *how to assess the impacts of legacy phosphorus in streams on water quality and evaluate dredging for reducing phosphorus*? Legacy phosphorus, often referred to as accumulated P in agricultural soils, can deteriorate water quality and

be remobilized or recycled as a continuous source to downstream surface waters for years, decades, or even centuries (McDowell et al., 2002). Reduction of nonpoint source pollution from uplands is successfully addressed by field management practices (e.g., cover crops, no tillage, fertilizer reductions) and watershed management practices (e.g., converting land use, creating detention ponds, and meandering stream networks). Nevertheless, the intent of reducing load downstream by these practices results in P accumulation, leading to erosion and diffusion of legacy P as an unintended source. As a result, legacy P may mask or buffer load reductions and remediation of legacy P has yet to be addressed in the Yahara Lakes.

1.2 Research objectives

The aims of this dissertation are to address flood risks and present solutions to improve water quality in the Yahara chain of lakes. Specifically, four overarching objectives of this dissertation are as follows:

1) Develop and provide real-time water information including of a RCL system for effective and timely water level management to the public, managers, and researchers.
2) Examine flood risks from environmental, social, and economic perspectives in a river chain of lakes.
3) Test an innovative Water Exclosure Treatment System (WETS) to reduce beach closures from cyanobacteria and *E. coli* bacteria originating from either offshore or onshore.
4) Investigate impacts of legacy phosphorus in streams before and after dredging stream sediments.

1.3 Outline of the dissertation

Chapter 2 aims to characterize water level fluctuations and provide timely water information in Yahara Lakes. Specifically, the Integrated Nowcast and Forecast Operation System (INFOS) is developed to provide reliable and timely information for the Yahara RCL for sharing information to the community, planning for water use and delivery, and management. The system infrastructure comprises a web portal to retrieve and display observations that are used to drive models under a high performance computing server. Water level and flow information are obtained from a suite of models that directly simulate the RCL system. Two key contributions of this chapter are: first, a new data assimilation technique based upon flow routing algorithm and a nested-mesh domain reduction is developed to update the Manning's roughness. Second, INFOS provides real-time water level information in a RCL for the first time. Chapter 2 was published in *Journal of Water Resources Management* (2016).

In Chapter 3, the objective is to present a sustainability assessment of flood risks from environmental, social, and economic perspectives in a RCL. A flood assessment framework consisting of five components including compiling data, modeling, mapping, estimating loss, and risk is employed to characterize sustainability. Flood risk is shown to have different environmental, economic, and social impacts depending on storm duration and return period (rainfall amount). The key contribution of this chapter is revealing the unrecognized flood risks from a sustainability perspective and how they are influenced by rainfall amounts and duration. Chapter 3 is in preparation to be submitted to *Science of the Total Environment*.

Chapter 4 aims to test the hypothesis that that an innovative Water Exclosure Treatment System (WETS) can prevent algal scums and reduce beach closures from cyanobacteria and *E. coli* bacteria originating from either offshore or onshore in inland lakes. WETS consists of an

"exclosure" with a five-sided polypropylene, barrier that excludes offshore lake contaminated water from the swimming area. Inside the exclosure, water is pumped to a portable filtration-ultraviolet treatment sub-system. Computational fluid dynamics modeling with a Lagrangian particle-tracking method are employed to determine sizing of the treatment system and reveal the residence time for the duration of particles within the swimming area. In this chapter, the key contribution is the development of an innovative Water Exclosure Treatment System to provide safe, clean water inside the exclosure for minimizing beach closures. Chapter 4 was published in *Science of the Total Environment* (2019).

In Chapter 5, the objective is to investigate impacts of legacy phosphorus in before and after dredging stream sediments in an agricultural watershed. Before stream dredging, microcosm experiments in the laboratory were performed to measure P diffusion into the stream water. After stream dredging, mesocosm experiments in the field were conducted to evaluate reductions in P concentrations. Overall water quality response before and after dredging was evaluated from long term gage station data. The key contribution of this chapter is to evaluate legacy P and reveal water quality improvements due to removal of legacy P from stream dredging. Chapter 5 is in preparation to be submitted to *Journal of Environmental Management.*

Lastly, in Chapter 6, a summary and recommendations for future work are presented.

1.4 References

Aikman, F., Mellor, G.L., Ezer, T., Sheinin, D., Chen, P., Breaker, L., Bosley, K., Rao, D. B., 1996 Towards an operational nowcast/forecast system for the U.S. East Coast. Modern Approaches to Data Assimilation in Ocean Modeling. Elsevier Oceanography Series, **61**, 347-376.

Ashbullby, K.J., Pahl, S., Webley, P., White, M.P., 2013. The beach as a setting for families' health promotion: a qualitative study with parents and children living in coastal regions in southwest England. Health & Place 23, 138–147.

Baptista, A.M., Wilkin, M., Pearson, P., Turner, P., McCandlish, C., Barrett, P., Das, S., Sommerfield, W., Qi, M., Nangia, N., Jay, D., Long, D., Pu, C., Hunt, J., Yang, Z., Myers, E., Darland, J., Farrenkopf, A., 1998 Towards a multi-purpose forecast system for the Columbia River Estuary. Ocean Community Conference 199. Baltimore, MD.

Betz, C. R., Balousek. J., Fries, C., Nowak, P. 2005. Lake Mendota: improving water quality. LakeLine 25:47-52.

Carpenter, S.R., Lathrop, R.C., Nowak, P., Bennett, E.M., Reed, T., Soranno, P. A., 2006. The ongoing experiment: restoration of Lake Mendota and its watershed. Pages 236-256 in J. J. Magnuson, T. K. Kratz, and B. J. Benson, editors. Longterm dynamics of lakes in the landscape: long-term ecological research on north temperate lakes. Oxford University Press, Oxford, UK.

Englebert, E.T., McDermott, C., Kleinheinz, G.T., 2008. Effects of the nuisance algae, Cladophora, on Escherichia coli at recreational beaches in Wisconsin. Science of the Total Environment 404, 10-17.

Gillon, S., Booth, E.G., Rissman, A. R., 2016. Shifting drivers and static baselines in environmental governance: challenges for improving and proving water quality outcomes. Regional Environmental Change, 16, 759-775.

Houston, J.R., 2008. The economic value of beaches - a 2008 update. Shore & Beach 76 (3), 22–26.

Isthmus., 2007. Getting too high on the lake. https://isthmus.com/opinion/opinion/getting-too-high-on-the-lake/

Lanerolle, L., Patchen, R.C., Aikman, F., 2011 The Second Generation Chesapeake Bay Operational Forecast System (CBOFS2): Model Development and Skill Assessment. NOAA Technical Report NOS CS 29, Silver Spring, MD.

Lathrop, R. C., 2007. Perspectives on the eutrophication of the Yahara lakes. Lake and Reservoir Management 23(4):345-365.

Lathrop, R.C., Bradbury, K., Halverson, B., Potter, K., Taylor, D., 2005. Groundwater, stream flow, and lake level responses to urbanization in the Yahara lakes basin. LakeLine 25:39-46.

Lathrop, R.C., Nehls, S.B., Brynildson, C.L., Plass, K.R., 1992. The fishery of the Yahara Lakes. Department of Natural Resources Technical Bulletin, No. 181.

McDowell, R.W., Sharpley, A.N., Chalmers, A.T., 2002. Land use and flow regime effects on phosphorus chemical dynamics in the fluvial sediment of the Winooski River, Vermont. Ecological Engineering. 18, 477–487.

Motew, M.M., Kucharik, C. J., 2013. Climate-induced changes in biome distribution, NPP, and hydrology in the Upper Midwest U.S.: a case study for potential vegetation. Journal of Geophysical Research: Biogeosciences 118(1):248-264.

Nyberg, L., Evers, M., Dahlstrom, M., Pettersson, A., 2014. Sustainability aspects of water regulation and flood risk reduction in Lake Vanern. Aquatic Ecosystem Health & Management, 17 (4), 331-340.

Patz, J.A., Vavrus, S.J., Uejio, C.K., McLellan, S.L., 2008. Climate change and waterborne disease risk in the Great Lakes Region of the U.S. American Journal of Preventive Medicine 35 (5): 451-458.

Reimer, J.R., Wu, C.H., 2016. Development and Application of a Nowcast and Forecast System Tool for Planning and Managing a River Chain of Lakes. Water Resources Management, 30(4), 1375-1393.

Schmalz, R.A., 2011. Three-Dimensional Hydrodynamic Model Developments for a Delaware River and Bay Nowcast/Forecast System. NOAA Technical Report NOS CS 28, Silver Spring, MD, 199pp.

Schwab, D.J., Bedford, K.W., 1995. Operational three-dimensional circulation modeling in the Great Lakes. Computer Modeling of Seas and Coastal Regions II. 2nd International Conference on Computer Modelling of Seas and Coastal Regions Location: Cancun, 387-395.

Stedman, R.C., Lathrop, R. C., Clark, B., Ejsmont-Karabin, J., Kasprzak, P., Nielsen, K., Osgood, D., Powell, M., Ventelä, A.-M., Webster, K.E., Zhukova. A., 2007. Perceived environmental quality and place attachment in North American and European temperate lake districts. Lake and Reservoir Management 23(4):330-344.

Wardropper, C.B., Chang, C., Rissman, A.R., 2015. Fragmented water quality governance: constraints to spatial targeting for nutrient reduction in a Midwestern USA watershed. Landscape and Urban Planning 137:64-75.

Wei, E., Zhang, A., 2011 The Tampa Bay Operational Forecast System (TBOFS): model development and skill assessment. NOAA Technical Report NOS CS 30, Silver Spring, MD, 119pp.

Wheeler, B.W., White, M., Stahl-Timmins, W., Depledge, M.H., 2012. Does living by the coast improve health and wellbeing? Health & Place 18 (5), 1198–1201.

Wisconsin Initiative on Climate Change Impacts, WICCI., 2011. Wisconsin's Changing Climate: Impacts and Adaptation.

2. Development and Application of a Nowcast and Forecast System Tool for Planning and Managing a River Chain of Lakes

The following has been published in *Journal of Water Resources Management*

Reimer, J.R., Wu, C.H., 2016. Development and Application of a Nowcast and Forecast System Tool for Planning and Managing a River Chain of Lakes. Journal of Water Resources Management. 30:1375-1393.

2.1 Introduction

Planning and managing a river chain of lakes (RCL) is a challenging task that requires the consideration of public interest for each individual lake and the chain of lakes among several municipalities and entities. Oftentimes, "correct" lake level orders are continuously debated, particularly in high water flooding or low water drought periods. Different from a river chain of reservoirs that usually are controlled by hydraulic structures, e.g., sluice gates, dams, weirs, or culverts (Afshar et al., 2011; Fallah-Mehdipour et al., 2013), a RCL, defined here, is connected with rivers with or without hydraulic control structures. If episodic storms or sustained droughts happen, the lake level orders, usually set by regulatory agencies, cannot be complied due to larger watershed runoff into the lakes greater that can be delivered through the RCL. As a result, better predicting the response of a RCL will provide timely information to release an appropriate amount of water from upstream lakes during certain time duration to downstream lakes for effective planning and management of an RCL.

Several factors affect the response of a lower gradient RCL system that can determine the overall water levels of lakes and discharge capacity in rivers. For the connected rivers, backwater caused by the downstream lakes influences the release of water from the upstream lake. Channel narrowing due to bridges create flow constriction (Hunt et al., 1999; Kaatz and James, 1997) or

flow choking (Sturm, 2001). Seasonal aquatic plant density in the connected channel can vary friction, affecting channel-conveyance capacity (Kowen and Fathi-Moghadam, 2000; Tsihrintzis and Madiedo, 2000; Green, 2005). For lakes, rainstorms can cause each lake to rise at different rates due to varying lake sizes and watershed characteristics. In addition, storm-induced water levels due to wind can push water towards one end of the lake, which can impede river discharge and even cause reverse flow. Peters and Buttle (2010) showed that the outflow obstruction of lakes within a river-lake-delta system can act as a 'hydraulic dam', temporarily leading to reverse flow. To address the complex response of an RCL system due to several factors mentioned above, reliable and timely water information is crucial.

In the recent years, timely water information obtained from nowcast and forecast systems have become more popular due to research, public, and management needs. Recognizing the importance of water level fluctuations, Schwab and Bedford (1995) first developed a hindcast and forecast online system for the hydrodynamics in the Great Lakes. Afterwards, substantial progress on online web infrastructure has been made to characterize the ocean and estuary environment, e.g., the East Coast Ocean Forecast System (Aikman et al. 1996); the Tampa Bay Operational Forecast System (Wei and Zhang, 2011); Delaware River and Bay Operational Forecast System (Schmalz, 2011); Chesapeake Bay Operational Forecast System (Lanerolle et al., 2011); and the Columbia River estuary (CORIE) nowcast and forecast system (Baptista et al., 1998). For riverine environment, the NWS River Forecasting System (NWSRFS) has been used by National Oceanic and Atmospheric Administration (NOAA) National Weather Service to issue forecasts for the nation's major rivers over the last thirty years. In NWSRFS, hydrologic and hydraulic models are used to calculate runoff (watershed overland flow) and channel routing processes to produce flood outlooks (Day, 1985). Due to the limited capability in forecasting ability, a new operational

infrastructure, known as the Community Hydrologic Prediction System (CHPS), was recently advanced by Roe et al. (2010). CHPS employs the Delft Flood Early Warning System (FEWS) that combines the U.S. Army Corps of Engineers (USACE) hydrologic and hydraulic models. Nevertheless the connection between hydraulic river routing and reservoir/lake modeling is still lacking. Taking the advantage of flexible unstructured grids, Anderson et al. (2010) developed the Huron to Erie Connecting Waterways Forecasting System (HECWFS) to provide real-time discharge and water level information on Lake St. Clair and the St. Clair River. In view of the great progress in developing online systems for rivers, estuaries, or oceans, to date little attention has been paid to obtain online water level fluctuations and flow dynamics in a RCL system.

Several modeling approaches are available for predicting discharge and water level changes for a RCL system. Rating curve models have been commonly used to estimate river discharge based on water levels (Fread, 1975). However, backwater or unsteady flow due to floods and flow reversal complicates the development of rating curve models (Herschy, 2009) and often requires continuous field measurements to correct rating curves that may not be timely for water level management decisions. A lumped hydrologic water balance model was used to determine the appropriate amount of water released through hydraulic structures to meet the regulated target water levels (Krug, 1999). Water balance models may be timely; however, hydraulic river process including flow constrictions and backwater could not be addressed. To remedy this issue, a one-dimensional hydraulic river model was employed to connect each lake treated as a reservoir with a control gate. Nevertheless, reverse flows caused by downstream lake motions (i.e. hydraulic dam effects) cannot be simulated. Twigt et al., (2009) proposed to couple a two-dimensional lake model with a one-dimensional river model for a RCL system but special care for matching the boundaries between of two models is required (Lai et al. 2013). One approach is to use one-way nesting by

passing output of a river model to a lake model (Steinebach et al., 2004); but this approach can introduce conservation errors due to different mass or momentum exchanges between the models. Another approach is to simultaneously employ river and lake models without matching boundary conditions (Fernandez-Nieto et al., 2010). Nevertheless the time steps required for each model can be different, which could lead to computational stability issues (Morales-Hernandez et al., 2013). To date, there has been no attention paid to reliably predict real-time reverse flow for RCL with controlled hydraulic structures, as far as the authors are aware.

The overall objective of this paper is to provide real-time water information including water level and discharge of a RCL system. Specifically, we incorporate a new data assimilation technique to an Integrated Nowcast and Forecast Operation System (INFOS) that can automatically retrieve real-time observations and drive models under a high performance computing server. Accuracy and efficiency of the INFOS are carefully compared and examined. Outcomes of INFOS are used for sharing information to the community, planning for water use and delivery, and managing water levels in an RCL system.

2.2 Material and methods

2.2.1 Study site

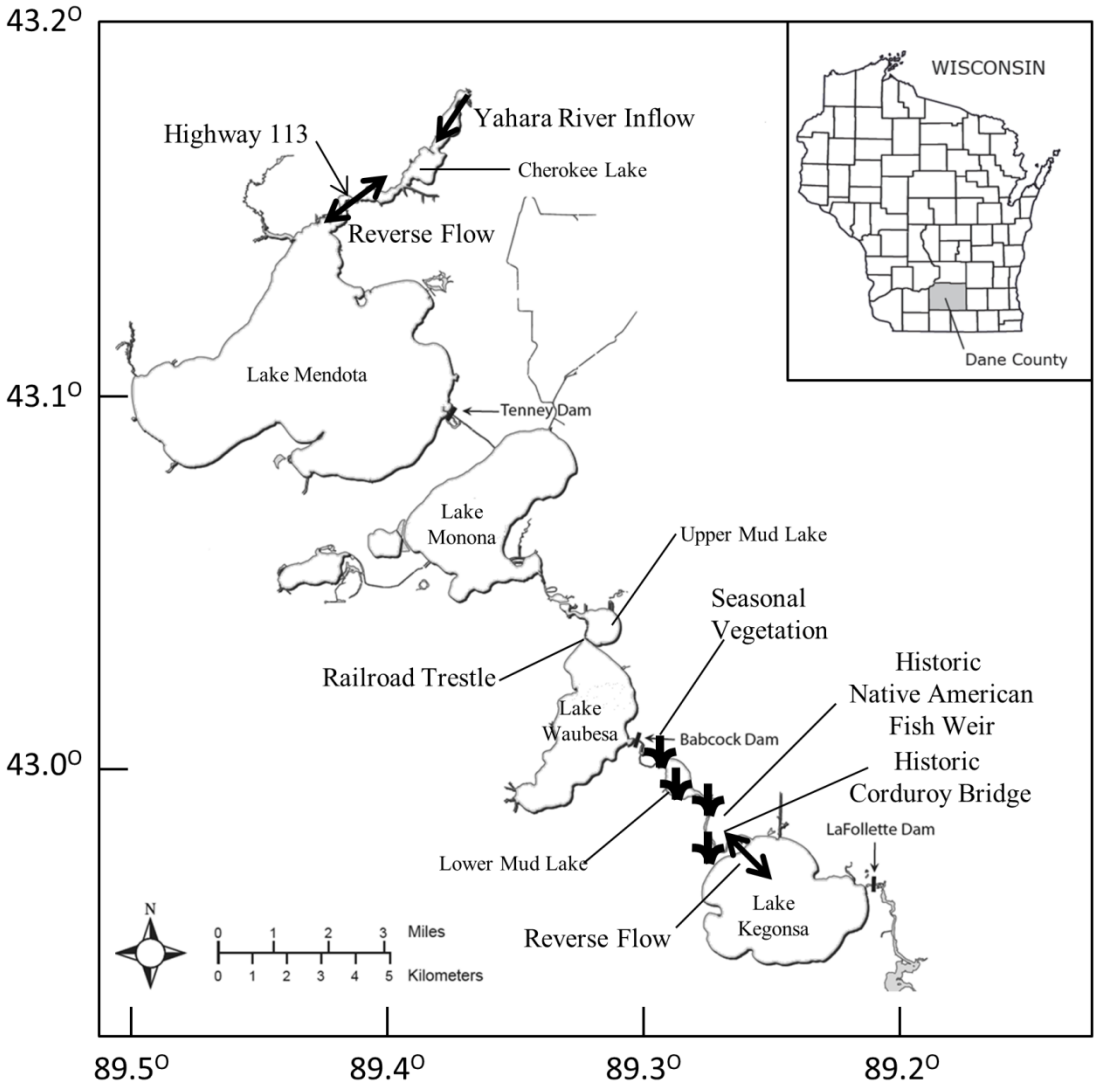

Fig 2-1. The Yahara River chain of lakes study site located in the state of Wisconsin, United States.

The Yahara RCL, located in Dane County, Wisconsin, is made up of a chain of lakes including Cherokee, Mendota, Monona, Upper Mud, Waubesa, Lower Mud, and Kegonsa

connected in between lakes by approximately 18 km of river (Fig 2-1). The RCL system is not a supply for drinking water or agriculture use, but does provide recreation purposes and ecological services. The Yahara RCL is a mixed system featuring natural channels and several bridges that narrow river cross sections. In addition, there are three human-operated control dams. The Yahara River inflow enters Cherokee Lake and discharges into Lake Mendota through a narrow channel at Highway 113 Bridge, which causes backwater flow. Due to the flat gradient between Cherokee Lake and Lake Mendota (i.e., the bottom slope is less than 0.002%), flow reversals with flow rates up to 14.2 m^3/s can occur. According to the USGS station (05427850) at Highway 113, five reverse flow events greater than 14.2 m^3/s occurred over a five year period from 2008 to 2012. At Lake Mendota, the water level is controlled by the Tenney Dam, which raised the original water level by 1.4 meters after its construction in 1847. Water released from Lake Mendota enters Lake Monona, travels through the uncontrolled natural channel to the Upper Mud Lake, and eventually reaches Lake Waubesa whose water level is controlled by the Babcock Dam. After the dam, the water flows along the Lower Mud Lake river corridor featuring the Native American fish weir and historic corduroy log bridge. Under high water levels, both native and historic features are submerged to cause flow restriction. Furthermore, seasonal aquatic plant growth and flow reversal between Lake Waubesa and Lake Kegonsa inhibit water delivery. To mitigate the flow restriction along the river, plant harvesting is regularly performed during the summer season which is accounted for in the modeling using a time Manning *n* friction coefficient. Due to the wind setup, reverse flows are frequently observed at the location before the water from the river enters Lake Kegonsa. Finally the water level at Lake Kegonsa is controlled by the LaFollette Dam. Overall, this complex mixed natural-manmade system presents several challenges to meet the regulated target water levels (Table 2-1). Dane County Land & Water Resources (DCLWRD) is charged to

manage the water levels for the chain of lakes through the operation of dam control structures to deliver water from upstream to downstream.

Table 2-1. Regulatory levels for the Yahara Lakes (elevation in meters above mean sea level, NGVD29)

Lake Name	Annual Maximum m, (ft)	Summer Minimum (March-October) m, (ft)	Winter Minimum (November-February) m, (ft)	100-Year Flood Elevation m, (ft)
Mendota	259.11 (850.10)	258.96 (849.60)	258.53 (848.20)	259.94 (852.80)
Monona	257.62 (845.20)	257.47 (844.70)	256.71 (842.20)	258.38 (847.70)
Waubesa	257.56 (845.00)	257.41 (844.50)	256.64 (842.00)	258.17 (847.00)
Kegonsa	257.10 (843.50)	256.95 (843.00)	256.60 (841.85)	257.62 (845.20)

2.2.2 Nowcast and Forecast System

2.2.2.1 Components

Three major components for INFOS are observations, modeling, and high performance computing server (Fig 2-2). Observations include the United States Geological Survey (USGS) for surface water level and discharge data, as well as NOAA, UW-Madison Atmospheric Oceanic and Space Sciences (http://metobs.ssec.wisc.edu/aoss/), and the Lake Mendota buoy (http://metobs.ssec.wisc.edu/buoy/) for meteorological data. Supplemental water level stations, using in-situ water level loggers with an accuracy of 0.1%, and rain gauges with accuracy of 1%, are also added for further calibrating models. Webcams, installed at Lake Mendota, the Babcock Dam, and LaFollette Dam, are used for management of lake levels to observe real-time environmental conditions and visual observations of water levels and obstructions to flow that need attention.

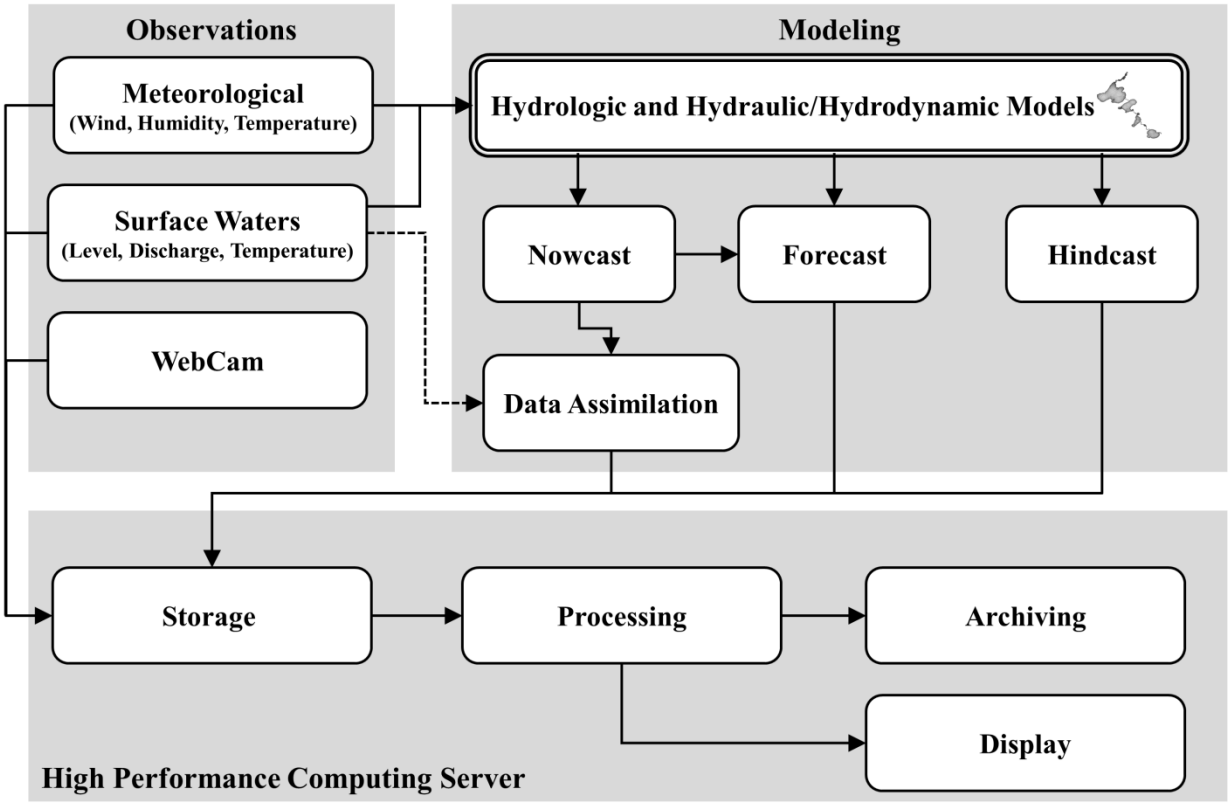

Fig 2-2. INFOS Infrastructure consisting of observations, modeling, and a high performance computing server.

The infrastructure of INFOS consists of a suite of integrated models in INFOS (Fig 2-2) that features hydrologic process for runoff, hydraulic river flows and water levels, and lake hydrodynamic circulation and temperature. In the Yahara RCL system, there are fifteen tributaries where only certain tributaries contain a gauge station. The hydrologic model is used to provide ungauged stream and storm sewer discharge. At present time, the Soil Conservation Service dimensionless unit hydrograph (Mockus, 1972, Yen et al., 1997) is employed by relating watershed

characteristics, e.g. shape, size, and slope, with rainfall properties like storm pattern, duration, and amount with peak flow rate (m^3/s)

$$q_P = \frac{KAR}{T_P} \tag{1}$$

where q_p is the peak flow rate (m^3/s), A is the drainage area (km^2), R is the total runoff depth (cm), T_p is the time to peak (hr), K is constant of 2.083. Even though the unit hydrograph method has been developed since Sherman (1932) it is still being applied and adopted today (Bhuyan et al., 2015). An example of real-time results of the integrated hydrological model can be found at http://www.infosyahara.org/monona. Overall, the hydrologic model serves to provide the water budget of each lake, which is then used for hydraulic/hydrodynamic modeling.

A hydrodynamic model is implemented to provide linkage between lake circulation and river hydraulic flow for the Yahara RCL system. Specifically, the Finite Volume Coastal Ocean Model (FVCOM) is utilized, developed by Chen et al. (2003) for modeling estuaries and oceans (Weisberg and Zheng, 2006; Chen et al., 2008). The hydrodynamic model solves the continuity equation (Eq. 2), horizontal momentum equations (Eq. 3 and Eq. 4), vertical hydrostatic pressure equation (Eq. 5), and temperature equation (Eq. 6) on horizontal unstructured meshes with a vertical sigma coordinate system as follows

$$\frac{\partial u}{\partial x} + \frac{\partial v}{\partial y} + \frac{\partial w}{\partial z} = 0 \tag{2}$$

$$\frac{Du}{Dt} - fv = -\frac{1}{\rho_0}\frac{\partial P}{\partial x} + \frac{\partial}{\partial z}\left(K_m \frac{\partial u}{\partial z}\right) + F_u \tag{3}$$

$$\frac{Dv}{Dt} - fu = -\frac{1}{\rho_0}\frac{\partial P}{\partial y} + \frac{\partial}{\partial z}\left(K_m \frac{\partial v}{\partial z}\right) + F_v \tag{4}$$

$$\frac{\partial P}{\partial z} = -\rho g \tag{5}$$

$$\frac{DT}{Dt} = \frac{\partial}{\partial z}\left(K_h \frac{\partial T}{\partial z} \right) + F_T \tag{6}$$

where u, v, and w are velocity components (m/s) in the x, y, and z the Cartesian coordinates, respectively; T is temperature (^oC), ρ is density ρ_o is reference density (kg/m^3); P is pressure (N/m^2); f is the Coriolis parameter ($1/sec$) ; g is gravitational acceleration (m/sec^2); K_m is vertical eddy viscosity coefficient (m^2/sec); K_h is thermal vertical eddy diffusion coefficient (m^2/sec); F_u and F_v are horizontal momentum diffusion terms (m/sec^2); and F_T is horizontal thermal diffusion term ($^oC/sec$). The bottom boundary condition for the momentum equation is

$$K_m\left(\frac{\partial u}{\partial z}, \frac{\partial v}{\partial z} \right) = \frac{1}{\rho_o}\left(\tau_{bx}, \tau_{by} \right) \tag{7}$$

where $\left(\tau_{bx}, \tau_{by} \right) = \rho_o g \frac{n^2}{D^{1/3}} C_D \sqrt{u^2 + v^2}\,(u, v)$ are the bottom stress (N/m^2) in the x and y components; D is water depth (m), and n is the Manning's roughness. The choice of the Manning roughness coefficient plays an important role in simulating reverse flows, seasonal evolution of aquatic plants, and the heterogeneity of bottom morphology (i.e. boulders, submerged weirs, and the historical submerged bridge).

The domain for the hydrodynamic model is determined by the following two steps. First, merging land topography measured from LiDAR with a vertical root mean square error of 24.7 cm at 95% confidence interval (Ayres Associates, 2010) and underwater bathymetry measured from an acoustic sub-bottom profiler with a vertical resolution of 1.8 cm, within 1% of the measurement range as described in Lin et al., 2009. Second, the 100 year floodplain is mapped to define the size of the model domain. The LiDAR data describes floodplain storages and connectivity to the rivers and lakes (Teng et al., 2015) applying a flooding/drying technique (Chen et al. 2008). To incorporate dams, an internal boundary condition is used, instead of separating the river chain of

lakes into different portions (Fread, 1978). Specifically, the discharge for the unstructured mesh elements intersecting the dam are replaced by the discharge of dam delivery curves, obtained from historical measurements of known gate heights and lake stage. Finally, discharge at the dam is obtained based on the gate opening height as an input. Flexible, unstructured meshes are employed to characterize different sizes of the lakes and rivers. The meshes are designed to have smaller sizes (~5m) in rivers and larger sizes (~100m) in lakes, allowing for accurate representation of the river hydraulics and reliable characterization of lake circulation. The sizes of meshes are determined by the balance of computational cost and resolution of flow resolved. Fig 2-3 shows the unstructured meshes with 17,565 meshes and 10,340 nodes in the Yahara RCL. The meshes overlay the water surface including the river chain of lakes and land surfaces including the 100 year floodplain. The multi-scale of meshes, ranging from 5 meters in the rivers to 100 meters in the lakes, maintains optimal number of meshes, thereby greatly reducing model computational cost on the whole domain of the Yahara RCL system.

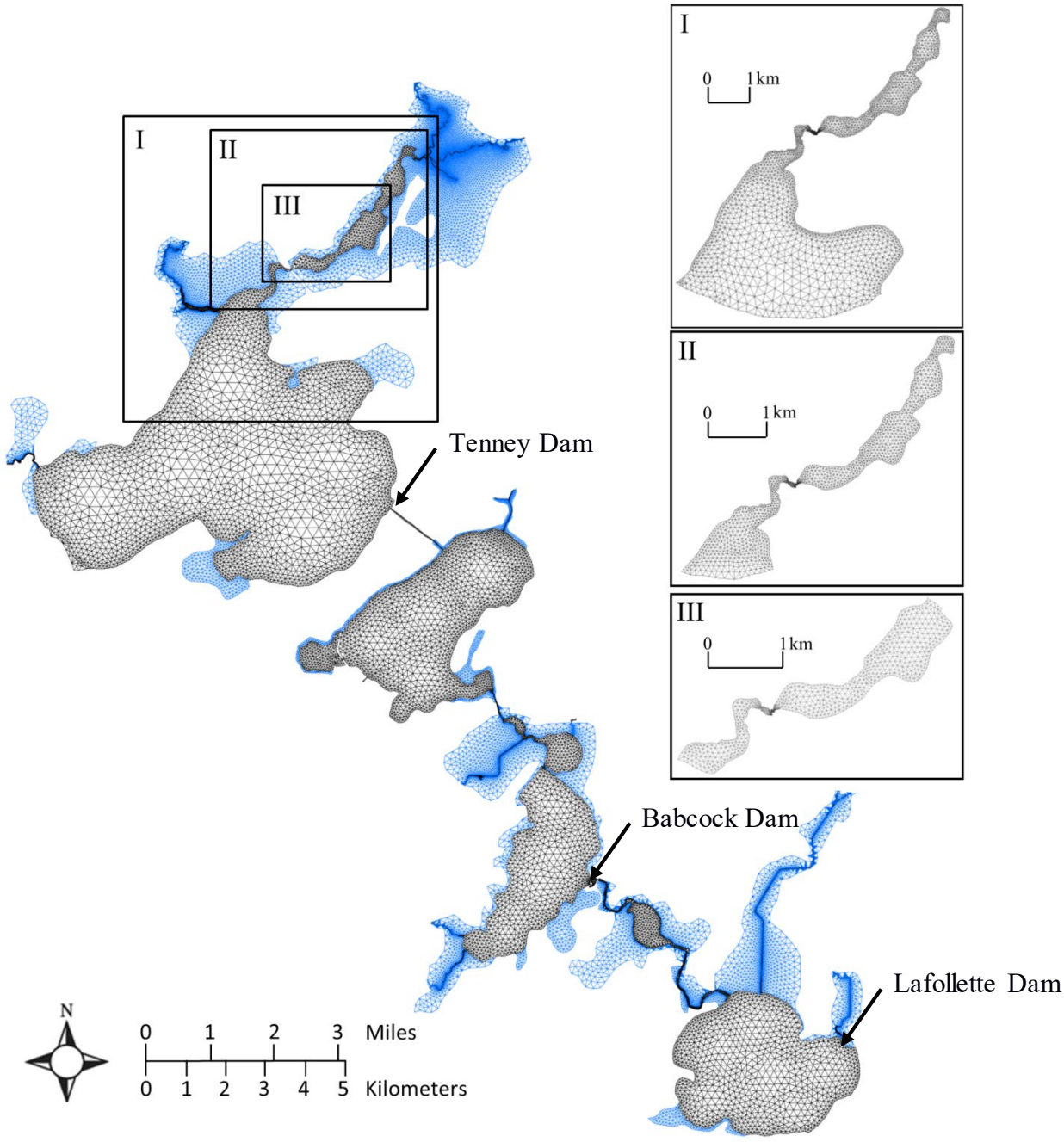

Fig 2-3. The computational meshes of the INFOS model on the Yahara RCL and the floodplain areas (blue). I, II, and III are the three different sizes of the nested domains.

A new data assimilation technique, different from Hsu et al. (2006), is developed in this paper to update the dynamic Manning roughness coefficient n in INFOS modeling. Two approaches are discussed here and compared. The first approach is based upon several flow routing algorithms including the steady state equation (Eq. 8), diffusive wave equation (Eq. 9), and fully dynamic wave equation (Eq. 10), (Chow 1959, Quinn and Wylie, 1972, Akan 2006), as follows:

$$n = \frac{AR^{2/3}S_o^{1/2}}{Q} \tag{8}$$

$$n = \left[\frac{AR^{4/3}}{gQ|Q|} \times \left(g - \frac{Q^2T}{A^3}\right)\frac{\partial h}{\partial x}\right]^{1/2} \tag{9}$$

$$n = \left[\frac{AR^{4/3}}{gQ|Q|} \times \left(\frac{1}{A}\frac{\partial Q}{\partial t} - \frac{2QT}{A^2}\frac{\partial h}{\partial t} + \left(g - \frac{Q^2T}{A^3}\right)\frac{\partial h}{\partial x}\right)\right]^{1/2}$$

(10)

where A is cross sectional area (m^2), Q is observed real-time discharge (m^3/sec), R is hydraulic radius (m), T is top width of the cross section area (m), h is the water level (m), and S_o is river bottom slope. For the dynamic wave equation, the unsteady terms $\frac{\partial Q}{\partial t}$ and $\frac{\partial h}{\partial t}$ are obtained from the real-time observations at and previous time step values. The second approach is based upon a nested mesh to reduce computational domain. For example, three sizes (i.e., I, II, and III in Fig 2-3) of nested computational domain are employed. The procedure for the two-way nested approach starts with a global domain for the Yahara RCL, yielding water level boundary conditions at upstream and downstream locations of a nested domain. Afterwards, the water level and velocity field within the nested domain are computed. The Manning roughness n is thereby updated using one of three Eqns (8), (9), or (10), and is feedback to the global computational domain for the next

step simulation. Details of the two different approached will be compared and discussed in the result section.

A high performance computing (HPC) server was used to efficiently perform data storage, processing, archiving, and display. Specifically the server utilizes Rocks Cluster 6.0, an open-source Linux cluster distribution capable of scalable and parallel computing. The server uses AMD Opteron 3.2 GHz Processor and consists of 64 Central Processing Units (CPUs). Model input data is temporarily stored on the server for model simulation. Afterwards, each model simulation runs in parallel mode with 8 CPUs. In the modeling configuration, the time ratio of run time to modeled time is 1:72. Modeling results and observations are processed using Mathworks-Matlab and Perl scripts in the forms of JavaScript Object Notation (JSON), American Standard Code for Information Interchange (ASCII) text files, comma separated value (CSV) files, and Google Keyhole Markup Language (KML or zip format KML known as KMZ). Data produced from modeling and observations are archived to the server for the use of historic and future water planning and management scenarios. The webserver is provided by Apache HTTP Server Project. The display is written in combined codes including HyperText Markup Language (HTML), Adobe Flash, JavaScript, and Google Maps JavaScript API.

2.2.2.2 Functions

Three functions, including hindcast, nowcast, and forecast, are incorporated in the INFOS. The hindcast function in INFOS is used to calibrate the hydrologic and hydrodynamic models and provide historical information of the Yahara RCL system. For the nowcast/forecast functions, previous/current observations including water levels, discharge, and meteorological data are required. Wind data obtained from the Lake Mendota buoy and weather stations is interpolated by

inverse distance weighted method over the model domain. Tributary discharge is obtained from real-time gauge stations or the hydrologic model with a time interval of 5 minutes. To reliably predict flow in the current condition, we develop a new data assimilation technique to adjust river roughness parameters based on observed water levels as targets to account for reveres flow. For the forecast function, the roughness parameters are assumed the same as those in the nowcast mode. Predicted precipitation amounts from the National Weather Service (NWS) are prescribed into the hydrologic model to estimate future tributary lake inflows. To address various time intervals used in models, the 5-minute tributary flows and 1-minutes weather observations are linearly interpolated to prescribe to the hydrodynamic model with a time step of 0.6 seconds. The hydrodynamic model projects 24-hour prediction of lake water levels and river discharges with the purpose of providing flood outlooks or warnings. The nowcast and forecast functions provide crucial water information for managing the Yahara RCL system.

2.3 Results and discussion

2.3.1 Flow reversal

Lake currents driven by winds are responsible for mixing and transport of nutrients or chemicals (Gardner et al., 2006, Moskalsi et al., 2011). In the low gradient of the Yahara RCL, flow reversals caused by winds are frequently observed. For example, a southern wind can push the water toward the northern shore of Lake Mendota, causing the downstream water level higher than the inlet of the Yahara River to yield flow reversal. If the direction or magnitude of the wind changes, the water level fluctuates and sways back and forth. This is called seiches, first termed by the Swiss hydrologist François-Alphonse Forel in 1890 (Darwin, 1898). These oscillations of water with periods, depending on the size of water body, interact with the river flow and temporally

cause flow reversal. For example, the type of flow reversal has been commonly found in an estuary-delta environment like Delaware Bay (Moskalsi et al., 2011) and the Slave River Delta (Gardner et al., 2006). Seiche events reverse river flows which can result in upstream flooding of lagoons and wetlands as well, which is the case on River Murray, Australia (Webster et al., 1997). On the Yahara RCL, lake seiches can reverse flow from the Yahara River daily. Based upon the water level records at the Highway 113 on Lake Mendota (USGS 05427850 gauge, Fig 2-1), the occurrence of flow reversals ranges from 1 to 5 times per day over the ten-year period from 2003 to 2013. As a result, the ability on measuring and modeling flow reversals, influenced by meteorological wind forcing and opposing hydraulic flows, is crucial to address the overall inflow from the Yahara River to Lake Mendota.

Two types of flow reversals are identified at the Highway 113. First, wind-forcing can induce reverse flow. As shown in Fig 2-4, a south wind of 8.5 m/s sustainably blew across Lake Mendota from 14:00 to 18:00 on 7/25/12, creating the wind setup on the north side of lake to cause flow reversal up to -5.66 m^3/s. The strength of the reversed flow depends on the magnitude of the wind stresses. As soon as the wind decreased, the wind setup also became smaller and flow reversal disappeared. In contrast to the sustained reverse flow, the second type is transient reverse flow caused by seiching. On the same day, the wind direction changed to be northerly, which is in the same direction as the incoming flow at 22:00 and thus the water level on the southerly end of the lake was raised. As the wind decreased gradually, the water level imbalance in Lake Mendota forced the water to slosh back to the north, creating seiches with an approximate 25 minute period of repeated transient reverse flow events with magnitude up to 7.0 m^3/s until 3:00 on 7/26. To compare with the theoretical period of a seiche in an enclosed body of water, Merian's formula (Merian, 1828, Proudman, 1953) can be applied:

$$T = \frac{2L}{\sqrt{gh}} \tag{8}$$

where T is the longest natural period (sec), g the acceleration of gravity (m/s^2), and L and h are the length and the average depth of the body of water (m), respectively, is used. The theoretical period of seiches for Lake Mendota is estimated to be 27.1 minutes, further supporting the common occurrence of this type of flow reversal. In the past, modeling dynamic flow reversals, influenced by meteorological wind forcing and opposing hydraulic flow, has been challenging due to the difficulties in parameterizing the Manning roughness coefficient to address high frequency water level fluctuations and flow direction changes.

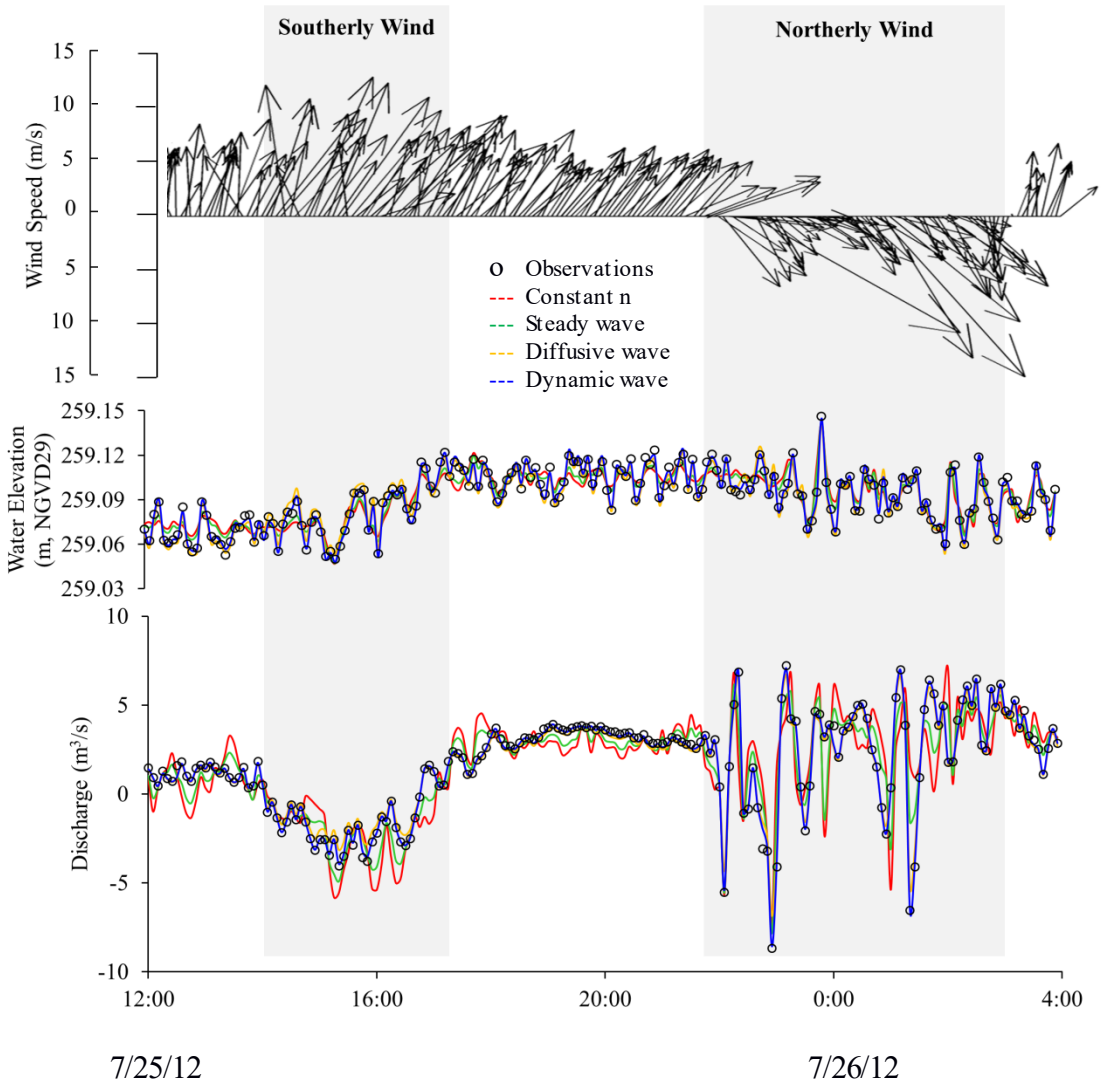

Fig 2-4. The time series of (a) wind field, (b) water level, and (c) discharge for the Yahara River inflow at Highway 113. The shadow zones delineate two reverse flow events.

In this paper, a new data assimilation technique for accurately simulating flow reversal is developed. Results of the two approaches (i.e. flow routing algorithm and nested-mesh domain reduction), described previously, are shown here. Table 2-2 summarize results using three flow routing algorithms based upon steady state Manning's equation, diffusive wave equation, and

dynamic wave equation to simulate flow reversals at Highway 113 on Lake Mendota. In comparing with constant Manning roughness without data assimilation, the daily average iterations on July 25, 2012 is 12 times using the steady Manning equation, greater than the 7 times based upon the diffusion and dynamic equations. For the computational cost, a 3-day simulation period is used here. It is found that the run time for the diffusive and dynamic equations is 1.44 and 1.45 hours, respectively, versus 2.40 hours using steady state Manning equation. The results indicate that the average iteration number for the diffusion and dynamic wave equations is the approximately the same; and the root mean square deviation (RMSD) for the dynamic wave equation algorithm is further reduced. Fig 2-4 shows the two types of flow reversals are well resolved by the dynamic wave equation algorithm (blue solid line) with the local and convective accelerations, which are absent from the steady Manning equation (green solid line) and diffusion wave equations (orange solid line).

Table 2-2. Comparison of algorithm and domain approaches on number of iterations, statistical results (R^2), and computation speed.

Approach	Case	Number of Iterations	Discharge RMSD (m^3/s)	3 Day Simulation Run Time	Computation Speed
None	None	0	1.73	0.91 hr	1:78.6
Algorithm	Manning's	10	1.08	2.40 hr	1:30.0
Algorithm	Diffusive	7	0.41	1.44 hr	1:50.1
Algorithm	Dynamic	7	0.23	1.45 hr	1:49.8
Domain	I	7	0.23	1.20 hr	1:60.2
Domain	II	7	0.23	1.04 hr	1:69.4
Domain	III	7	0.23	1.00 hr	1:72.1

The computational efficiency is further addressed by the second approach based upon a nested-mesh domain reduction. Table 2-1 shows the computational time linearly decreases for the three nested domains (Fig 2-3) using the dynamic wave flow routing algorithm approach. It is also noted that the reduction of the nested domain does not affect RMSD for the three domains, indicating the efficiency and effectiveness of the new data assimilation technique. Similar flow reversal at the inlet of Lake Kegonsa (Fig 2-1) is also modeled using INFOS with the data assimilation technique with a 1:90 computation speed with a nested domain and dynamic flow routing algorithm but not shown here for brevity. Overall, it is demonstrated that the INFOS model based upon the new data assimilation technique for obtaining Manning roughness coefficients can reliably and effectively model real-time flow reversals, which have not yet been appeared in the literature as far as the authors are aware.

2.3.2 Flow choking

In open channel hydraulics, specific energy is defined as energy head relative to channel bottom, or the sum of the water depth and velocity head (Bakhmeteff in 1932). For flow to pass a channel section, a minimum specific energy is needed (Sturm, 2001). If the flow does not have the minimum specific energy needed to pass a channel section, it would adjust itself to increase the specific energy, decrease the discharge, or both. This is often referred to as flow choking (Sturm, 2001). Flow choking can occur due to a constriction caused by narrowing river widths, rise in bed elevation, or both that influences the upstream flow and/or water level (Henderson, 1966). In this paper, the authors employ the INFOS model for flow choking that occurs among 10 of the 14 bridge constrictions along the Yahara River. Specifically, the Railroad Trestle constriction (Fig

2-1) that connects Lake Monona and Lake Waubesa is presented. The finding is critical for future decisions regarding widening the channel at the Railroad Trestle.

Two cases are presented to examine if specified flow rates can be passed through a narrow channel width (i.e. 26 m) of the Railroad Trestle under the summer minimum water level of 257.41 m (NGVD29) at the downstream, Lake Waubesa. Depending on the condition at the Railroad Trestle, the upstream water level (Upper Mud Lake) may adjust itself or maintain the same flow condition. First, for a flow rate of 5.66 m^3/s (200 cfs), Fig 2-5a shows the water depth (referenced to summer minimum water level in NGVD29) versus specific energy diagram, obtained from the INFOS model. Three cross sections are examined here. At the upstream of the Trestle (point G), the channel width is 405 m, yielding the discharge per unit width q = 0.014 m^2/s and the water depth of 0.55 m. At the Trestle (point H), the cross section becomes narrower with a width of 26 m, yielding q = 0.222 m^2/s. The water depth drops to 0.51 m under the same specific energy (0.54 m). At the downstream of the Trestle (point I), the cross section becomes wider with the channel width of 45 m, yielding q = 0.125 m^2/s. The water depth increases up to 0.53 m. Overall the flow can pass from the upstream G, through the Trestle H, and to the downstream I, indicating the feasibility of operating to 5.66 m^3/s discharge condition without choking to alter the specific energy. Fig 2-5b shows the corresponding water surface profile. To compare the modeled water surface profile (solid line), the normal depth (dashed line) is plotted, computed from the Manning's equation. The modeled water profile is greater than the normal depth indicating an M1 water profile. At a distance of 0.3 km the modeled and normal depth profiles intersect the so-called long channel. The intersection indicates that the Railroad Trestle does not impact water levels on Lake Monona under the 5.66 m^3/s flow condition.

For the second case, a higher flow rate 11.32 m^3/s (400 ft^3/s) is set with the same summer minimum water level at the downstream, Lake Waubesa. Using the INFOS modeling, Fig 2-5c shows the modeled specific energy diagram versus water depth under this condition. At the upstream G, the initial water depth is 0.55 m and the specific energy is 0.56 m with the discharge per unit width $q = 0.028$ m^2/s. To reach the Trestle H with the discharge per unit width $q = 0.446$ m^2/s, the minimum specific energy is around 0.61 m, which is larger than that of G (0.55 m). As a result the flow does not have the minimum specific energy to pass through the Trestle, causing the flow choking to occur. The specific energy is raised to 0.61 m at G', in which the water depth is also elevated to 0.61 m. After passing the Trestle, the widening cross section at I yield the water depth to decreases to 0.58 m under the discharge per unit width $q = 0.251$ m^2/s, still equivalent to total flow rate of 11.32 m^3/s. Fig 2-5d shows the water surface profile from Lake Monona (0 km) to Lake Waubesa (3.2 km). At a distance of 2.9 km (Point G'), an M1 water profile curve would form, followed by a water drop through the Railroad Trestle. In this mild channel, the normal depth line (dashed line) does not intersect with the modeled water surface profile (solid line), yielding a so-called a short-channel condition between the Trestle and Lake Monona (Akan, 2006). Since the choke occurs at the Railroad Trestle, an increase in water depth upstream of the Trestle would propagate through the short connecting river, which would impact the water level in Lake Monona. Overall, the two cases for examining flow choking are successfully addressed, demonstrating the capability of the INFOS model to provide real-time choked flow conditions.

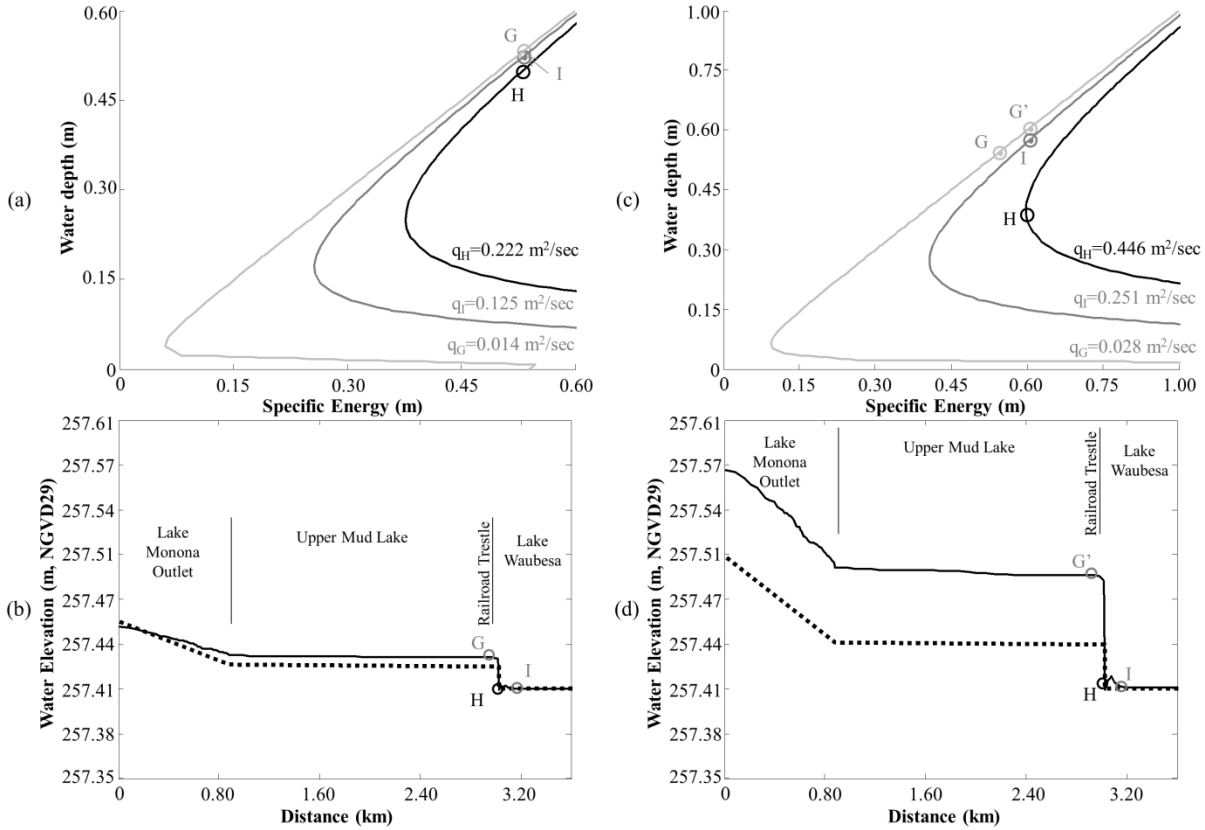

Fig 2-5. (a) The specific energy diagram at the upstream (light gray line), downstream (dark gray line), and the Railroad Trestle (black line) for Q = 5.66 m^3/s; (b) The modeled water surface profile (solid line) and normal depth (dashed line) from Lake Monona at distance = 0 km to the Railroad Trestle at distance = 2.9 km; (c) Same as (a) except for 11.33 m^3/s discharge; (d) Same as (b) except for Q = 11.33 m^3/s.

2.3.3 Planning of water levels in the RCL

Planning scenarios for plausible circumstances to create the desired water level of each lake are employed. These scenarios are examined through the aid of INFOS lake-river modeling for an example for water levels on Lake Monona that are prone to flooding due to several extreme rainfall storm events in June 2008. The storm caused tremendous damage and economic loss of $77.9 Million in Dane County (County of Dane Emergency Management, 2014). Water release

from Lake Monona travels through an uncontrolled river channel with a narrow cross section at the Railroad Trestle. During flood periods with high flow, choking can occur (Fig 2-5) so as to block the flow release and increase the water level in Lake Monona. The regulatory maximum water level orders, listed in Table 2-1, for Lake Monona and Lake Waubesa are 257.62 and 257.56 meter, respectively. Between the two lakes, 0.06 meter difference in water levels is regulated. Nevertheless, there was 0.21 meter of water level difference between the two lakes for approximately half of a month.

Previous studies for reducing water levels include the use of wetlands (Tsihrintzis et al., 1998), dams (Montaldo et al., 2004, Onusluel et al., 2010), and levees (Gergel et al., 2002; Castellarin et al., 2011). In this paper, the authors address this issue by altering downstream river geometries due to limitations (e.g., private ownership, permitting) with altering adjacent land. Fig 2-6 shows the outcome of the three planning scenarios. For the first scenario, the Railroad Trestle is widened to 49 m from the original 24 m width but bottom depth remained unchanged. The Railroad Trestle widening does not change the long-standing water level in Lake Monona, suggesting that flow choking still exists. For the second scenario, the entire channel is dredged 1.52 to 3.05 meter deep with 0.3 meter increment but maintained the width of the Railroad Trestle. Due to the entire river being affected versus local widening at the Railroad Trestle, the systems thereby responds more to dredging. As a result, it is found that dredging 2.45 m deep (shown in Fig 2-6 for brevity) would mitigate the water level on Lake Monona below the 100 year flood elevation. For the third scenario, both dredging and railroad widening actions are considered. The difference of water level between Lake Waubesa and Lake Monona is decreased to 0.055 m, lower than the required order of 0.061 m. The results from the three planning scenarios obtained from the INFOS modeling provide quantitative measure for lake management to reduce the magnitude

of extreme water levels and the occurrences of violations of regulatory water level orders. In this paper, the INFOS model is used to assess the impacts of future climate scenarios on high or low water levels in an RCL system.

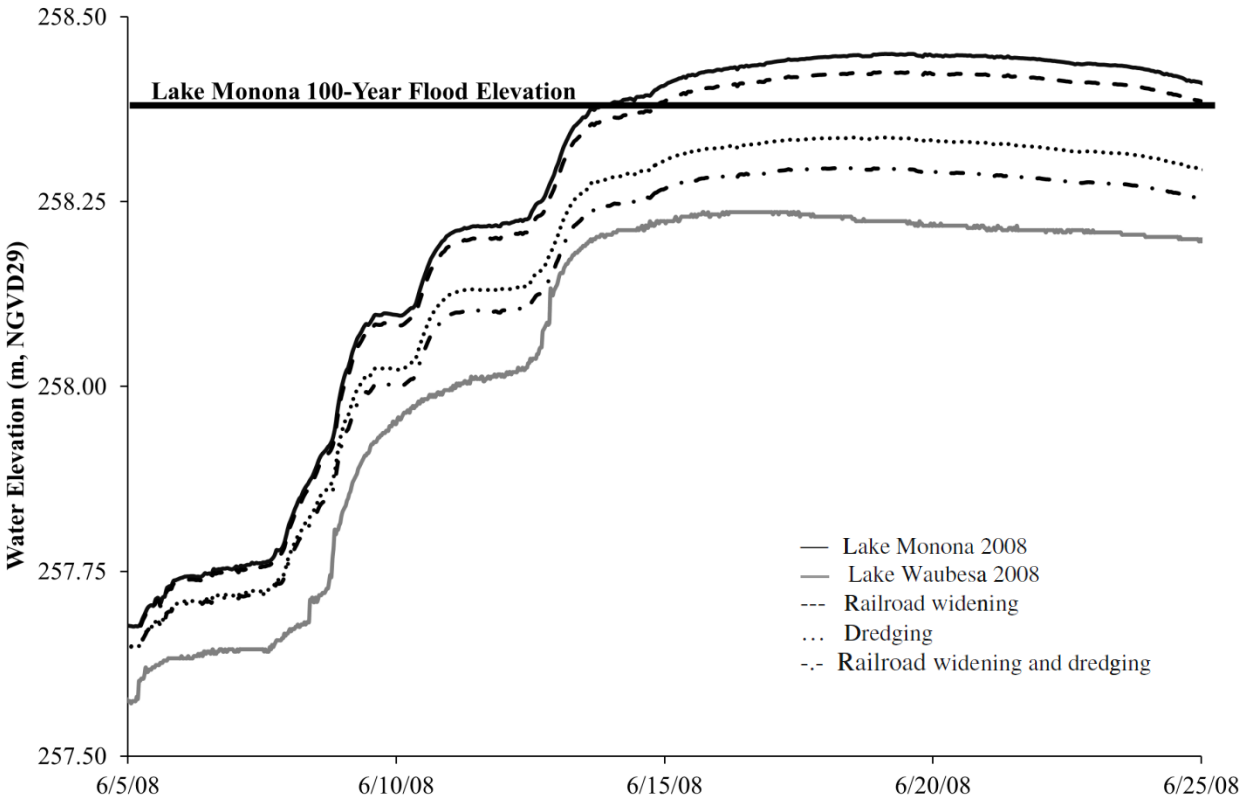

Fig 2-6. The time series water elevations during the extreme storm events in 2008 and Lake Monona of the three planning scenarios.

2.3.4 Management of RCL

Water level management of an RCL involves full consideration for delivering an appropriate amount of water (i.e. discharge) to each lake to achieve regulated water levels for the entire chain of lakes system. Water level operating ranges (Table 2-1) for each lake in the Yahara RCL were set by the Wisconsin Department of Natural Resources (Morrisette, 1979). Large or repetitive rainfall events can quickly cause water levels to become out of compliance. Challenges are to determine the amount and the time to release water by operating the three dams in the Yahara RCL (Fig 2-1) to meet water level orders timely. Currently the midrange of the set lake level orders was operated (County of Dane, 2010). Two other management philosophies have been debated. First, the flow-through management aims to quickly release water, which would lower water level on its supporting lake but increase the risk of causing high water levels in the downstream lakes. Second, the storage management targets to store water on its supporting lake to reduce the risk of flooding on downstream lakes. The authors employ INFOS to compare the outcomes of the current operation with those by the other two management philosophies.

Fig 2-7 shows the water elevations and the duration of flooding for an extreme (i.e. 50-year) rainfall event in June 2008 that caused Lake Mendota and Lake Waubesa to experience 53 days and 52 days above the targets (black lines), respectively. In comparison, the authors employ the flow-through management by setting the targeted water level at the 3 inches and 6 inches higher than the midrange of the lake level, i.e., 259.04 m. As a result, Lake Mendota would experience 49 days (dotted black line) and 45 days (dashed black line) above the target level due to the immediate release of water to the downstream. Lake Waubesa would increase of the flooding period from 52 days (black line) to 58 days (dotted black line) and 64 days (dashed black line). In other words, in comparison with the current target lake levels, the flow-through management

would reduce the flood duration of Lake Mendota by 4 (= 53-49) days and 8 (= 53-45) days and increase the flood duration of Lake Waubesa to 6 (=58-52) days and 12 (64-52) days, respectively. In contrast, employing the storage management by setting water level lower than the midrange of the lake level would extend the flood duration of Lake Mendota from 53 days to 57 days (dotted gray line) and 60 days (dashed gray line), but reduce that of Lake Waubesa from 52 days to 43 days (dotted gray line) and 35 days (dashed gray line) for at the 7.62 cm inches and 15.24 cm, respectively. While the duration of flooding in Lake Waubesa is reduced at the cost of flood extension in Lake Mendota, the peak water level of Lake Waubesa is reduced by approximately 1 foot as compared to the current targets. Overall the flood durations for the Yahara RCL system under the current operation and the two management philosophies can be quantitatively obtained and compared using INFOS. This information, not available in the past, nowadays provides sound and scientific justification for managing the water level orders for the Yahara RCL. Future research that considers multi-purpose water body networks (Anand et al., 2013) is currently underway.

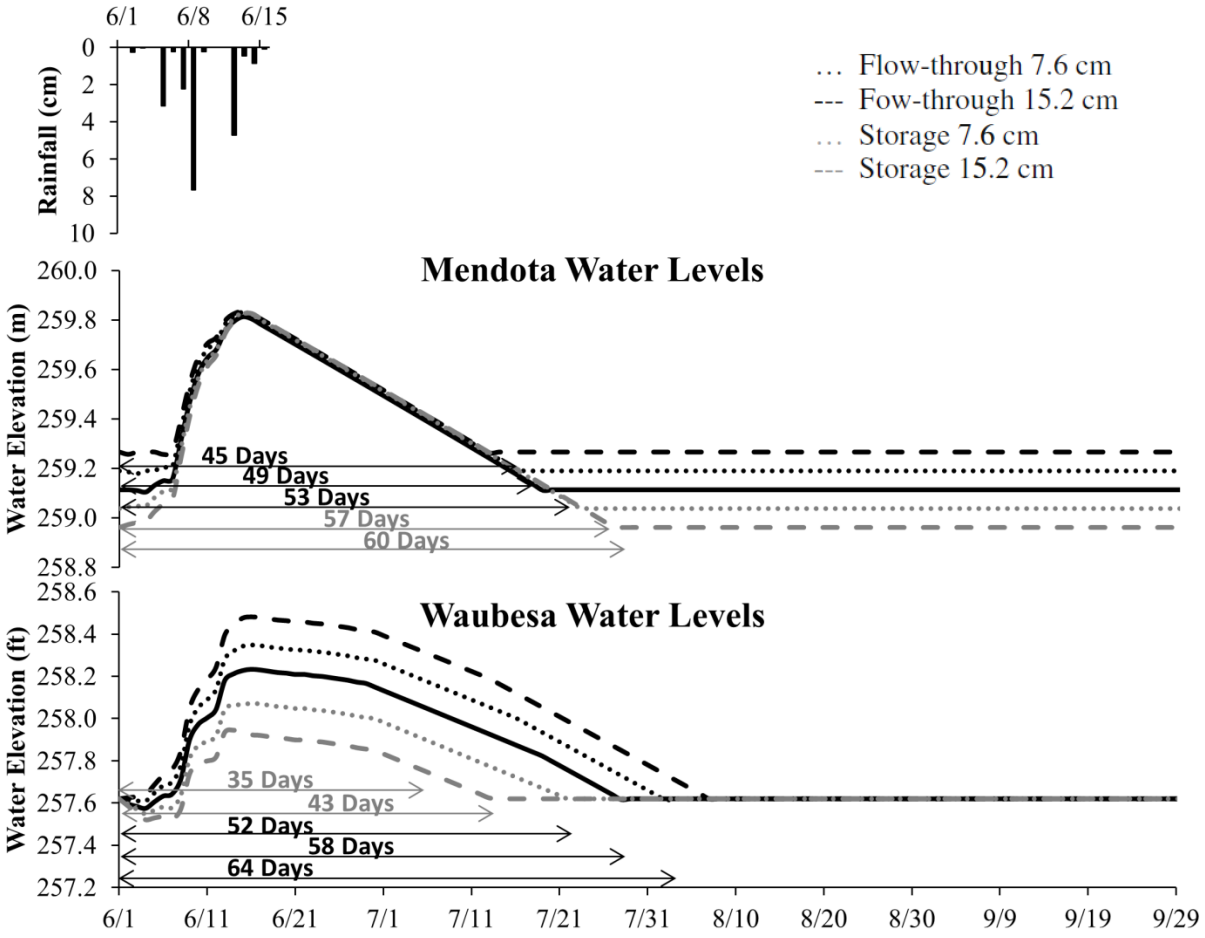

Fig 2-7. The extreme rainfall event and water elevations (solid lines) of Lake Mendota and Lake Waubesa in June 2008, compared with those by two strategies based upon flow-through and storage management.

2.4 Summary and conclusions

In this paper, an Integrated Nowcast Forecast Operation System (INFOS), consisting of observations, modeling, and high performance computing server, is developed to provide real-time water information including water level and discharge of the Yahara RCL system. Specifically, a new data assimilation technique based upon flow routing algorithm and nested-mesh domain reduction is developed to update the Manning's roughness. It is demonstrated that the INFOS can reliably and effectively model real-time sustained reverse flow due to wind forcing and transient reverse flow due to seiches, which have not yet been appeared in the literature as far as the authors

are aware. INFOS can also predict flow choking condition that can provide the information to release an appropriate amount of water for the overall Yahara RCL system. Applications of the INFOS are illustrated both planning and management. Specifically the INFOS model is employed to effectively assess the compliance of water level orders for all lakes under extreme rainfall storm events through planning scenarios like river channel widening, dredging, or both. Moreover, INFOS is used to address the suitability of the current dam operation, compared with two other management philosophies. The flood durations of the Yahara RCL system are quantitatively obtained and compared, providing sound and scientific justification for managing the water level orders for the Yahara RCL. Through the illustration, INFOS is shown to successfully provide for reliable and timely nowcasting and forecasting water information of the Yahara RCL system for the public, managers, and researchers.

2.5 Acknowledgements

This research was funded in part by the National Science Foundation DEB-0941510, Dane County Land and Water Resources Department (DCLWRD) MSN126143, and the City of Madison, Wisconsin 97235340-1. Specifically the authors thank Mr. Kevin Connor, Director of DCLWRD, and Mr. Greg Fries, Principal Engineer, at the City of Madison for their continuous support of the INFOS development and applications. Mr. Jeremy Balousek and Mr. Josh Harder at DCLWRD for their comments and suggestions to address complex hydraulics on the Yahara RCL are highly acknowledged. The authors also thank Dr. Paul Hanson at the Center of Limnology, University of Wisconsin-Madison for the collaboration of the deployment of the real-time Lake Mendota buoy (http://www.infosyahara.org/dbbadger). In addition, Ms. Sue Josheff at Wisconsin Department of Natural Resources for her assistance to provide permit for installing water level gauges is highly acknowledged. Finally, both authors thank Dr. Yin-Tien (Kevin) Lin and Mr. William Kasch to assist data collection of lake bathymetry and water level.

2.6 References

Afshar, A., Shafii, M., Haddad, O.B., 2011. Optimizing multi-reservoir operation rules: an improved HBMO approach. Journal of Hydroinformatics. 13 (1), 121-139.

Akan, O.A., 2006. Open Channel Hydraulics. Elsevier, Oxford.

Aikman, F., Mellor, G. L., Ezer, T., Sheinin, D., Chen, P., Breaker, L., Bosley, K., Rao, D. B., 1996. Towards an operational nowcast/forecast system for the U.S. East Coast. Modern Approaches to Data Assimilation in Ocean Modeling. Elsevier Oceanography Series, 61, 347-376.

Anand, A., Galelli, S., Samavedham, L., Sundaramoorthy, S., 2013. Coordinating multiple model predictive controllers for the management of large-scale water systems. Journal of Hydroinformatics. 15 (2), 293-305.

Anderson, E.J., Schwab, D.J., Lang, G.A., 2010. Real-time hydraulic and hydrodynamic model of the St. Clair River, Lake St. Clair, Detroit River system. Journal of Hydraulic Engineering ASCE. 136 (8), 507-518.

Ayres Associates., 2010. GPS survey for LIDAR control. Report, Madison, WI.

Bakhmeteff, B.A., 1932. Hydraulics of Open Channel Flow. McGraw-Hill, New York.

Baptista, A.M., Wilkin, M., Pearson, P., Turner, P., McCandlish, C., Barrett, P., Das, S., Sommerfield, W., Qi, M., Nangia, N., Jay, D., Long, D., Pu, C., Hunt, J., Yang, Z., Myers, E., Darland, J., Farrenkopf, A., 1998. Towards a multi-purpose forecast system for the Columbia River Estuary. Ocean Community Conference 199. Baltimore, MD.

Bhuyan, M.K., Kumar, S., Jena, J., Bhunya, P.K., 2015. Flood hydrograph with synthetic unit hydrograph routing. Water Resources Management. 29, 5765-5782.

Castellarin, A., Domeneghetti, A., Brath, A., 2011. Identifying robust large-scale flood risk mitigation strategies: A quasi-2d hydraulic model as a tool for the Po river. Physics and Chemistry of the Earth. 36 (7-8), 299-308.

Chen, C., Liu, H., Beardsley, R.C., 2003. An unstructured grid, finite-volume, three-dimensional, primitive equations ocean model: Application to coastal ocean and estuaries. Journal of Atmospheric and Oceanic Technology. 20 (1), 159-186.

Chen, C.S., Qi, J.H., Li, C.Y., Beardsley, R.C., Lin, H.C., Walker, R., and Gates, K., 2008. Complexity of the flooding/drying process in an estuarine tidal-creek salt-marsh system: An application of FVCOM. Journal of Geophysical Research. 113, C07052.

Chow, V.T., 1959. Open Channel Hydraulics, McGraw-Hill, New York.

County of Dane, 2010. Dane County lake level management guide for the Yahara chain of lakes. Dane County and Water Resources, Madison WI.

County of Dane Emergency Management, 2014. Dane County Natural Hazard Mitigation Plan. https://www.countyofdane.com/emergency/mitigation_plan.aspx.

Darwin, G.H., 1898. The tides and kindred phenomena in the solar system. Houghton, Boston.

Day, G.N., 1985. Extended streamflow forecasting using NWSRFS. Journal of Water Resource Planning and Management ASCE. 111 (2), 157-170.

Fallah-Mehdipour, E., Bozorg Haddad, O., Marino, M.A., 2013. Developing reservoir operation decision rule by genetic programming. Journal of Hydroinformatics. 15 (1), 103-119.

Fernandez-Nieto, E.D., Marin, J., Monnier, J., 2010. Coupling superposed 1D and 2D shallow-water models: source terms in finite volume schemes. Computers & Fluids. 39, 1070-1082.

Fread, D.L., 1978. Numerical hydrodynamic modeling of rivers for flood forecasting by the National Weather Service, NOAA Technical Report, Silver Spring, MD, 14pp.

Gardner, J.T., English, M.C., Prowse, T.D., 2006. Wind-forced seiche events on Great Slave Lake: hydrologic implications for the Slave River Delta, NWT, Canada. Hydrological Processes. 20 (19), 4051-4072.

Gergel, S.E., Dixon, M.D., Turner, M.G., 2002. Consequences of human-altered floods: levees, floods, and floodplain forests along the Wisconsin River. Ecological Applications. 12 (6), 1755-1770.

Green, J.C., 2005. Modeling flow resistance in vegetated streams: review and development of new theory. Hydrological Processes. 19 (6), 1245-1259.

Henderson, F.M., 1966. Open Channel Flow. MacMillan, New York.

Herschy, R.W., 2009. Streamflow Measurement. Taylor & Francis, New York.

Hunt, J., Brunner, G.W., Larock, B.E., 1999. Flow transitions in bridge backwater analysis. Journal of Hydraulic Engineering ASCE. 125 (9), 981-983.

Hsu, M.H., Fu, J.C., Liu, W.C., 2006. Dynamic routing model with real-time roughness updating for flood forecasting. Journal of Hydraulic Engineering ASCE. 132 (6), 605-619.

Kaatz, K.J., James, W.P., 1997. Analysis of alternatives for computing backwater at bridges. Journal of Hydraulic Engineering ASCE. 123 (9), 784-792.

Krug, W.R., 1999. Simulation of the effects of operating Lakes Mendota, Monona, and Waubesa, south-central Wisconsin, as multipurpose reservoirs to maintain dry-weather flow. U.S. Geological Survey Open-File Report, 99-67.

Lakes and Watershed Commission, 2013. Aquatic Plant Management. http://www.danewaters.com/management/AquaticPlantManagement.aspx.

Lai, X.J. Jiang, J.H., Liang, Q.H., Huang, Q., 2013. Large-Scale hydrodynamic modeling of the middle Yangtze River Basin with complex river-lake interactions. Journal of Hydrology. 492, 228-243.

Lanerolle, L., Patchen, R.C., Aikman, F., 2011. The Second Generation Chesapeake Bay Operational Forecast System (CBOFS2): Model Development and Skill Assessment. NOAA Technical Report NOS CS 29, Silver Spring, MD.

Lin, Y.T., Schuettpelz, C.C., Wu, C.H., Fratta, D., 2009. A combined acoustic and electromagnetic wave-based techniques for bathymetry and subbottom profiling in shallow waters. Journal of Applied Geophysics. 68 (2), 203-218.

Mockus, V., 1972. Soil Conservation Service National Engineering Handbook, U.S. Department of Agriculture, Washington, D.C.

Montaldo, N., Mancini, M., Rosso, R., 2004. Flood hydrograph attenuation induced by a reservoir system: analysis with a distributed rainfall-runoff model. Hydrological Processes. 18 (3), 545-563.

Morales-Hernandez, M., Garcia-Navarro, P.,Burguete, J., Brufau, P., 2013. A conservative strategy to couple 1D and 2D models for shallow water flow simulation. Computers & Fluids. 81, 26-44.

Morrissette, D., 1979. In the Matter of Reestablishment of Water Levels for Lakes Monona and Waubesa, Dane County. Docket No. 3-SD-77-819.

Merian, J.R., 1828. Ueber die Bewegung tropfbarer Flüssigkeiten in Gefässen [On the motion of drippable liquids in containers, thesis in German. Basel: Schweighauser.

Olsen, N.R.B., Hedger, R.D. George, D.G., 2000. 3D numerical modeling of Microcystis distribution in a water reservoir, Journal of Environmental Engineering. 126(10), 949-953.

Onusluel Gul, G., Harmancioglu, N., Gul, A., 2010. A combined hydrologic and hydraulic modeling approach for testing efficiency of structural flood control measures. Natural Hazards. 54 (2), 245-260.

Pahl-Wostl, C., 2007. Transitions towards adaptive management of water facing climate and global change. Water Resources Management. 21, 49-62.

Peters, D.L., Buttle, J.M., 2010. The effects of flow regulation and climatic variability on obstructed drainage and reverse flow contribution in a northern River-Lake-Delta Complex, Mackenzie Basin Headwaters. River Research and Applications. 26 (9), 1065-1089.

Proudman, J., 1953. Dynamical Oceanography. London: Methuen. 117, 225 pp.

Roe, J., Dietz, C., Restrep, P., Halquist, J., Hartman, R., Horwood, R., Olsen, B., Opitz, H., Shedd, R., Welles, E., 2010. NOAA's Community Hydrologic Prediction System. 2nd Joint Federal Interagency Conference. Las Vegas, NV.

Schmalz, R.A., 2011. Three-Dimensional Hydrodynamic Model Developments for a Delaware River and Bay Nowcast/Forecast System. NOAA Technical Report NOS CS 28, Silver Spring, MD, 199pp.

Schwab, D.J. Bedford, K.W., 1995. Operational three-dimensional circulation modeling in the Great Lakes. Computer Modeling of Seas and Coastal Regions II. 2nd International Conference on Computer Modelling of Seas and Coastal Regions Location: Cancun, 387-395.

Sherman LK., 1932. Streamflow from rainfall by the unit hydrograph method. Engineering News Record. 108, 501–505

Steinebach, G., Rademacher, S., Rentrop, P., Schulz, M., 2004. Mechanisms of coupling in river flow simulation systems. Journal of Computation and Applied Mathematics. 168, 459-470.

Sturm, T.W. 2001 Open Channel Hydraulics. McGraw-Hill, New York.

Teng, J., Vaze, J., Dutta, D., Marvanek, S., 2015. Rapid inundation modeling in large floodplains using LiDAR DEM. Water Resources management. 29, 2619-2636.

Tsihrintzis, V.A., John, D.L., Tremblay, P.J., 1998. Hydrodynamic Modeling of Wetlands for Flood Detention. Water Resources Management. 12 (4), 251-269.

Tsihrintzis, V.A., Madiedo, E.E., 2000. Hydraulic resistance determination in marsh wetlands. Water Resources Management. 14, 285-309.

Twigt, D.J., De Goede, E.D., Zijl, F., Schwanenberg, D., Chiu, A.Y.W., 2009. Coupled 1D-3D hydrodynamic modelling, with application to the Pearl River Delta. Ocean Dynamics. 59(6), 1077-1093.

Webster, I.T., Maier, H., Baker, P., Burch, M., 1997. Influence of wind on water levels and lagoon-river exchange in the River Murray, Australia. Marine and Freshwater Research. 48 (6), 541-550.

Wei, E., Zhang, A., 2011. The Tampa Bay Operational Forecast System (TBOFS): model development and skill assessment. NOAA Technical Report NOS CS 30, Silver Spring, MD, 119pp.

Weisberg, R.H., Zhen, L.Y., 2006. Circulation of Tampa Bay driven by buoyancy, tides, and winds, as simulated using a finite volume coastal ocean model. Journal of Geophysical Research. 111 (C1), C01005.

Yen, B., Lee, K.T., 1997. Unit hydrograph derivation for ungauged watersheds by stream-order laws. Journal of Hydrologic Engineering. 22 (1), 925-933.

YLAG2, 2012. Yahara Lakes Water Level Advisory Group. https://www.countyofdane.com/lwrd/landconservation/ylag.aspx.

3. Sustainability Assessment of Flood Risks for a River Chain of Lakes

The following is in preparation to be submitted to *Science of the Total Environment*.

3.1 Introduction

Flooding has devastating consequences that can impact the environment, the economy, and society across the world (Dottori et al., 2018). Among the natural disasters, flooding accounts for 24% of deaths (CRED, 2019), prompts evacuation of people (Simonovic and Ahmad, 2005), and makes millions of people homeless (Faganello and Attewill, 2005). From the environmental aspect, high water levels and elevated flow velocities due to flooding can dislodge hazardous storage tanks, rupture underground gas pipelines, and disrupt water purification or sewage disposal systems (Schmidt, 2000). Runoff from flooding can transport nutrients and contaminats, which can threaten human health (Albering et al., 1999; Konat and Kowaleska, 2001; Sarria-Villa et al., 2016) and impact aquatic integrity for fish and other aquatic species (Aborgiba et al., 2016). From the economic aspect, flooding can cause damage to infrastructure (Petit-Boix, et al., 2017), reduction in tourism and business (Chatterton et al., 2010, Holmes et al., 2010), destruction to roads and transportation (Kubal et al., 2009), and a decrease in agricultural productivity (Posthumus et al., 2009). In 2018, $90.5 US billion of economic loss was caused by storms and flooding (CRED, 2019). From the societal aspect, some governments and communities seeking for financial assistance to cope with flooding resulted in debt that took decades to repay (Grahn and Nyberg, 2014). Countries diverting vital resources to flood relief have set back their own economic growth (Loayza et al., 2012). In view of the consequences of flooding, a holistic approach to flooding is crucially needed.

Sustainability assessment for flooding, critical for the stability, progress, and wellbeing to benefit communities, consists of three steps (The National Academies, 2012). First, hazards (e.g., rainfall) with flood probabilities are determined. Second, flood vulnerabilities (e.g., buildings, roads, land) are characterized. Third, risk or loss due to flood are evaluated through the three aspects of sustainability including environmental, economic, and social perspectives (UNCED, 1992). Specifically, environmental assessment of flood risk considers metrics such as inundation area (Snoussi et al., 2007), landscape changes (Brouwer and van Ek, 2004), pollutants (Krüger et al., 2005), and habitat and biodiversity loss (Apel et al., 2004). Economic assessment of flood risk evaluates financial losses to building property and utility infrastructure (Meyer et al., 2009; Kubal et al., 2009). Social assessment of flood risk focuses on health and psychological effects (Brouwer and van Ek, 2004; Tapsell et al., 2002); injuries to people (Hall and Solomatine, 2008); and population estimates exposed to flood risk (Johnson et al., 2007b; Middelkoop et al., 2004) that can affect people and their wellbeing and livelihood (Hall and Solomatine, 2008). Several methodologies for holistic sustainability assessment for flooding such as optimization (Fu, 2008; Malekmohamma de et al., 2011), ranking (Vaidya and Kumar, 2006; Li et al., 2011), and goal-orientated acceptability (Behzadian et al, 2012; Lee et al., 2015), etc., have been implemented in rivers (Ahmadisharaf et al., 2017; Edjossan-Sossou et al., 2014; Lee et al., 2018), coast areas (Harwell, 1998; McGahey et al., 2009), and lakes (Harvey et al., 2009; Chen et al., 2017). To date, no study on sustainability assessment of flooding in river chains of lakes has been reported in the literature, as far as the authors are aware.

Flooding in a river chain of lakes (RCL), defined as a series of lakes connected with rivers with or without hydraulic structures (Reimer and Wu, 2016), is one of the most demanding issues due to competing environmental, economic, and social interests as evident in the Yahara RCL

(Capital Times, 2018). For example, controlling water levels in a RCL during flooding is often contested among municipalities or entities within in each individual lake to the whole connected lakes (Wisconsin State Journal, 2018a) from environmental, economic, and social perspectives. Due to various characteristics of watersheds in a RCL system, rainstorm induced runoffs entering into each distinct lake can yield water level rise at different rates. In the connected rivers between lakes, discharge or conveyance capacity can be limited due to increased resistance of seasonal aquatic plant density (Kowen and Fathi-Moghadam, 2000; Green, 2005) and backwater effect caused by the downstream lake water level, bridge constriction, or hydraulic control structure (Hunt et al., 1999; Kaatz and James, 1997). Recently, an Integrated Nowcast, Forecast Operation System (INFOS), developed by Reimer and Wu (2016), was employed for managing water levels in the Yahara RCL system and to cope with flood hazards (Isthmus, 2007). Nevertheless, regulating water level within the targeted range for each lake during flooding are continuously challenging and even controversial to meet both social and economic concerns (Nyberg et al., 2014). To date, no study on sustainability assessment of flood risks for RCL systems has been reported in the literature, as far as the authors are aware.

The objective of this paper is to present sustainability assessment of flood risks from environmental, social, and economic perspectives in a river chain of lakes. Specifically, the flood risk assessment framework consists of six components including data compiling, modeling, mapping, risk calculation, loss estimating, and sustainability assessment. A stochastic storm transposition tool is employed to generate 35 rainfall scenarios comprising of 7 return periods (1, 10, 25, 50, 100, 250, and 500 year) and 5 rainfall durations (2, 4, 6, 8, and 10-day). Environmental, social, and economic impacts and their associated flood risk are determined for individual and the entire lakes with their competing outcomes emphasized. At last, the importance of rainfall duration

and actions to improve flood resiliency are discussed for individual and all lakes within a RCL system.

3.2 Methods

3.2.1 Study site

The Yahara RCL, spanning 28.5 kilometers in length in Dane County, Wisconsin, consists of a series of lakes including Cherokee, Mendota, Monona, Wingra, Upper Mud, Waubesa, Lower Mud, and Kegonsa (Fig 3-1). Water from the Yahara River enters Lake Cherokee and flows through the narrow river at Highway 113 Bridge.to Lake Mendota. The Tenney Dam consisting of two 3.7-meter wide tainter gates and one lock chamber was built in 1847 on the east side of Lake Mendota to raise the lake water level of 1.4 meters. Lake Monona surrounded by an urban watershed is vulnerable to flooding due to the input of water from upstream Lake Mendota and stormwater runoff. Water continuously flows through a relatively flat bottom gradient (i.e. slope is less than 0.004%) of an uncontrolled natural channel to the Upper Mud Lake consisting of a large wetland complex and a narrow cross section of Railroad Trestle at the outlet to Lake Waubesa. Babcock Dam consisting of two automated sluice gates, two stoplog weirs, and one lock chamber is located at the downstream of Lake Waubesa to regulate water discharge to the Lower Mud Lake river-wetland corridor. Previous study (Reimer and Wu, 2016) showed that several features including a Native American fish weir, historic sunken corduroy bridge, and seasonal aquatic vegetation growth within the Lower Mud Lake River corridor could cause flow choking and inhibit water delivery to Lake Kegonsa. At last, the LaFollette Dam consisting of one automated sluice gate, two stoplog weirs, and one lock chamber is located at the outlet of Lake Kegonsa to regulate flow out of the Yaraha RCL system.

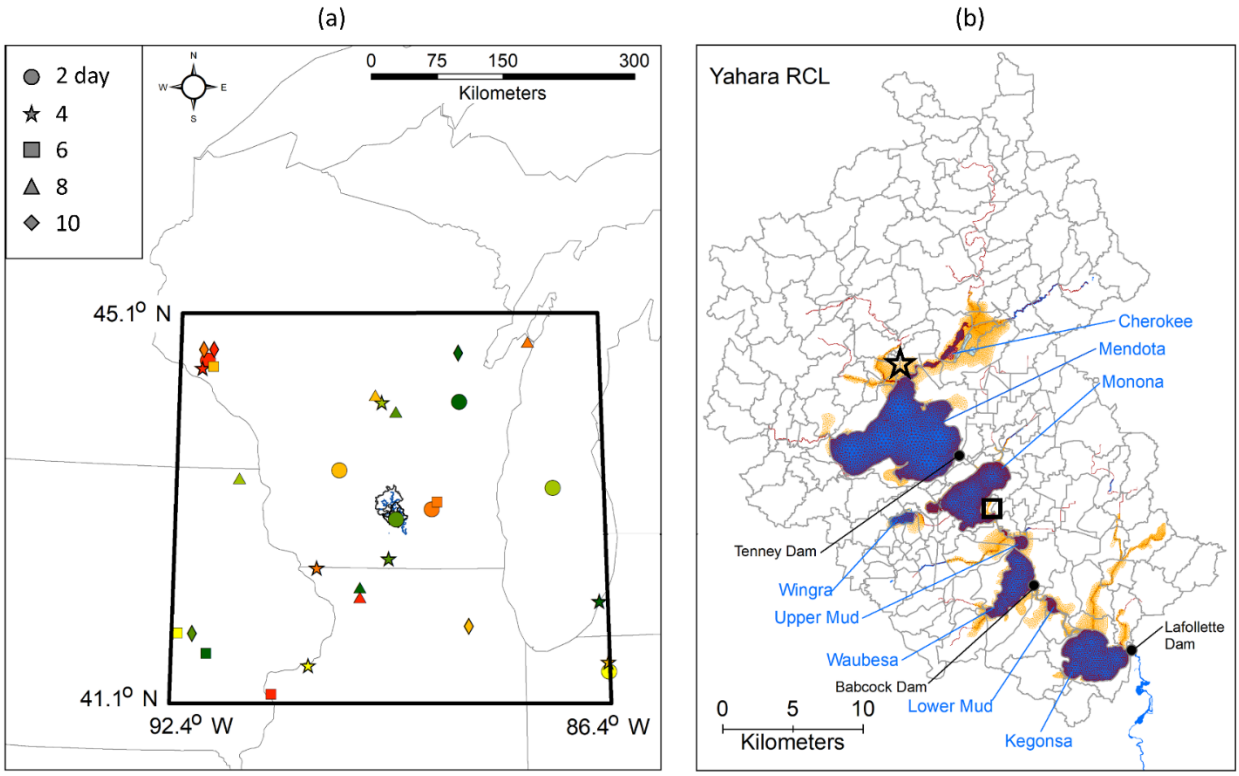

Fig 3-1. (a) The study site is located in Wisconsin, United States (left). The black bounding box represents the stochastic storm transposition domain. Colors of the symbols represent the locations of the 1 (dark green), 10 (green), 25 (light green), 50 (yellow), 100 (orange), 250 (dark orange), and 500 (red) year return periods. The 2-day (circles), 4-day (stars), 6-day (squares), 8-day (triangles), and 10-day (diamonds) storm durations are denoted (b) The Yahara River Chain of Lakes (right) shows the sub watershed boundary (gray and hydraulic model grids of water (dark red) and overland (orange).

Over the last century, the Yahara RCL experienced frequent flooding events (Reimer et al., 2019). Since 1916, the top ten highest recorded water levels of Lake Mendota occurred in years 2000, 2008, 2018, 1993, 1959, 2007, 2004, 1980, 1978, and 1996. Seven of the top ten floods occurred in the past 25 years. The two recent floods, June of 2008 and August of 2018, resulted in property damage and infrastructure loss that were estimated approximately $35.8 Million and $154 Million USD, respectively (DC Emergency Management, 2018). As a result, flooding in the Yahara RCL has been the top concern for the communities (Channel 3000, 2018; Wisconsin Public Radio, 2018; Wisconsin State Journal, 2018b)

3.2.2 Flood risk assessment framework

The framework of flood risk assessment for the RCL, shown in Fig 3-2, consists of six components. First, data is compiled in three main databases: rainfall hazard, land information (digital elevation model, soils, and use), and building asset. Second, flood vulnerability modeling employs an integrated hydrologic-hydrodynamic model (Arnold et al., 1998, Reimer and Wu, 2016) to simulate water level inundations on the Yahara RCL under a range of rainfall occurrence conditions. Third, a Geographic Information System (GIS) is used to map flood inundation areas and damage locations over the Yahara watershed. Fourth, economic loss of buildings and social loss of people displaced are estimated using Hazus. Fifth, flood risk is calculated by the product of the probability of a given rainfall hazard and estimated loss. Lastly, sustainability assessment is performed using analytic hierarchy process. Details of each component is described in the following sub-sections.

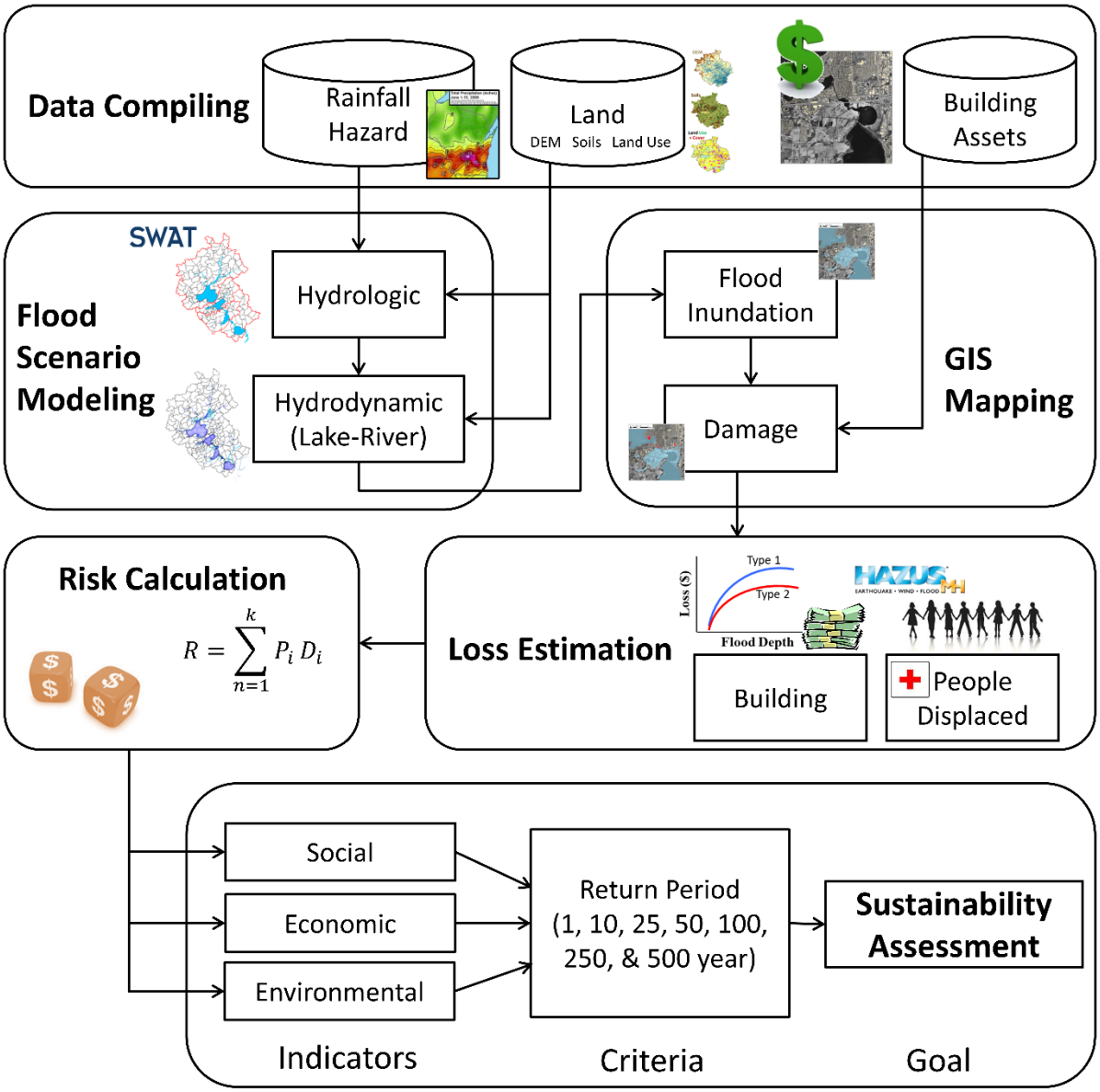

Fig 3-2. Flood risk assessment framework consisting of six components including data compiling, flood scenario modeling, GIS mapping, Loss estimation, risk calculation, sustainability assessment.

3.2.2.1 Data Compiling

Datasets for flood risk assessment can be classified into three types. First, the rainfall dataset is used an input to a hydrologic model to generate runoff hydrographs. Rainfall hazards can be characterized by point precipitation frequency analysis like NOAA ATLAS 14 (Stedinger et al., 1993, Perica et al., 2013), deterministic storm transposition with probabilistic storms of exceedance probability and uncertainties (Merz et al., 2008; Nicholas et al., 2017), and stochastic storm transposition (Wright et al., 2017). Previously, a deterministic storm transposition was conducted by transporting the preserving intensity and timing of rainfalls from an event occurring approximately 50.5 km north-west in Baraboo, WI (329.9 mm) in 2008 to the Yahara RCL system (Hayden et al., 2016). In this study, we employ a stochastic storm transposition approach for the purpose of creating a dataset with various rainfall durations and return periods for evaluating flood risks. Specifically, the RainyDay toolkit (Wright et al, 2017) is utilized that combines 2002-2017 rainfall data from Stage IV radar (Lin and Mitchell, 2005) with rain gages, satellite rainfall estimates from the National Weather Service Next-Generation Radar network (Crum and Alberty, 1993). Table 3-1 shows a total of 35 rainfall scenarios comprising 7 return periods (1, 10, 25, 50, 100, 250, and 500 year) and 5 rainfall durations (2, 4, 6, 8, and 10-day) with the cumulative rainfall amounts (in mm). Fig 3-1a shows generated rainfall data with the specified colors for return periods and shapes by durations over an area of 4km x 4km (see the black box with latitude and longitude coordinates).

Table 3-1. Cumulative rainfall (in millimeters) from 35 scenarios of various return periods and rainfall durations.

Return Period (years)	Rainfall Duration (days)				
	2	**4**	**6**	**8**	**10**
1	13	13	17	8	16
10	103	120	136	149	162
25	142	157	166	192	198
50	172	192	189	227	229
100	204	217	221	249	267
250	264	286	241	272	329
500	288	337	252	293	346

Second, a land dataset, consisting of elevations, soils, and land use is used for hydrological and hydraulic models to delineate watersheds, determine water flow paths, configure computational mesh extents, generate runoffs, and map vulnerable areas susceptible to flooding. Specifically, a digital elevation model (DEM) data is created by merging land topography measured from LIDAR with a vertical root mean square error of 24.7 cm at 95% confidence interval (Ayres Associates, 2010) and underwater bathymetry measured from an acoustic sub-bottom profiler with a vertical resolution of 1.8 cm, within 1% of the measurement range (Lin et al., 2009). Soil texture classifications and soil hydrologic groups are compiled from the Soil Survey Geographic (SSURGO) database. Land use data including mapped areas of agriculture, airport, commercial, industrial, residential, roadway, utility, and wetland are obtained from the Soil Survey Geographic database (NRCS).

Third, a building asset dataset is used to estimate loss based upon inundation depths (FEMA, 2018). Specifically, we use an inventory created by the Capital Area Regional Planning Commission in 2010 (CARPC, 2020). Based upon a Geographical Information System (GIS),

identified building footprints are classified into residential, industrial, commercial, and agricultural types. In addition, identified building footprints categorized into different foundation type (basement, crawlspace, and floor slab) and exterior siding types (wood, brick, vinyl, composite) that are joined with tax records to provide economic damage to buildings.

3.2.2.2 Flood vulnerability modeling

Flood vulnerability are assessed by common methods like empirical-based interpolation models and physically-based hydraulic models for quantifying the extent of flood inundation (Apel et al., 2009). Based upon simulated water level inundation, physical stage-damage functions and environmental impacts can be obtained (HEC, 1998, Smith, 1994). In this study, an integrated hydrologic model for watershed runoff and a hydraulic-hydrodynamic model for river flows and lake water levels in the Yahara RCL system are employed to obtain flood outcomes of 35 stochastic rainfall scenarios. The Soil and Water Assessment Tool (SWAT) model (Montgomery Associates, 2011; Neitsch et al., 2002) with a total of 201 subwatersheds ranging from 1 to 40 square kilometers (see Fig 3-1) were created to simulate watershed hydrology for overland, tributary, and channel flow. DEM data of 3 meter horizontal spacing is used to delineate flow paths of perennial and intermittent streams. Land use and cover data are used to estimate model parameters such as curve number and overland flow Manning's roughness. To calculate infiltration, the Green-Ampt model based on 1-hour rainfall input and channel routing with an hourly time step is used (Arnold, 1998). Overall, the SWAT hydrologic model yields an amount of water discharge (i.e., runoff hydrographs), which is used to the input to the hydraulic-hydrodynamic model.

A hydraulic-hydrodynamic model, implemented by Reimer and Wu (2016), is used to calculate river discharges and lake levels for the Yahara RCL. The model is based upon the Finite

Volume Coastal Ocean Model (FVCOM, developed by Chen et al. 2003) that solves the governing equations are the continuity equation, momentum equation, and temperature equation under hydrostatic pressure assumption. Fig 3-1b shows the unstructured meshes containing 21,965 elements and 12,925 nodes in the Yahara RCL, determined from bathymetry data and DEM topography with the 500-year floodplain. The meshes connect the water surface including the river chain of lakes and land surfaces for the floodplain, as shown in blue/red and orange color areas, respectively, in Fig 3-1b. The multi-scale of meshes with smaller sizes (~ 3m) in rivers and larger sizes (~100 m) in lakes are designed to accurately represent river hydraulics and reliably characterize lake surge and circulation (Reimer and Wu, 2016). The flooding/drying technique (Chen et al. 2008) is employed to simulate flood inundation area.

3.2.2.3 Flood mapping

To map flood area in the Yahara RCL, we use a Geographical Information System (GIS) based upon the horizontal datum North American Datum of 1983 (NAD83) and vertical datum called National Geodetic Vertical Datum of 1929 (NGVD29). The flood vulnerability map includes infrastructures and properties susceptible to overland flood inundation, damaged buildings associated with magnitude of loss to aid in mitigation strategies, building relocations, development restriction areas, and communications for increasing public awareness of flood risks (Jalayer et al., 2014). Additional layers of map include land use, transportation (streets, bike paths, bus routes), and utilities (water, sanitary, and storm water) to assess economic and social impacts. For example, transportation impacts include street closures that could hinder emergency service response such as fire or ambulance services. Utility service outages impact includes drinking water or sewer backups in basements causing further economic and health risks. The flood mapping data

combined with additional layers provide sustainability assessment of flood risks to address environmental-social-economic impacts.

3.2.2.4 Flood risk calculation

Flood risk including inundation impact, economic impact due to financial loss to buildings, and social impact due to temporary displacement of people is calculated. Specifically, risks for the 35 rainfall scenarios are obtained by multiplying the probability (return period) with economic (USD) and social loss, i.e. people displaced with the purpose of examining the most at risk for future planning efforts. A large risk can arise from a high probability of a flood with only minor vulnerabilities or a small probability of a flood (e.g. 500 year) with high vulnerabilities (National Academies, 2000) such as near populated areas of the isthmus area in downtown Madison. Due to spatial variability in vulnerabilities (people and buildings), flood risk for individual lake (Mendota, Monona, Waubesa, and Kegonsa) on the Yahara RCL is calculated and compared.

3.2.2.5 Loss estimate

Flood loss for social and economic impacts is characterized using HAZUS-MH, a multi-hazard risk assessment and loss estimation software program developed by Federal Emergency Management Agency (FEMA) in collaboration with the National Institute of Building Sciences (Smith, 1994; Scawthorn et al., 2006; Schneider et al., 2006; Remo et al., 2016; FEMA, 2018). Specifically, more than 900 damage curves relating inundation depth to loss have been provided by FEMA and US Army Corps of Engineers (FEMA, 2018). In this paper, the default damage curves developed in Hazus-MH (Schneider and Schauer, 2006) are applied to estimate losses for all rainfall scenarios. Damage loss estimate is determined by the multiplication of percent damaged

within census block (Remo et al., 2016) and user supplied buildings (Scawthorn et al., 2006) with weighted by the area of inundation for an average flood depth. Note that the composition of the building stock within a given census block is commonly assumed to be evenly distributed throughout the block (FEMA, 2018). Nevertheless, higher valued buildings are generally located adjacent to lakes and rivers for the Yahara RCL. We employ spatially defined building locations and associated economic data. Loss for the number of individuals who need short-term shelter and to be evacuated is calculated by the number of displaced people and not on the degree of damage to structures (Scawthorn et al., 2006). Flood damages for each building is determined and aggregated within a 1 kilometer radius. Specifically, the expected annual damage (EAD), defined as yearly flood damage times the probabilities occurring at all return periods (Dierauer et al., 2012; Guida, et al., 2016), and is

$$EAD = \int_0^1 D(p)\,dp \quad (1)$$

where D is flood damage loss in 2018 US dollars and p is the probability of the corresponding rainfall event. In this study, the EAD is calculated for two limiting the return periods: 100 year (probabilities of 0.1, 0.04, 0.02 and 0.01) and 500 year (probabilities of 0.1, 0.04, 0.02 and 0.01, 0.004 and 0.002) for comparison.

3.2.2.6 Sustainability assessment

In this study, the analytic hierarchy process (AHP) by Saaty (1980) is employed to the Yahara RCL. The AHP has three main levels including indicators (social, economic, environment), criteria (return period), and goals of sustainability assessment, as shown in Fig 3-2. The criteria in the AHP is determined using return period. A pairwise comparison matrix is conducted as shown in Table 3-2 with judgement values ranging from 1 to 9 where a higher number indicates that return

period is considered more important. The matrix is designed where it is more important to consider sustainability impacts at lower (e.g. 10 year) versus higher (e.g. 500 year) return periods because they are more likely to occur. For example, comparison of 10 year (.1) and 500 year (0.002) yields a value of 50 (1/0.002) which is normalized to 6.04 using the formula Cij=1.2873*ln(RPi/RPj)+1, where where Cij is the judgement value of the criterion in the pairwise comparison matrix and RP is the return period. Other literature has reported consistency concerns when developing the pairwise matrix when there are three or more criteria (Maiolo & Pantusa, 2018; Piengang, Beauregard, & Kenné, 2019; Sarmiento & Vargas-Berrones, 2018). To address this concern, a Consistency Ratio (CR) is calculated to show if judgements in the pairwise comparisons are appropriate. If CR exceeds 0.1, the set of judgements may be too inconsistent to be reliable. Otherwise, if the CR is less than 0.1, then the comparison matrix can be considered to have an acceptable consistency.

Table 3-2. AHP matrix judgements, criteria weights (PV), and consistency measure (CM).

	1year	10year	25year	50year	100year	250year	500year	Sum	PV	CM
1year	1.00	3.96	5.14	6.04	6.93	8.11	9.00	40.18	0.45	7.67
10year	0.25	1.00	2.18	3.07	3.96	5.14	6.04	21.65	0.20	7.53
25year	0.19	0.46	1.00	1.89	2.78	3.96	4.86	15.15	0.13	7.32
50year	0.17	0.33	0.53	1.00	1.89	3.07	3.96	10.95	0.09	7.16
100year	0.14	0.25	0.36	0.53	1.00	2.18	3.07	7.54	0.06	7.06
250year	0.12	0.19	0.25	0.33	0.46	1.00	1.89	4.25	0.04	7.07
500year	0.11	0.17	0.21	0.25	0.33	0.53	1.00	2.59	0.03	7.18
Sum	1.99	6.36	9.67	13.11	17.35	24.00	29.82		1.00	

The CR is calculated from three steps. First, the consistency measure (CM) is calculated by multiplying PV (Equation 3) by the weighted sum of the normalized criteria weights and is provided in Table 3-2.

$$X_{ij} = \frac{c_{ij}}{\sum_{i=1}^{n} c_{ij}} \quad (2)$$

$$PV_{ij} = \frac{\sum_{j=1}^{n} X_{ij}}{n} \quad (3)$$

where Cij is the value of the criterion in the pairwise comparison matrix, Xij is the normalized score, PVij is the priority vector of a criteria. Second, the consistency index (CI) is calculated as described in equation 4 where λmax is the sum of CM divided by n which equals 123.

$$CI = \frac{(\lambda_{max-n})}{(n-1)} \quad (4)$$

Third, the consistency ration (CR) is determined by dividing the consistency index by the random index (CI/RI). Since the number of criteria in this study is 7, the RI is 1.32 as given by Saaty (1980).

$$CR = \frac{(\lambda_{max-n})}{(n-1)} \quad (4)$$

In our study the CR is found to be 0.04 which indicates a reasonable level of coherency in the pairwise comparison.

Three indicators of social, economic, and environment were evaluated in the AHP using the results of the flood risk calculation. Specifically, four criteria for each indicator are created with judgement values ranging from 1 to 4 where a higher number means that the chosen risk is considered more important than the other risk used in the comparison. The AHP provides outputs of importance of each sustainability and are compared by lake in the results. Also, comparisons are made for individual sustainability perspectives by lake.

3.3 Results

3.3.1 Rainfall hazards

Rainfall hazards to the Yahara RCL, characterized by stochastic storm transposition and statistical approaches, are presented here. Fig 3-3a shows the 35 scenarios of rainfall depth-frequency curves as in the gray bounds. Specifically, the 4-day (solid blue line) and 10-day (solid red line) of the RainyDay results are compared with those (dashed lines) obtained by the NOAA

Atlas 14, based upon L-moment regionalization techniques to combine with observations from 5 rain gages from 1896 to 2010 (Perica et al., 2013). For return periods less than 50-year, rainfall hazards based upon the RainyDay are lower than those based upon NOAA Atlas 14. Conversely, for return periods greater than 100-year, rainfall hazards by the RainyDay are higher, which may be attributed to increasing intense precipitation storm events in the last ten years (WICCI, 2020). Three rainfall observations are compared with the rainfall depth-frequency curves by NOAA Atlas 14 and the RainyDay. First, the 10-day rainfall depth in June 2008 storm in Madison was 267.2 mm, corresponding to close return periods: 96-year (crossing red solid line) by Rainy Day and 94-year (crossing red dashed line) by NOAA Atlas 14. Second, the same storm with higher 10-day rainfall in Baraboo was 329.9 mm, corresponding to a return period of 237-year (crossing red solid line) by RainyDay but a larger return-period of 413-year (crossing green dashed line) by NOAA Atlas 14. Third, the 4-day rainfall depth in July 2007 storm in Madison was 145.1 mm, corresponding to similar return periods: 19-year (crossing blue solid line) by Rainy Day and 14-year (crossing blud dashed line) by NOAA Atlas 14. In short, rainfall hazards obtained from the RainyDay of return periods less (more) than 50-year, are lower (larger) than those from NOAA Atlas 14. Furthermore, RainDay based upon stochastic storm transposition approach faithfully characterizes the rainfall hazards in the Yahrara RCL.

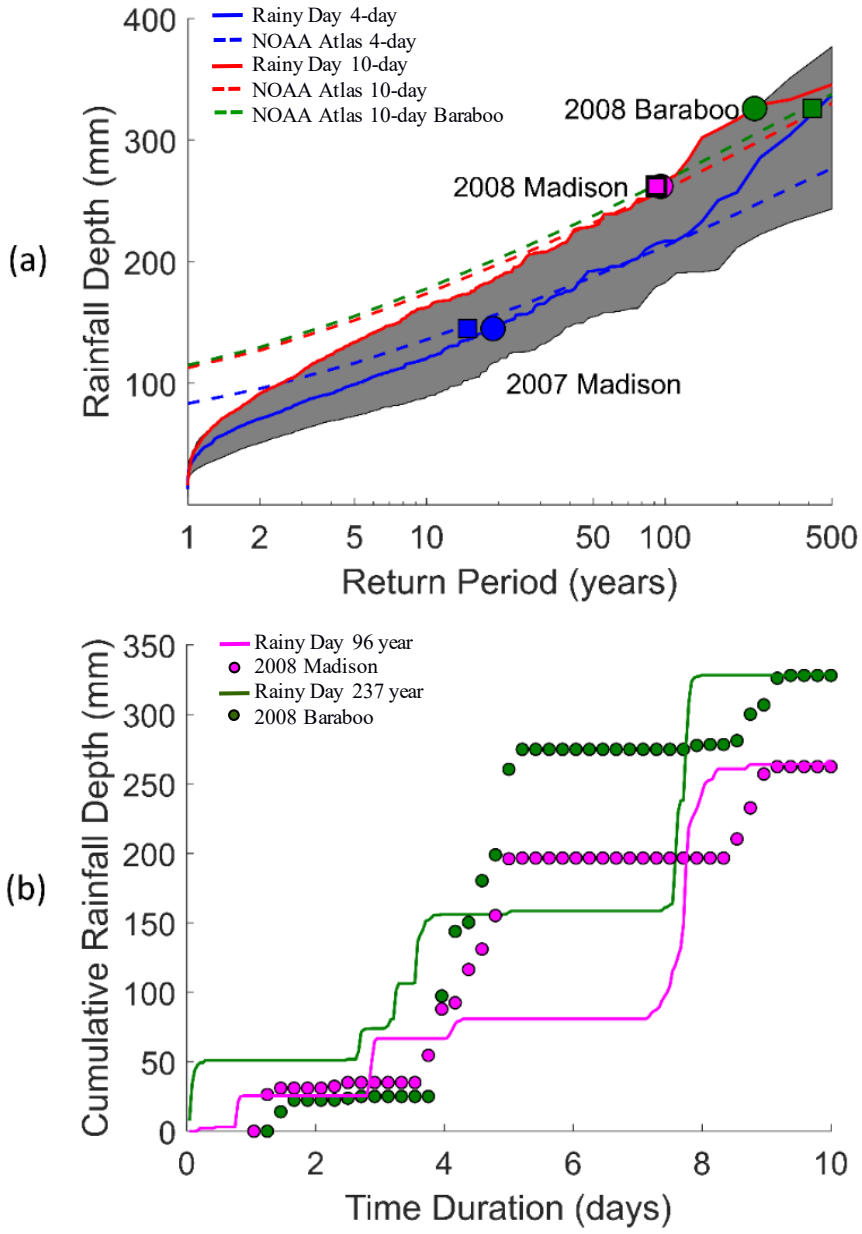

Fig 3-3. (a) The rainfall depth-frequency curves for the Rainy Day results for 1-day to 10-day rainfall duration shown in the gray bounds. Specifically, the 4-day rainfall duration (blue solid line) and 10-day duration (red solid line) is plotted to compare with NOAA Atlas 14, 4-day (blue dashed line) and 10-day duration (red dashed line). Most recently, large rainfall occurred in 2007 in Madison (blue), 2008 in Madison (magenta), and Baraboo (green) shown by square and circle markers. (b) Cumulative rainfall is compared for 2008 Madison (magenta circles) and corresponding Rainy Day 96 year return period results (magenta solid line). Also, 2008 Baraboo (green circles) and corresponding Rainy Day 237 year return period results (green solid line) is shown.

Cumulative rainfall over a specified duration obtained by the RainyDay are compared to observations of 2008 rainfall events in Fig 3-3b. Both cumulative rainfalls, RainyDay 96-year return period (solid magenta line) and 2008 rainfall observations in Madison (magenta circles), at day 10 are the same while the intensity and rainfall timing over the 10-day duration between the two are different. Comparable results can be seen in the RainyDay 237-year return period results (solid green line) and 2008 rainfall observations in Baraboo rainfall (green circles). Furthermore, results of the 2007 4-day duration of 2007 storm in Madison, not shown for brevity, are similar. Overall, cumulative rainfalls obtained by the stochastic RainyDay storm transposition toolkit for a given duration and return period represent total rainfalls but not the incremental rainfalls.

3.3.2 Flood inundation impacts

Inundation spatial extents and locations of building damage impacted by 100 and 500-year return periods over 4-day and 10-day durations of flood are depicted here. For urban areas around Lake Monona (see the square in Fig 3-1b), Fig 3-4a shows that the 100-year flood inundation extents (light orange) over the 10-day duration are slightly larger than those over the 4-day duration (light blue). Additional damaged buildings (yellow and red dots) caused by the 10-day flood duration are seen, compared to those (red dots only) over the 4-day duration. Fig 3-4b shows that the 500-year flood inundation extents (light orange) over the 10-day duration are nearly equal to those over the 4-day (light blue). Similar damaged buildings are seen for both 10- and 4-day inundation. In other words, extreme (e.g., 500-year) flood-induced inundation impacts on the highly urbanized Lake Monona areas are not sensitive to storm durations. Nevertheless, longer durations of 100-year floods are of concerns to inundation impacts on spatial extents and locations of building damage.

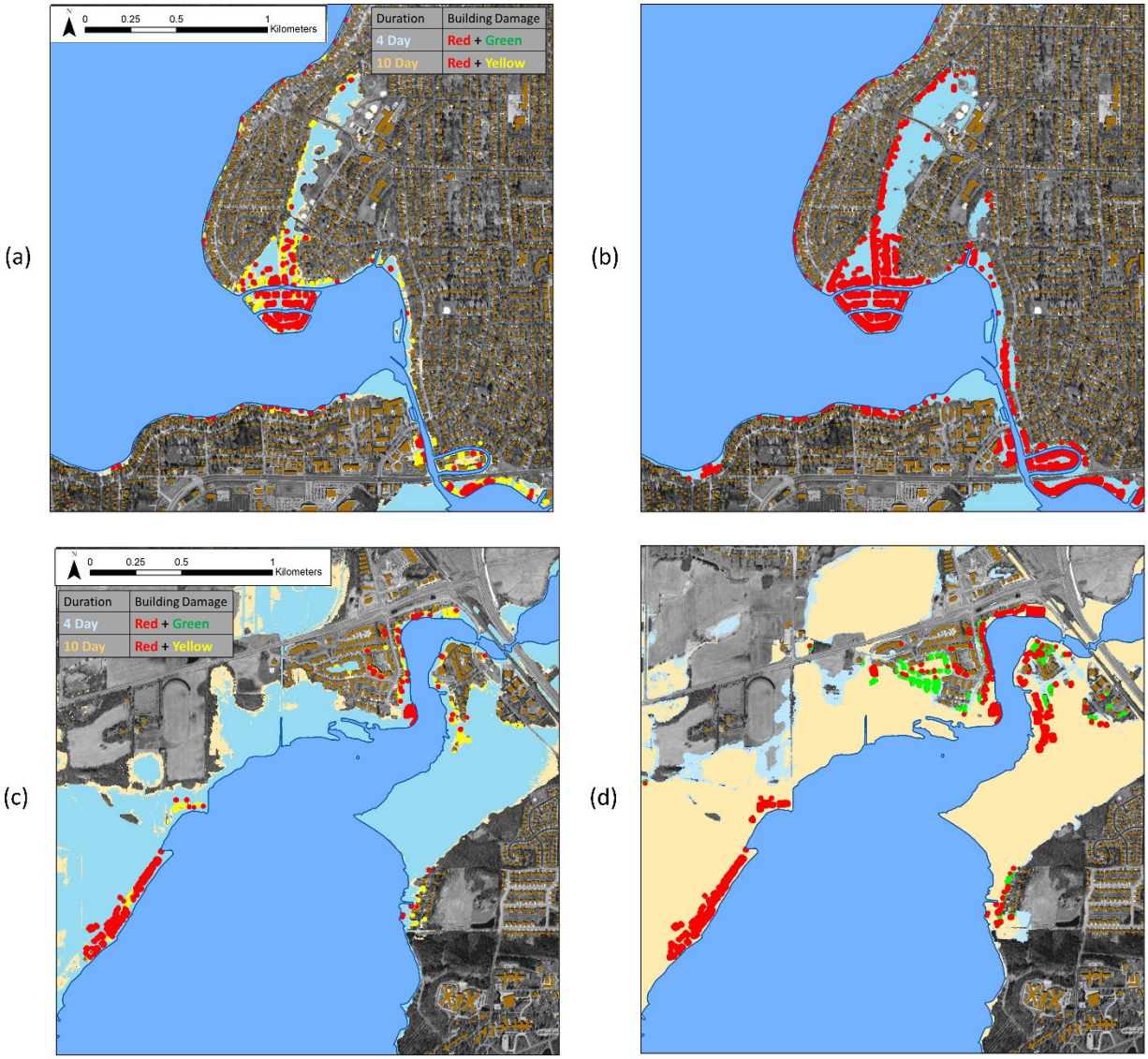

Fig 3-4. (a) Lake Monona 100 year flood inundation (light blue) and building damage locations (red) for 4-day rainfall duration in comparison to inundation (light orange) and building damage locations (red and yellow) for 10 day rainfall duration. (b) Lake Monona 500 year flood inundation (light blue) and building damage locations (red and green) for 4-day rainfall duration in comparison to inundation (light orange) and building damage locations (red) for 10 day rainfall duration. (c) Lake Mendota 100 year flood inundation (light blue) and building damage locations (red) for 4-day rainfall duration in comparison to inundation (light orange) and building damage locations (red and yellow) for 10 day rainfall duration. Shown in dark orange are building footprint locations. (d) Lake Mendota 500 year flood inundation (light blue) and building damage locations (red and green) for 4-day rainfall duration in comparison to inundation (light orange) and building damage locations (red) for 10 day rainfall duration.

For sub-urban areas like the entrance of Lake Mendota (see star in Fig 3-1b), similar results of flood inundation extents and damaged building are found to those of Lake Monona under the 100-year flood (Fig 3-4c). In contrast, Fig 3-4d shows the 500-year flood inundation extents (light blue) over the 4-day duration are larger than those over the 10-day duration (light orange). Additional damaged building locations (red and green dots) over the 4-day duration, in comparison with those over the 10-day (red dots only), are clearly seen. In other words, shorter durations of extreme (e.g. 500-year) flood-induced inundation impacts on sub-urban upstream areas of Lake Mendota are noted. Similar flood results are found in sub-urban areas in Lake Waubesa and Lake Kegonsa, not shown here for brevity. Overall, flood inundation impacts indicate that the importance of flood return periods and durations on inundation spatial extents and locations of building damage can vary depending on the urban and sub-urban areas on the Yahara RCL.

3.3.3 Social impacts

Social impacts due to flooding are assessed and examined. Fig. 4-5a shows inundation extents and various social vulnerabilities on the Madison isthmus area caused by the 500-year flood over the 4-day duration. Specifically, a large portion of the isthmus area is inundated (light blue), affecting homes and businesses access like flooded bus stops (red dots), bike paths (purple lines), and streets (satellite image) as well as threatening utility services such as sanitary pump stations (green dots), storm sewer manholes (magenta dots), and water hydrants (yellow triangles). The east side of Madison, in comparison with the west, is depicted to be more vulnerable to these social impacts.

Social vulnerabilities including land use types, transportation means, and utility services of all the Yahara RCL area (solid lines) and the Madison downtown area (dashed lines) due to the

4-day storm duration are quantified in Figs 4-5b, c, and d. In each figure, two flood return periods, 100-year (blue) and 500-year (red), are portrayed and compared. Fig 3-5b shows areas of land use type affected by flooding, measured in hectares. The shapes of two radar charts caused by the 100 and 500-year return period are similar except for different sizes of polygons, indicating that inundation areas of land use types increase with respect to larger return periods. Comparing all Yahara Lakes (solid lines) to Madison isthmus (dashed lines) for the same return period (e.g. 500-year, red), relative flood impacted areas of land use types are different. For example, areas of agriculture and woodland land use in all the Yahara Lakes, relative to the urbanized Madison isthmus, are more vulnerable to flood. Fig 3-5c shows lengths of transportation means like streets, bus routes, bike paths, and railroads affected by flooding, measured in kilometers. The transportation means are vulnerable to floods under 100-year and 500-year return periods except that railroads are of concerns for 500-year return period. Inundation lengths of transportation means of the all the Yahara Lakes (solid line) are much larger than those of Madison isthmus (dashed line), suggesting the importance of ensuring transportation means in flood assessment from the regional Yahara River watershed aspect. Fig 3-5d shows malfunction of utility services affected by flooding, measured in numbers. All utility services that can impact sewage to pose economic and health risks are susceptible to floods under 100-year and 500-year return periods. Specifically, numbers of stormwater conveyance systems are much larger than those of sanitary sewer networks. Numbers of impacted utilities between Yahara Lakes (solid lines) to Madison isthmus (dashed lines) are similar, indicating the emphasis of ensuring utility services under rainfall hazards in the urban Madison areas. In summary, vulnerabilities of land use types, transportation means, utility functions impacted by flood inundation of all the Yahara RCL area

and the Madison downtown area under 100- and 500 year return periods are examined and compared.

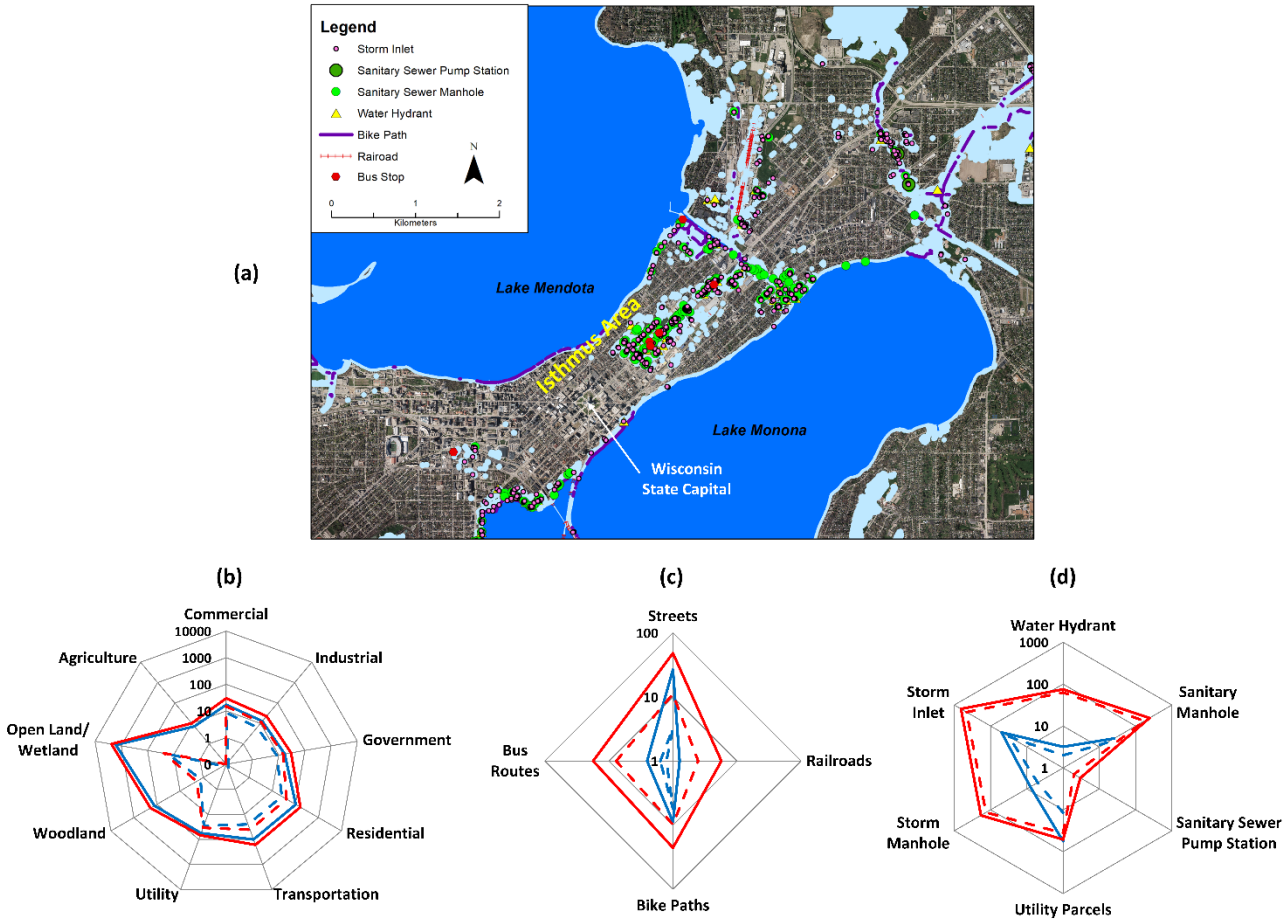

Fig 3-5. (a) Map of flood inundation (light blue) and vulnerabilities impacted. Radar charts showing vulnerabilities by (b) land use types in hectares, (c) transportation means in kilometers, and (d) malfunction of utility services in numbers. Four cases are presented showing the 500 (red) and 100 (blue) year return periods for Madison isthmus area (dashed line) and all Yahara Lakes (solid line).

Vulnerability of people evacuation on the Yahara RCL due to a range of flood return periods of the 10-day duration are compared. Fig 3-6a shows that numbers of people displaced are the highest in Lake Monona (red line), followed by Lake Mendota (blue line), Lake Waubesa (orange line), and Lake Kegonsa (green line). In comparison with the other three lakes, the rate of

people displaced on Lake Monona rapidly increases from 5 to 25-year return periods, indicating the importance of reducing flood inundations of these return periods in Lake Monona. Fig 3-6b shows the risk of people displaced among the four lakes. In particular, the highest risk occurs between 5-year and 25-year flood return periods; the risk of people displaced on Lake Monona is approximately 4, 7, 8 times greater than that of Lake Mendota, Lake Waubesa, and Lake Kegonsa, respectively. Overall, social impacts of land use types, transportation means, utility services, and people evacuation due to rainfall flood hazard are assessed and examined. The outcomes provide critical information to address social impacts for individual lake and the entire Yahara RCL.

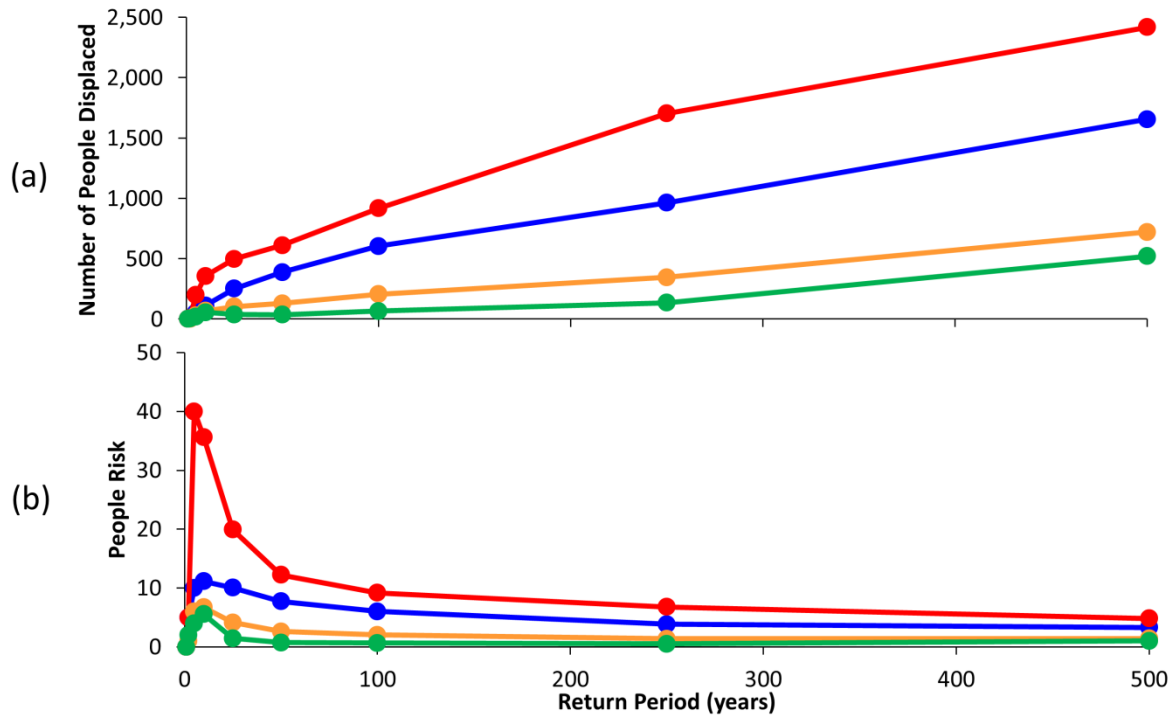

Fig 3-6. (a) Number of people displaced and (b) risk of people displaced versus return periods of the 10-day flood duration on Lakes Mendota (blue), Monona (red), Waubesa (orange), and Kegonsa (green).

3.3.4 Economic impacts

Risks of damaged buildings under the three return periods (10, 100, and 500-year) flooding on Lake Mendota (blue), Monona (red), Waubesa (orange), and Kegonsa (green) are assessed in Fig 3-7. For the 10-year return period (Fig 3-7a), economic risks of all lakes, i.e., $7,016 to $34,700, linearly increases five times as storm duration increases from 2 days to 10 days, indicating the importance of storm duration in economic risks. In comparison among the lakes, the risk of Lake Monona (red bar) for the 2 day storm duration is largest, suggesting that Lake Monona is more vulnerable to short-duration tense storms. For the 100-year return period (Fig 3-7b), the risks of all lakes increase with respect to storm duration. Nevertheless, risks of each lake tend to be similar under all storm duration. For the 500-year return period (Fig 3-7c), a trend of similar risks of each lake is seen but the economic risk of all lakes is nearly two times from $19,082 to $39,651, corresponding to 2 days and 10 days flood durations. The largest risk occurring under 10-day duration is $39,651, which is smaller than $42,479 for the entire Yahara RCL occurring under the 100-year return period with 10-day duration. Overall, for the Yahara RCL, an economic risk increases with longer storm durations, larger return periods, or combination of the two. Individually, Lake Monona (red bars) and Mendota (blue bars) experiences the largest risk at the 10 year return period ($20,924) and 500 year ($15,070), respectively. The assessment provides critical economic risks of entire Yahara RCL and individual lake susceptible to flooding.

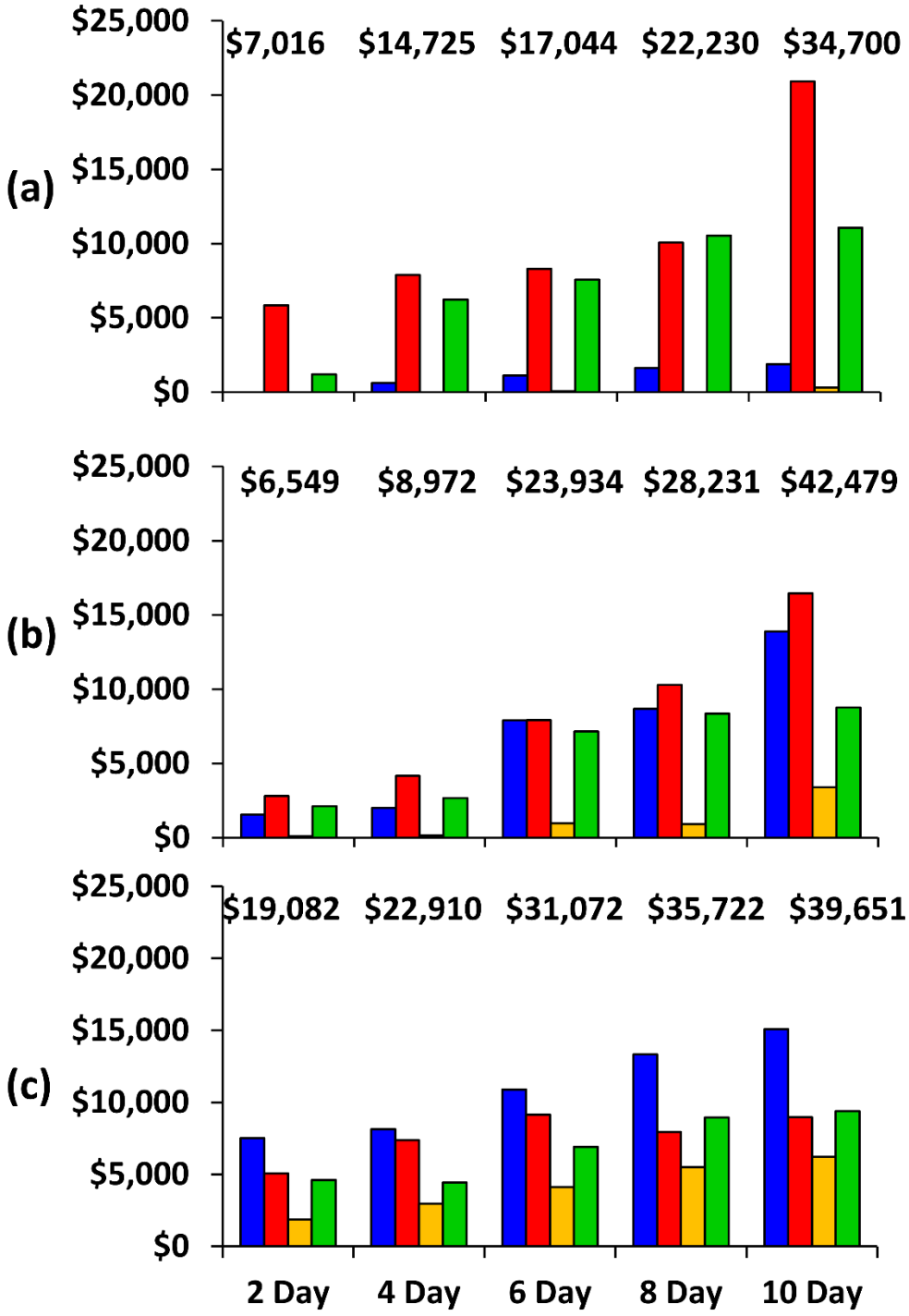

Fig 3-7. The risk of buildings is estimated for the (a) 10, (b) 100, and (c) 500 year return period. The colors blue, red, orange, and green represent Lakes Mendota, Monona, Waubesa, and Kegonsa, respectively. The risk in US Dollars of the sum of all lakes is displayed above each bar.

Spatial distributions of expected annual damage (EAD) for the entire Yahara RCL are assessed here. For the 500-year return period, Fig 3-8a shows that the largest EADs for Lake Monona, Lake Mendota, Lake Kegonsa, and Lake Waubesa are $147k, $45k, 41K, and 8k, respectively. The top two EADs occur at the two vulnerable locations: the urban area around Lake Monona and the sub-urban areas around Lake Mendota illustrated in Fig 3-4. In comparison, EAD of building on the Madison isthmus area is relatively smaller. From the whole lake perspective, the sums of EADs of each lake in the descending order are $190k (Lake Monona), 167K (Lake Kegonsa), 67K (Lake Mendota), and 27K (Lake Waubesa). The results provide the matrices for the priority to protect flood damage. If the 100 year return period is used to estimate EAD, Fig 3-8b shows that the EADs are smaller and the general spatial pattern of EADs (values greater than $10k) are similar. Nevertheless, EADs become zero at several vulnerable locations, e.g. Madison isthmus area of $5k, which can lead to underestimate of EADs. Therefore, the 500-year return period for estimating EAD is strongly recommended. Overall, the spatial distributions of EADs on each individual lake and the entire Yahara RCL provide information on locations for flood mitigation response during the floods.

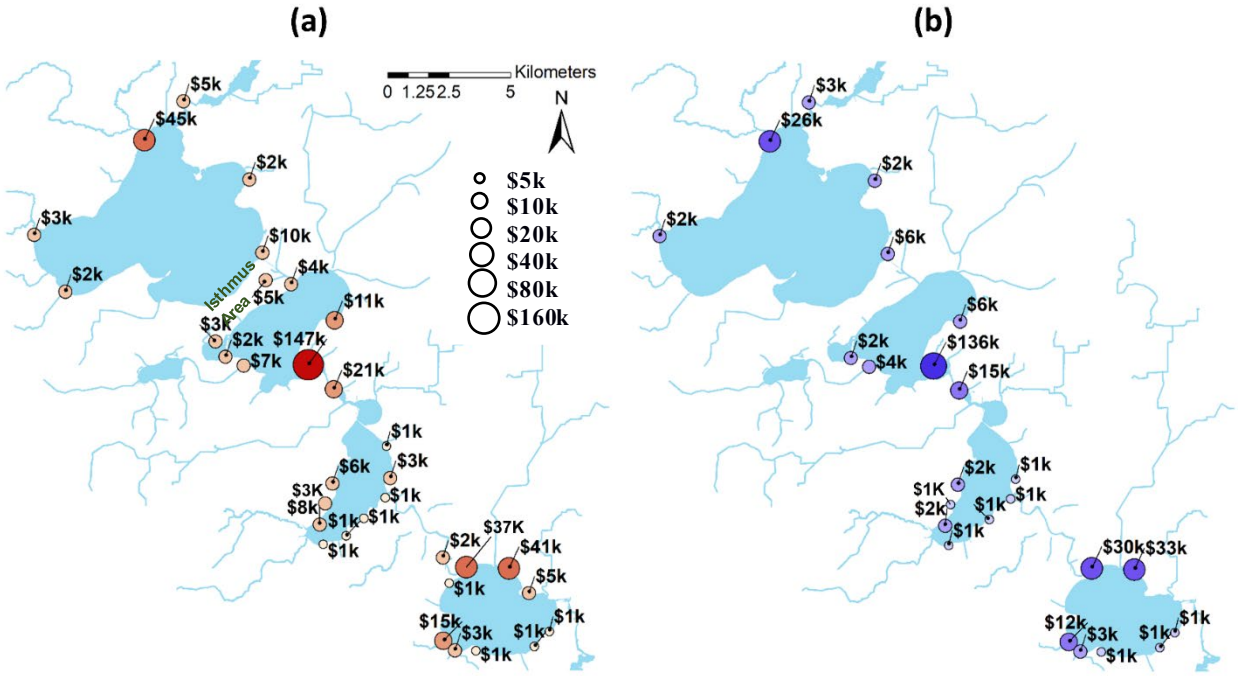

Fig 3-8. Spatial distributions of expected annual damage (EAD) that are aggregated within a 1 kilometer radius in $1,000 US dollars over the 10 day storm duration of the return periods of (a) 500 year and (b) 100 year.

3.3.5 Sustainability assessment

Sustainable assessment of three perspectives of social (people evacuation), economics (US dollars), and environment (area of inundation) are summarized by lake in Fig 3-9 using AHP. In Fig 3-9a, Lake Mendota is most at risk economically (0.40, light orange) as compared to social (0.33, light blue) and environment (0.28, light green). For Lake Monona, a similar order of perspectives are witnessed to that of Lake Mendota; however, there is greater economic risk. For Lake Waubesa (Fig 3-9c), the largest risk is witnessed to the environment which is different than lakes Mendota and Monona which showed the lowest impact. Environmental impacts on Lake Waubesa is mainly attributed to inundation on the southwest shore where the Waubesa Wetlands reside that are of high quality and diversity. Lake Kegonsa (Fig 3-9d) is most at risk economically

(0.43) followed by environment (0.31) and social (0.25). Overall we see a response of the three sustainability perspectives which have different sequences of risk impacts for each individual lake.

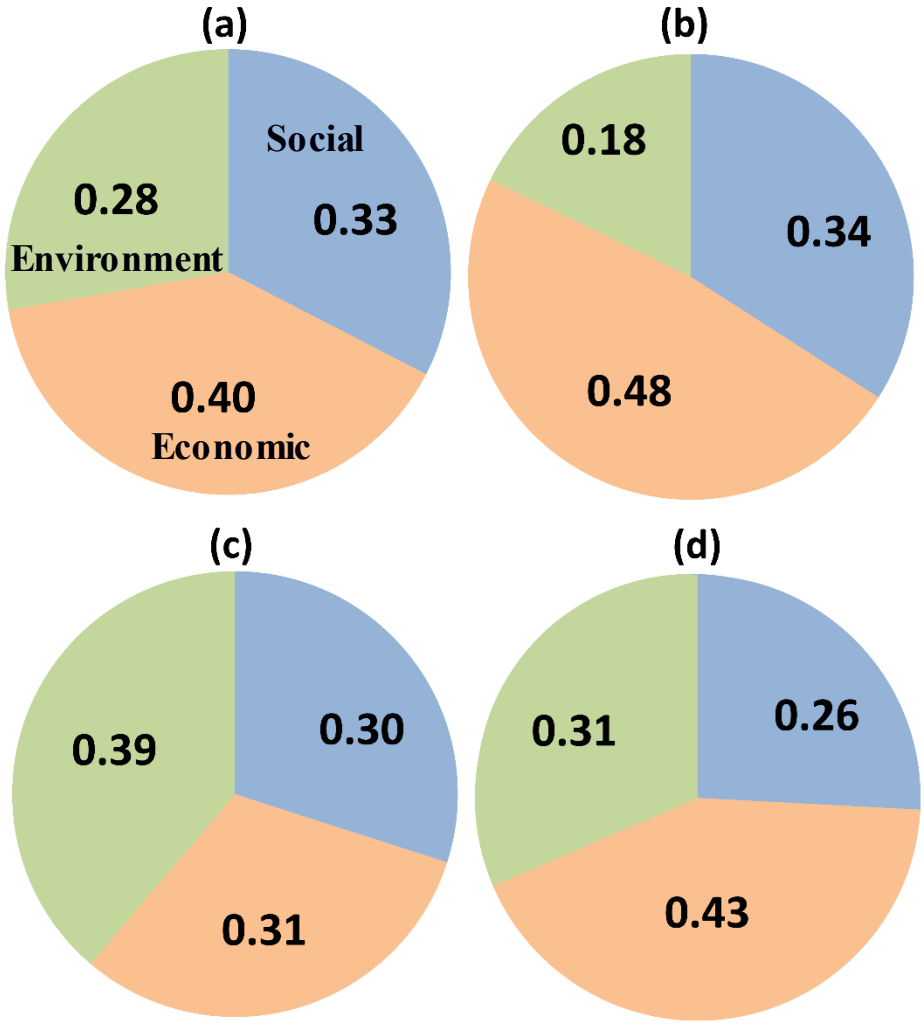

Fig 3-9. Comparison of social (light blue), economic (light orange), and environment (light green) risk for Lake Mendota (a), Monona (b), Waubesa (c) and Kegonsa (d).

To assess sustainability perspectives of social, economic, and environment differences between lakes, AHP results are shown in Fig 3-10. The largest social risk occurs on Lake Monona (0.40, red), followed by Lake Mendota (0.22, blue), Waubesa (0.20, orange), and Kegonsa (0.17, green). Similarly, economic risk on Lake Monona is nearly two times more than that of any other lake in the Yahara RCL. Lastly, environmental risks of inundation are pretty well balanced among lakes. Overall, Lake Monona is most at risk socially and economically than the other lakes and suggests flood mitigation efforts to improve Lake Monona would be beneficial. However, if management efforts are attempted to store and delivery flood waters on other lakes, that could result in negative affects socially, environmentally, and economically.

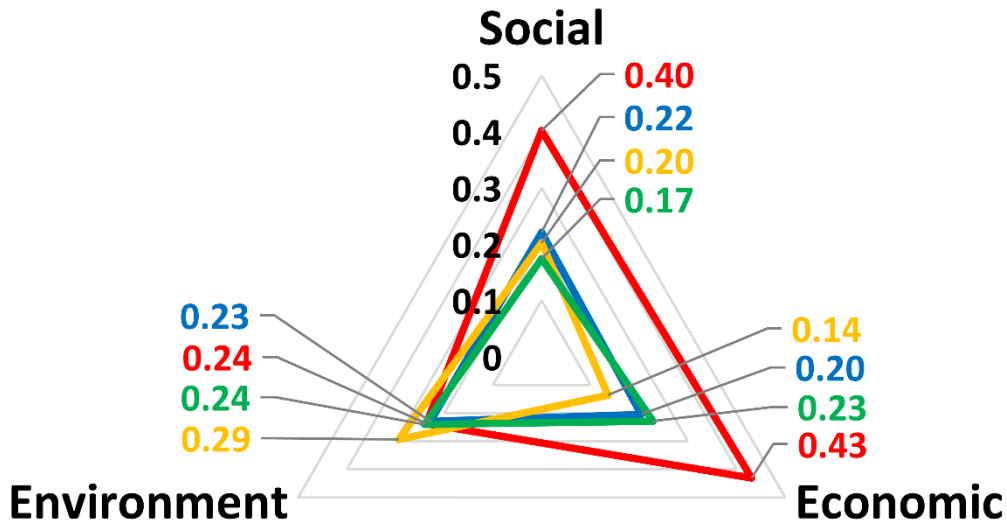

Fig 3-10. Comparison of social, economic, and environment for Lake Mendota (blue), Monona (red), Waubesa (orange) and Kegonsa (green).

3.4 Discussion

3.4.1 Rainfall duration

Rainfall duration affects flood loss and risk differently for each lake in the Yahara RCL. Generally, in urban areas, greatest loss occurs at shorter durations (e.g. hourly) where rainfall intensities are large. For the Yahara RCL losses are experienced at longer durations (e.g. daily) but vary due to dam operations and water release from lake to lake. The largest flood loss as shown in the economic results occurs at the 500-year return period. For rainfall duration, the three lakes Mendota, Waubesa, and Kegonsa experience peak flood loss of $6.7M, $2.8M, and $4.5M, respectively at the 8-day. However, Lake Monona loss of $4.6M is experienced at the 6-day which is mainly attributed to its flashy, urbanized watershed and storage of water on upstream Lake Mendota to provide protection during larger rainfall durations. Assessing a variety of rainfall durations is valuable to determine peak loss in a RCL otherwise flood loss may be under predicted. For example, if the 8-day duration was only used to characterize loss then Lake Monona would be under predicted by 13%. Similarly, if the 6-day duration was used then loss would be under predicted by 18%, 25%, and 23% for Lakes Mendota, Waubesa, and Kegonsa, respectively. On the extreme, if a shorter duration of 2-day was only assessed on all lakes, then significant under prediction of loss would be experienced by 44%, 45%, 66%, 48%, for Mendota, Monona, Waubesa, and Kegonsa, respectively. Overall, flood loss in the Yahara RCL is highly dependent on rainfall duration is an important factor to consider.

Peak flood risk also depends on rainfall duration and varies among lakes in the Yahara RCL. For the two lower lakes of Waubesa and Kegonsa, the largest risk occurs at the 8-day which is similar duration as flood loss but with different return periods. For lakes Mendota and Monona,

the peak flood risk both occur at a 10-day duration versus 8 and 6-day peak flood loss, respectively revealing that peak risk and loss is experienced at different durations. Peak risk in the Yahara RCL generally occurs at longer durations and for comparison to the 2-day, flood risk would significantly be under predicted from 44 to 76% depending on lake. Overall, the Yahara RCL experiences the largest risk and loss with various rainfall durations ranging from 6 to 10 day and are noted to be of most concern.

3.4.2 Sustainability assessment approach

Sustainability assessment in this study utilized AHP where the pairwise judgement values were calculated based on return period probability. Alternatively, surveys from the community or expert opinions may be carried out to determine judgment values and AHP repeated as a representation of people's views. To test the sensitivity of AHP to different judgement values such as a community survey, integer values ranging from 1 to 7 were input for each criteria. Specifically, judgement values of 1 year compared to 10 year return period was 2, 1 year compared to 25 year return period was 3, and so on. AHP results using integer values showed similar outcomes for economic, environmental, and social perspectives of that using return period probability to calculate judgement values. Overall, minor differences were found in the sustainability assessment with the largest variation less than 11%. These results suggest that different judgement values that consider low return period as more important than a high return period will generate similar outcomes in the Yahara RCL.

Other studies have identified alternative assessment approaches for sustainability and are noted for future study (Vaidya and Kumar, 2006; Fu, 2008; Li et al., 2011; Malekmohamma de et al., 2011; Behzadian et al, 2012; Lee et al., 2015). Alternatives to mitigate flooding such as storm

water control projects, improvements to river conveyance, or water level management may consider an optimization approach. For example, the objective function may consider to maximize the benefit to sustainability from social, economic, and environmental perspectives. The AHP method employed here has limitations to perform this analysis; however, the framework provided here could be applied to other sustainability assessment approaches such as optimization.

3.4.3 Flood actions

Recently, flood actions have been proposed to reduce flooding in the Yahara RCL due to 2018 event, costing millions of dollars of damage (Dane County Emergency Management, 2018). In response, a technical workgroup composed of engineers, researchers, scientists, and managers were brought together to evaluate various scenarios as shown in Table 3-3 that represents water level changes as compared to 2018. Also, a policy task force that consisted of members from the public, county board supervisors, and interest groups were charged to provide recommendations. The flood risk assessment modeling described in this paper was used to provide modeling results for various policy scenarios. As a result, two notable policy recommendations were made. First, updates to the stormwater ordinance for increased volume reduction measures (green infrastructure). Second, dredging the Yahara River to remove accumulated sediment and improve flow conveyance with an estimated $15 million budget. In summary, the development of the tools of flood risk assessment has been greatly beneficial to improve society impacts to flooding. Furthermore, this study provides useful results for further analysis in addressing community needs, policies, and actions to reduce flooding.

3.5 Conclusions

Flooding of the Yahara RCL has frequently occurred over the past few decades, resulting in large damage and economic loss. A sustainability assessment of flood risk was utilized to improve understanding of environmental, social, and economic impacts to flooding. Specifically, stochastic storm transposition results of RainyDay were cataloged for 35 rainfall scenarios from seven return periods (1, 10, 25, 50, 100, 250, and 500 year) and 5 rainfall durations (2, 4, 6, 8, and 10-day). Storm transposition results were utilized by integrated models to provide watershed runoff, river flow, and water levels. Outcomes of water levels for flooding were incorporated into Hazus-MH developed by Federal Emergency Management Agency (FEMA) to provide economic and social risks. The following conclusions can be made from the results of the study:

- Flood inundation in urban areas are not sensitive to storm durations under extreme rainfall.
- Flood inundation in non-urban areas are largest under shorter rainfall durations
- Largest social risk occurs between 5-year and 25-year flood return periods independent of rainfall duration.
- Economic risk is unbalanced among lakes in the Yahara RCL under low return periods as is mostly attributed to Lake Monona but becomes shared among all lakes under high return periods.
- Individually, Lake Monona (red bars) and Mendota (blue bars) experiences the largest economic risk at the 10 year return period ($20,924) and 500 year ($15,070), respectively.
- The 500-year versus 100-year return period for estimating EAD is strongly recommended.

- Sustainability assessments reveal Lake Monona is most at risk socially and economically when compared relative to other lakes.

3.6 Acknowledgements

This study was supported by the Dane County Land and Water Resources Department (DCLWRD) and College of Engineering at University of Wisconsin-Madison. We thank Ms. Michelle Richardson, GIS Analyst, at DCLWRD for her assistance in ArcMap software and GIS analysis.

4.7 References

Aborgiba, M., Kostic, J., Kolarevic, S., Kracun-Kolarevic, M., Elbahi, S., Knezevic-Vukcevic, J., Lenhardt, M., Paunovic, M., Gacic, Z., Vukovic-Gacic, B., 2016. Flooding modifies the genotoxic effect of pollution on a worm, a mussel and two fish species from Sava River. Science of the Total Environment.540, 358-367.

Adams, T.E., Chen, S., Dymond R., 2018. Results from operational hydrologic forecasts using the NOAA/NWS OHRFC Ohio River Community HEC-RAS Model. Journal of Hydrologic Engineering. 23 (7), 04018028.

Albering, H.J., Van Leusen, S.M., Moonen, E.J., Hoogewerff, J.A., Kleinjans, J.C., 1999. Human health risk assessment: A case study involving heavy metal soil contamination after the flooding of the River Meuse during the winter of 1993–1994. Environmental Health Perspectives, 107, 37-43.

Arnold, J.G, Srinivasan, R., Muttiah, R.S. and Williams, J.R., 1998. Large area hydrologic modeling and assessment - Part 1: Model development. Journal of the American Water Resources Association 34 (1), 73-89.

Ayres Associates. 2010 GPS survey for LIDAR control. Report, Madison, WI.

Behzadian, M., Otaghsara, S. K., Yazdani, M., and Ignatius, J., 2012. A state-of the-art survey of TOPSIS applications, Journal of Expert Systems and Applications. 39, 13051–13069.

Bradford, R.A., O'Sullivan, J.J., van der Craats, I.M., Krykow, J., Rotko, P., Aaltonen, J., Bonaiuto, M., De Deommonicis, S., Waylen, K., Schelfaut, K., 2012. Risk perception – issues for flood management in Europe. Natural Hazards and Earth System Sciences. 12, 2299-2309.

Browne, M.J., Hoyt, R.E., 2000. The demand for flood insurance: empirical evidence. Journal of Risk and Uncertainty. 20:3, 291-306.

Capital Area Regional Planning Commission (CARPC). 2020. Dane County Land Information Office. https://lio.countyofdane.com/

Capital Times. 2018. Watching the water: Torrential rains and flooding have renewed a debate over lake levels. https://madison.com/ct/news/local/environment/watching-the-water-torrential-rains-and-flooding-have-renewed-a-debate-over-lake-levels/article_0b439111-1173-5856-ba49-7f1bfefbc97c.html

Center for Research on the Epidemiology of Disasters (CRED)., 2019. Natural disasters 2018.

Channel 3000. 2018. 'It's been a lot of work': Monona residents prepare for flooding along Yahara Lakes. https://www.channel3000.com/its-been-a-lot-of-work-monona-residents-prepare-for-flooding-along-yahara-lakes/

Chatterton, J., Viavattene, C., Morris, J., Penning-Rowsell, E., Tapsell, S., 2010. The Costs of the summer 2007 floods in England, Environment Agency, Bristol, U. K.

Chen, C., Liu, H., and Beardsley, R.C., 2003. An unstructured grid, finite-volume, three-dimensional, primitive equations ocean model: Application to coastal ocean and estuaries. Journal of Atmospheric and Oceanic Technology. 20 (1), 159-186.

Chen, C.S., Qi, J.H., Li, C.Y., Beardsley, R.C., Lin, H.C., Walker, R., and Gates, K., 2008. Complexity of the flooding/drying process in an estuarine tidal-creek salt-marsh system: An application of FVCOM. Journal of Geophysical Research. 113, C07052.

Chen, X., Chen, Y., Shimizu, T., Niu, J., Nakagami, K., Qian, X., Jia, B., Nakajima, J., Han, J., Li, J., 2017. Water resources management in the urban agglomeration of the Lake Biwa

region, Japan: An ecosystem services-based sustainability assessment. Science of the Total Environment. 586 (2017), 174-187.

Chow, V.T., 1959. Open-channel hydraulics: New York, McGraw-Hill, 680 p.

Crum, T.D., Alberty, R.L., 1993. The WSR-88D and the WSR-88D operational support facility. Bulletin of the American Meteorological Society 74, 1669e1687.

Cunge, J.A., 1969. On the subject of a flood propagation computation method (Muskingum Method). Journal of Hydraulic Research. (7) 2, 205-230.

Dane County Emergency Management, 2018. Dane County Natural Hazard Mitigation Plan.

Dottori, F., Szewczyk, W., Ciscar, J.C., Zhao, F., Alfieri, L., Hirabayshi, Y., Bianchi, A., Mongelli, I., Frieler, K., Betts, R.A., Feyen, L., 2018. Increased human and economic losses from river flooding with anthropogenic warming. Nature Climate Change. 8, 781-786.

Edjossan-Sossou, A.M., Deck, O., Al Heib, M., Verdel, T., 2014. A decision-support methodology for assessing the sustainability of natural risk management strategies in urban areas. Natural Hazards and Earth System Sciences. 14, 3207-3230.

Falloon, P., Betts, R., 2010. Climate impacts on European agriculture and water management in the context of adaptation and mitigation – The importance of an integrated approach. Science of the Total Environment.408, 5667-5687.

FEMA. 2018, Hazus Flood Model User Guidance, 261p.

Fitzpatrick, F.A., Peppler, M.C., Walker, J.F., Rose, W.J., Waschbusch, R.J., and Kennedy, J.L., 2008. Flood of June 2008 in southern Wisconsin: U.S. Geological Survey Scientific Investigations Report 2008-5235.

Harvey, G.L., Thorne, C.R., Cheng, X., Evans, E.P., Han, S., Simm, J.D., Wang, Y., 2009. Qualitative analysis of future flood risk in the Taihu Basin, China. Journal of Flood Risk Management. 2(2009), 85-100.

Harwell, M.A., 1998. Science and environmental decision making in South Florida. Ecological Applications. 8(3), 580-590.

Hayden, N.G., Potter, K.W., Liebl, D.S., 2016. Evaluating infiltration requirements for new development using extreme storm transposition: A case study from Dane County, WI, Journal of American Water Resources Association, 1-9. DOI: 10.1111/1752-1688.12441.

Hijioka, Y., Lin, E., Pereira, J.J., Corlett, R.T., Cui, X., Insarov, G.E., Lasco, R.D., Lindgren, E., Surjan, A., 2014. Asia. In: Barros, V.R., Field, C.B., Dokken, D.J., Mastrandrea, M.D., Mach, K.J., Bilir, T.E., Chatterjee, M., Ebi, K.L., Estrada, Y.O., Genova, R.C., Girma, B., Kissel, E.S., Levy, A.N., MacCracken, S., Mastrandrea, P.R., White, L.L. (Eds.), Climate Change 2014: Impacts, Adaptation, and Vulnerability. Part B: Regional Aspects. Contribution of Working Group II to the Fifth Assessment Report of the Intergovernmental Panel on Climate Change. Cambridge University Press, Cambridge, United Kingdom and New York, NY, USA, 1327–1370.

Holmes, R.R., Koenig, T.A., Karstensen, K.A., 2010. Flooding in the United States Midwest, 2008, U.S. Gological Survey Porfessional Paper 1775, 64p.

Isthmus. 2007. Getting too high on the lake. https://isthmus.com/opinion/opinion/getting-too-high-on-the-lake/

Jalayer, F., De Risi, R., De Paola, F., Giugni, M., Manfredi, G., Gasparini, P., Elena Topa, M., Yonas, N., Yeshitela, K., Nebebe, A., Cavan, G., Lindley, S., Printz, A., Renner, F., 2014.

Probabilistic GIS-based method for delineation of urban flooding risk hotspots. Natural Hazards, 73, 975-1001.

Kang, M.G., Jeong, H.S., Lee, J.H., Kang, B.S., 2013. Assessing national flood management using a sustainable flood management framework. Water Policy, 48, 17-39.

Kellett, J., Caravani, A., 2013. Disaster Risk Reduction: A 20 year story of international aid. Global Facility for Disaster Reduction and Recovery. 280, 1-15.

Konat, J. and Kowaleska, G., 2001. Polychlorinated biphenyls (PCBs) in sediments of the southern Blatic Sea – trends and fate. The Science of the Total Environment. 280, 1-15.

Kundzewicz, Z.W., 2002. Non-structural flood protection and sustainability. Water International, 27, 3-13.

Li, F., Li, Z.-K., and Yang, C.-B., 2011. Risk Assessment of Levee Engineering Based on Triangular Fuzzy Number and Analytic Network Process and Its Application, in Modeling Risk Management in Sustainable Construction, edited by: Wu, D. D., Springer Verlag, Heidelberg, Berlin, 415–426.

Lee, G., Jun, K. S., and Chung, E.S., 2015. Group decision-making approach for flood vulnerability identification using the fuzzy VIKOR method, Natural Hazards and Earth System Science. 15, 863–874.

Lee, S., Lee, S., Lee, M.J. Jung, H.S., 2018. Spatial assessment of urban flood susceptibility using data mining and geographic information system (GIS) tools. Sustainability, 2018, 10, 648.

Levy, J.K., Hartmann, J., Li, K.W., An, Y., Asgary, A., 2007. Multi-criteria decision support systems for flood hazard mitigation and emergency response in urban watersheds. Journal of American Water Resources Association, 2007, 43, 346-358.

Lin, Y., Mitchell, K.E., 2005. The NCEP Stage II/IV hourly precipitation analyses: Development and applications. In: Preprints, 19th Conf. on Hydrology. American Meteorological Society, San Diego, CA, pp. 2e5, 9-13 January 2005, Paper 1.2.

Lin, Y.T., Schuettpelz, C.C., Wu, C.H., and Fratta, D., 2009. A combined acoustic and electromagnetic wave-based techniques for bathymetry and subbottom profiling in shallow waters. Journal of Applied Geophysics. 68 (2), 203-218.

Loayza, N.V., Olaberria, E., Rigolini, J., Christiaensen, L., 2012. Natural Disasters and Growth: Going Beyond the Averages. World Development. 40 (7), 1317-1336.

Mahmood, M.I., Elagib, N.A., Horn, F., Saad, S.A.G., 2017. Lessons learned from Khartoum flash flood impacts: An integrated assessment. Science of the Total Environment.601-602, 1031-1045.

Malekmohammadi, B., Zahraie, B., Kerachian, R., 2011. Ranking solutions of multi-objective reservoir operation optimization models using multi-criteria decision analysis. Expert Systems with Applications 38, 7851-7863.

Middelmann-Fernandes, M.H., 2010. Flood damage estimation beyond stage–damage functions: an Australian example. Journal of Flood Risk Management, 3, 88-96.

Montgomery Associates. 2011. Yahara Clean non-point source modeling report for the Dane County department of land and water resources.

National Academies. 2000. Risk analysis and uncertainty in flood damage reduction studies. The National Academies Press, Washington DC. 217p.

National Academies. 2012. Disaster resilience: A national imperative. The National Academies Press, Washington DC. 217p.

Neitsch, S. L., J. G. Arnold, J. R. Kiniry, R. Srinivasan, and J. R. Williams., 2002. Soil and Water Assessment Tool User's Manual Version 2000. GSWRL Report 02-02, BRC Report 02-06, TR-192. College Station, Texas: Texas Water Resources Institute, Texas A&M University.

Nyberg, L, Evers, M., Dahlstrom, M., Pettersson, A., 2014. Sustainability aspects of water regulation and flood risk reduction in Lake Vanern. Aquatic Ecosystem Health & Management, 17 (4), 331-340.

Park, J., Seager, T.P., Rao, P.S.C., Convertino, M., Linkov, I., 2013. Integrating risk and resilience approaches to catastrophe management in engineering systems. Risk Analysis. 33(3).

Perica, S., Martin, D., Pavlovic, S., Roy, I., St. Laurent, M., Tryupaluk, C., Unruh, D., Yekta, M., Bonnin, G., 2013. NOAA Atlas 14. Precipitation-Frequency Atlas of the United States Volume 8.

Petit,-Boix, A., Arahuetes, A., Josa, A., Rieradevall, J., Gabarrell, X., 2017. Are we preventing flood damage eco-efficiently? An integrated method applied to post-disaster emergency actions. Science of the Total Environment.580, 873-881.

Reimer, J.R. and Wu, C.H., 2016. Development and Application of a Nowcast and Forecast System Tool for Planning and Managing a River Chain of Lakes. Water Resources Management, 30(4), 1375-1393.

Reimer, J.R., Wu, C.H., Potter, K., Lathrop, R., Harder, J., Fries, G., Davis, R., Balousek, J., Allness, S., 2019. Technical Work Group Report: 2018 Yahara Chain of Lakes flooding https://lwrd.countyofdane.com/documents/pdf/Yahara-Flooding-Technical-Report-Final.pdf

Remo, J. W.F., Pinter, N., Mahgoub, M., 2016. Assessing Illinois's flood vulnerability using Hazus-MH. Natural Hazards, 81, 265-287.

Saaty, T.L., 1980. The Analytic Heirarchy Process. McGraw-Hill, New York.

Sarria-Villa, R., Ocamp-Duque, W., Paez, M., Schuhmacher, M., 2016. Presence of PAHs in water and sediments of the Colombian Cauca River during heavy rain episodes, and implications for risk assessment. Science of the Total Environment, 540, 455-465.

Scawthorn, C., Flores, P., Blais, N., Seligson, H., Tate, E., Chang, S., Mifflin, E., Thomas, W., Murphy, J., Jones, C., Lawrence, M., 2006. HAZUS-MH flood loss estimation methodology damage and loss estimation. Natural Hazards Review, ASCE 7(2), 72-81.

Schmidt, C.W., 2000. Lessons from the flood: will Floyd change livestock farming? Environmental Health Perspectives, 108, 74-77.

Schneider, P.J., Schauer, B.A., 2006. HAZUS-Its development and its future. Natural Hazards Review, ASCE 7(2), 40-44.

Schroter, K., Kreibich, H., Vogel, K., Riggelsen, C., Scherbaum, F., Merz, B., 2007. How useful are complex flood damage models?. Water Resources Research, 2014, 50, 3378-3395.

Simonovic, S.P., Ahmad, S., 2005. Computer-based model for flood evacuation emergency planning. Natural Hazards, 34, 25-51.

Smith, D.I., 1994. Flood damage estimation–a review of urban stage-damage curves and loss functions. Water SA. 20(3), 231–238.

Snoussi, M., Ouchani, T., Niazi, S., 2007. Vulnerability assessment of the impact of sea-level rise and flooding on the Moroccan coast: The case of the Mediterranean eastern zone. Estuarine, Coastal and Shelf Science, 77, 206-213.

Strope, S.A., Budikova, D., 2011. The 2008 spring Midwest floods: A signal of changing climate conditions. Journal of Physical Geography. 32 (4), 313-337.

Tate, E., Strong, A., Kraus, T., Xiong, H., 2016. Flood recovery and property acquisition in Cedar Rapids, Iowa. Natural Hazards. 80, 2055-2079.

U.S. Department of Commerce, 2013. NOAA Atlas 14 Precipitation-Frequency Atlas of the United States. Volume 8 Version 2.0: Midwestern States (Colorado, Iowa, Kansas, Michigan, Minnesota, Missouri, Nebraska, North Dakota, Oklahoma, South Dakota, Wisconsin). Silver Spring, Maryland.

Vaidya, O. S. and Kumar, S., 2006. Analytic hierarchy process: an overview of applications. European Journal of Operational Research. 169, 1–29.

Wisconsin Initiative on Climate Change Impacts (WICCI), 2020. Report to the Governor's task force on climate change: Strategies to improve Wisconsin's climate resilience and readiness. University of Wisconsin-Madison and Wisconsin Department of Natural Resources.

Wisconsin Public Radio. 2018. Dane County Readies For More Flooding As Additional Rain Passes Through. https://www.wpr.org/dane-county-readies-more-flooding-additional-rain-passes-through

Wisconsin State Journal. 2018. Climate, policy changes pose risk of major flooding on Madison's Isthmus. https://madison.com/wsj/news/local/environment/climate-policy-changes-pose-risk-of-major-flooding-on-madisons-isthmus/article_0c75f5c9-7410-5b6f-be3d-d6d7190b860e.html

Wisconsin State Journal. 2018. Flooding preparation continues in Madison, Monona ahead of Sunday's rainy forecast. https://madison.com/wsj/news/local/flooding-preparation-

continues-in-madison-monona-ahead-of-sunday-s/article_7d900867-b5ac-52a3-9d4b-10821eb6c655.html

Wright, D.B., Mantilla, R., Peters-Lidard, C.D., 2017. A remote sensing-based tool for assessing rainfall-driven hazards. Environmental Modelling & Software. 90 (2017), 34-54.

Yang, Z.Q., Khangaonkar, T., 2009. Modeling tidal circulation and stratification in Skagit River estuary using an unstructured grid ocean model. Ocean Modeling. 28 (1-3), 34-49.

4. Water Exclosure Treatment System (WETS): An innovative device for minimizing beach closures

The following has been published at *Science of the Total Environment*

Reimer, J.R., Wu, C.H., Sorsa, K.K., 2018. Water Exclosure Treatment System (WETS): An innovative device for minimizing beach closures. Science of the Total Environment. 625, 809-818.

4.1 Introduction

Beaches, a large part of the economies worldwide, provide well-being of local residents for swimming opportunities and attract tourism (Englebert et al., 2008; Houston, 2008; Wheeler et al., 2012; Ashbullby et al., 2013). Tourism in Wisconsin is a 12 billion dollar per year industry (Kleinheinz, 2003). Nevertheless, poor water quality at beaches can cause health threats or illness problems along shorelines for swimmers or recreational users (Patz et al., 2008). As a precautionary measure for the condition when water quality is below the standards, beach closures are issued. Surveys conducted by the Natural Resources Defense Council showed that over 20,000 beach closures every year were issued in the United States (Dorfman and Haren, 2013), yielding an estimated economic loss of approximately $35 for each person and up to $37,030 per day at a Lake Michigan beach (Rabinovici et al., 2004). Other economic impacts are medical costs to stricken beachgoers (Dwight et al., 2005). A previous study by Given et al. (2006) reported that each year, fecal contamination at Los Angeles and Orange County beaches caused between 627,800 and 1,479,200 gastrointestinal illnesses, resulting in a public health cost of $21 to $51 million USD. Furthermore, a recent study estimated that the cost of illness attributed to freshwater recreation was $1,676 per 1,000 people engaged in swimming or wading at freshwater and marine locations (DeFlorio-Barker et al., 2017). In view of these consequences, it is of high desire to

minimize beach closures to reduce health risk or medical cost and enhance economies through tourism.

Cyanobacteria and *E. coli* bacteria are two main causes of beach closures that pose a great health risk to recreation users. Cyanobacteria are a group of photosynthetic bacteria that can produce inherent toxins like hepatoxins, neurotoxins, cytotoxins, dermatoxins, and irritant toxins (Wiegand and Pflugmacher, 2005). Exposure to cyanobacteria hepato- and neurotoxins can cause impaired health or death of livestock wildlife, pets, and humans (Turner et al., 1990; Chorus and Bartram 1999; Falconer, 1999; Charmichael et al., 2001). Since many cyanobacteria contain gas vacuoles, they can form as floating scum mats regularly reported at downwind shorelines fouling beaches in the Yahara Lakes, Wisconsin (Lathrop et al., 2013). As a result, cyanobacteria scums are considered nuisance due to unaesthetic appearance and offensive odors associated with decomposition (Speziale and Dyck, 1992, Lathrop et al., 2013). Bacteria, present in fecal material, can be transmitted to humans during recreational water use via contaminated water carrying pathogens (McLellan and Salmore, 2003), posing a serious health concern to beach users. Possible sources of fecal organisms include humans (Lee et al., 2014), gulls (Araujo et al., 2014), geese, or domestic animals (Winfield and Groisman, 2003). For water quality monitoring, *Escherichia coli* (*E. coli*) is an indicator for fecal organisms for beach contamination (Kleinheinz and Englebert, 2005). Previous studies have shown that high occurrences of *E. coli* in water are associated with gastrointestinal disorders and other illnesses in swimmers (Dufour, 1984; Dufour and Cabelli, 1986; Pruss, 1998; Wade, 2003). Both cyanobacteria and *E. coli* can harbor within filamentous green algae (Whitman et al., 2003; Kleinheinz and Englebert, 2005; Englebert et al., 2008; Badgley et al., 2011; Vijayavel et al., 2013) that can then release free-floating bacteria and cyanobacteria by wave action, storms, and seasonal sloughing (i.e. detaching), accumulating along beach

shorelines (Whitman et al., 2003). In general, cyanobacteria and *E. coli* bacteria pose a threat to public health in recreational waters and beaches.

A great deal of efforts has been devoted to improving water quality, decrease contamination, and protect the health of beach users. For example, beach management practices often employed are stormwater runoff practices, combined sewer overflow mitigation, wildlife control, beach sediment nourishment, and source control policies. Based on the origination of contaminant, practices can be generally classified into two, onshore and offshore categories (Przybyla-Kelly, 2013). Onshore de-contamination practices like beach grooming are conducted to remove litter, vegetation, detritus, and animal fecal droppings in nearshore sand to reduce microbes harmful to human health (Sabino et al., 2014). As a result, fecal indicator bacteria can be reduced, improving beach water quality (Kinzelman et al., 2004). Similar onshore practice is to alter beach sediments from sand to gravel beaches to decrease concentrations of fecal bacteria (Aragones et al., 2016). Another onshore practice is to deter gull and geese populations from residing at beach areas, reducing bacteria concentration in the swimming water (Converse et al., 2012, Lee et al., 2013). Offshore de-contamination practices use devices to trap, deflect, or block offshore polluted lake water from entering swimming areas. For example, a floating boom to deflect long-shore currents in an inland lake in Wisconsin prevented swimming beaches to become fouled with blue-green algal (cyanobacteria) scums and other floating debris (Lathrop et al., 2013). This boom device was effective for blocking surface floating materials but could not prevent contaminants from entering into the swimming area through the open flowing water underneath of the floating boom. In comparison, a full depth permeable curtain was installed at Harbor Island Beach, New York within an ocean environment. The mechanism of tidal fluctuations provides the filtration to remove contaminants, effectively reducing *E. coli* by 81.9% (Lowe, 2008). A similar

filtering curtain was installed at Calumet Beach, Chicago but the swimming beach trapped more phytoplankton, higher *E. coli*, and turbidity (Przybyla-Kelly et al., 2013), suggesting that the effectiveness of full depth curtains depends on tides which are minimal at inland lakes. To date, little attention has been devoted to develop devices that minimize beach closures in inland, freshwater lakes where tidal effects are not significant.

The objective of this paper is to test the hypothesis that an innovative Water Exclosure Treatment System (WETS) can prevent algal scums and reduce beach closures from cyanobacteria and *E. coli* bacteria originating from either offshore or onshore in inland lakes. The WETS consists of two sub-system: an exclosure consisting of an impermeable curtain at the offshore and a water treatment device at the shore. The design of WETS water treatment intake and outlet piping locations were evaluated using computational fluid dynamics to estimate contaminant flushing and residence time scales. WETS was installed at a pilot beach in 2011 which has experienced contamination from onshore due to resident geese populations and offshore due to floating cyanobacteria scum and bacteria. The effectiveness of WETS in reducing cyanobacteria and *E. coli* concentrations to safe levels for beach users was evaluated. Overall it is found that WETS eliminated the need for beach closures in a non-tidal, freshwater lake.

4.2 Materials and methods

4.2.1 Study site

Brittingham Beach is located on the north shore of Monona Bay within the Yahara River Chain of Lakes in Dane County, Wisconsin, (see star location in Fig 4-1a). The beach, originally built in 1910, was the City of Madison's first water park boasting an expansive water slide and rental swimsuits. Brittingham Beach was one of the City's most popular beaches nearly 100 years

ago. Nevertheless, today it is one of the least frequented beaches due to poor water quality; high cyanobacteria and *E. coli* bacteria levels. From 2005 to 2009, the beach was closed 14 days due to high cyanobacteria and *E. coli* levels. As a result, Brittingham Beach was listed on the Environmental Protection Agency (EPA) 303(d) list of impaired beaches for high bacteria levels for several attributes. Onshore contamination is suspected to be a source of *E. coli* due to large numbers of waterfowl (i.e. geese and ducks) residing at the beach. Offshore contamination due to stormwater outfalls exits the shoreline riprap, approximately 350 feet away on each side of the beach. The outfalls drained from an urbanized and mixed use watershed where similar studies have shown that the discharge water contains pollutants such as oil and grease, chemicals, nutrients, metals, and bacteria (Brownell et al., 2007). Since the 1950's, Public Health of Madison and Dane County (PHMDC) has conducted sampling at Brittingham Beach. When water sampling shows elevated levels of cyanobacteria or *E. coli*, beach closing (a passive approach) is issued by PHMDC. Nevertheless, users may swim at their own risk. In this paper, we report an active approach, Water Exclosure-Treatment System (WETS, see Fig 4-1b) that was designed and installed at Brittingham Beach in 2011.

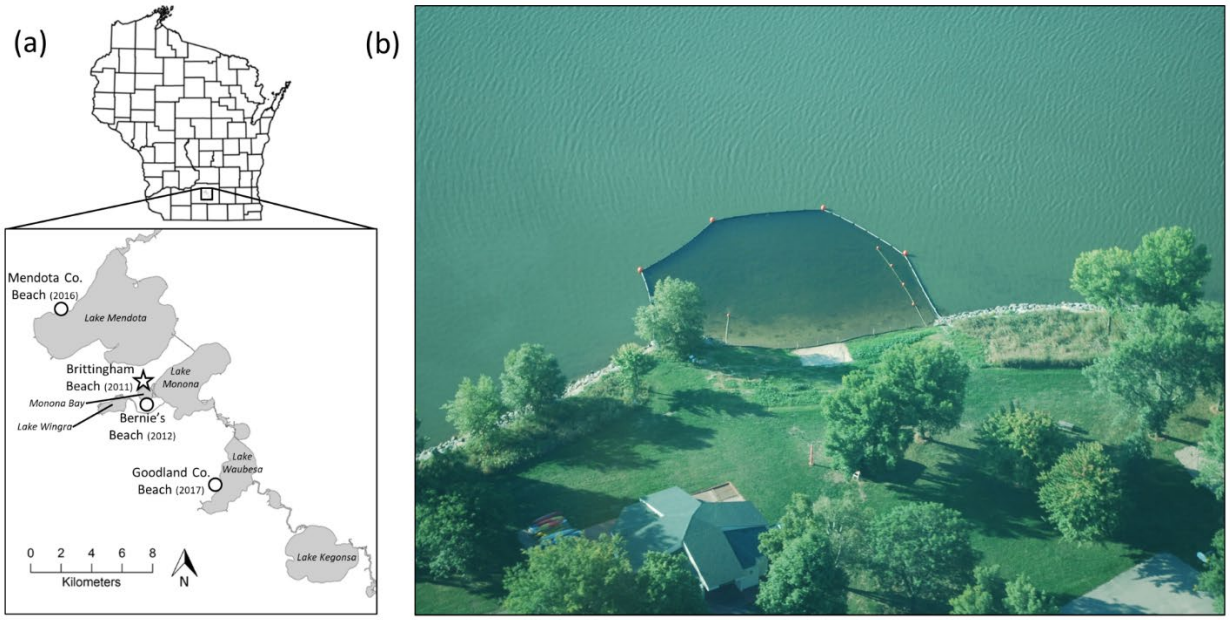

Fig 4-1. (a) The study site, Brittingham Beach (star on map), is located with the Yahara River Chain of Lakes, Dane County, Wisconsin, United States. WETS were also installed at other three sites (circle on map) that are Bernie's Beach, Mendota County Beach, and Goodland County Beach. (b) Aerial view of the Brittingham Beach with the exclosure system in the summer of 2011.

4.2.2 Water Exclosure-Treatment System

4.2.2.1 Exclosure sub-system

The exclosure sub-system consists of a five-sided polypropylene barrier (Seaman Corporation XR Membrane, 8130 X6-5) that excludes offshore contaminating lake water from the swimming area (Fig 4-2a). The total volume of water enclosed for swimming is 868 cubic meters. Each barrier contains a floatation boom consisting of five, 3.05-m long (15.25 meter total length) by 15-cm diameter styrofoam tubes. All five barriers were bolted together using a stainless steel accordion hinge to allow the floatation boom to freely float in response to fluctuating lake levels and waves. A tension steel cable located under the flotation boom traveled along the entire perimeter of the exclosure and anchored on shore to metal, tie-down rods. Each barrier was

designed to match the lake bathymetry with an additional 3 foot skirt with two ballast chains added to seal at the lake bottom, excluding lake water from swimming water (Fig 4-2b). An orange buoy marker is connected at each hinged section for two purposes. First, additional uplift is provided to counteract the downward force imposed from securing the barrier wall to the lake bed. Second, visibility for navigation to other lake users is addressed. Installation of the exclosure barrier was performed by using two barges and two boats to stretch out the exclosure at each orange buoy delivering tension on the exclosure. At last, each anchor weighing 300 pounds was chained to each orange buoy to retain tension for structure and prevent movement. The exclosure was deployed in the swimming season and removed after September.

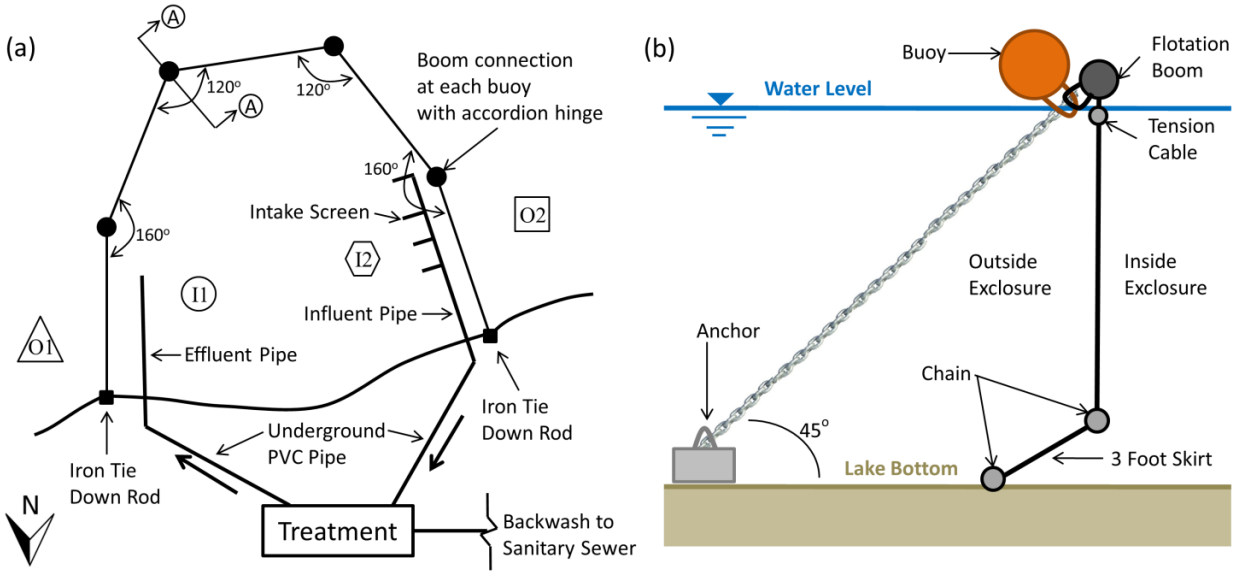

Fig 4-2. (a) The enclosure sub-system of WETs consists of five booms to separate the swimming area water from the lake proper. A treatment sub-system pumps influent water through a sand filter and ultraviolet disinfection, returning clean water to the swimming area and backwash water to the sanitary sewer. Labels O1, I1, I2, and O2 are the water sampling locations. (b) Section A-A shows the configuration of the exclosure sib-sub-system with the anchor.

4.2.2.2 Treatment sub-system

A strainer-filtration-ultraviolet treatment sub-system is housed inside an enclosed portable trailer (see Fig 4-3a). Lake water influent is entered through two-inch, underground polyvinyl chloride (PVC) pipes using a self-priming centrifugal pump (Gorman Rupp model 11-1/2A52-B). Fig 4-3b shows the three major components. First, a strainer (Eaton model 72 with ¼" perforated stainless steel strainer) is used to remove heavy debris such as aquatic plants. Second, a sand filter (Pentair model TR140C Triton Commercial Series) is utilized to remove fine particles with diameter greater than 40 microns. Third, two parallel ultraviolet (UV) disinfection purifiers (Atlantic Ultraviolet model S10,000C) are used to produce short wave radiation lethal to pathogens, cyanobacteria, bacteria, and viruses. The treated and clean water effluent is sent back to the swimming area through two-inch underground PVC piping (see Fig. 2a). A fully automated Programmable Logic Controller (PLC) is designed to execute commands based on pressure sensor readings (Fig. 3c). If the differential pressure across the sand filter is larger than a set threshold, the PLC would initiate a backwash by opening valves reversing lake water through filter media and discharging to the sanitary sewer. The differential pressure was set near 50 kPA which generated at least one backwash per day. The PLC also triggers alarms for low pumping pressure and dirty strainer conditions. The dirty filter alarm was triggered three times and occurred on days with many swimmers due to excessive aquatic plants uprooted or broken by swimming activity. The low pump pressure alarm occurred once and caused be fishing line tangled around the pump impellor. When an alarm is issued, the system shuts down to protect damage to the equipment. The automated treatment component was installed 1 week prior to the opening of beach season and was designed to run 24 hours a day.

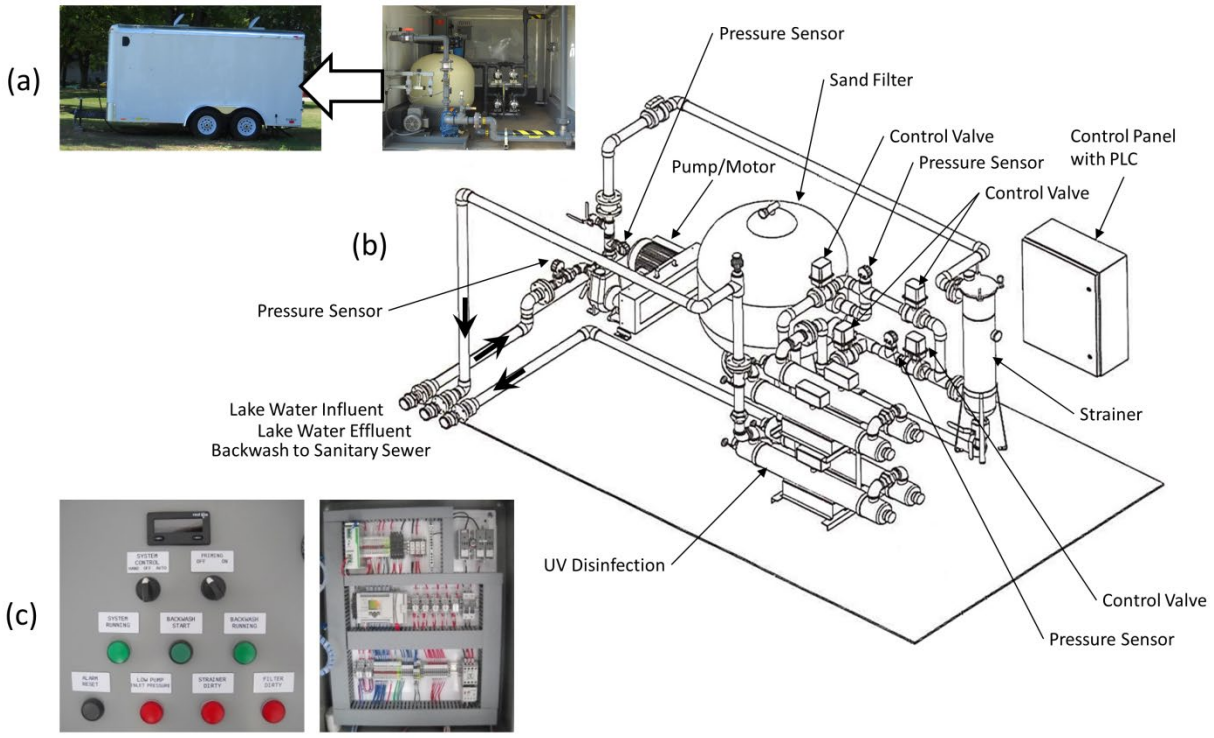

Fig 4-3. (a) A portable trailer enclosed with the treatment sub-system. (b) A schematic of the detailed components of the strainer-filtration-ultraviolet system. Lake water influent is pumped through a strainer removing heavy debris such as aquatic plant fragments, a sand filter removing fine particles, and ultraviolet water purifiers to produce short wave radiation lethal to microorganisms. The treated effluent water is returned to the swimming area. (c) An automatic logic control uses pressure sensors to monitor performance and trigger backwashing of the sand filter to the sanitary sewer.

4.2.2.3 Measurements and analysis

Water quality samples were collected in accordance with the EPA's national beach guidance and required performance criteria (USEPA, 2014). Specifically, grab water samples were collected within the swimming area and 6 meters outside of the barrier by placing a sample bottle 15.2 cm below the water surface within 76.2 cm of water. Samples were collected for turbidity, *E. coli*, cyanobacteria, and total phosphorus. The frequency of water quality sampling was conducted at least twice per week for the duration of the study period from Memorial Day to Labor Day.

Turbidity was measured on 26 samples for water outside (O1) and inside (I1) the exclosure as located in Fig 4-2. Turbidity measurements were performed using a Hach turbidity meter (NTU; 2100N Turbidimeter, Hach Company, Loveland, CO). *E. coli* is measured in many states, including Wisconsin, as an indicator organism of recent fecal contamination (Dufour, 1984; Dufour and Cabelli, 1986; Kleinheinz and Englebert, 2005). *E. coli* was measured on 24 samples to measure water outside (O1) and inside (I1) the exclosure. Samples for *E. coli* were analyzed using Colilert-18 defined substrate technique (IDEXX, Inc., Westbrook, ME). Testing results for E. coli were reported as most probable number (MPN) per 100 mL of water. A beach closure is issued if the *E. coli* count is greater than 1000 MPN/100 mL, consistent with Wisconsin DNR criteria for the Great Lakes beaches (WDNR, 2000).

Cyanobacteria samples were taken at two locations outside (O1 and O2) and two locations inside (I1 and I2). Cyanobacteria testing provided 644 data. Up to ten cyanobacteria genera were tested including *Aphanizomenon sp., Aphanocapsa sp., Anabaena sp., Cylindrospermopsis sp., Gloeotrichia sp., Limnothrix sp., Merismopedia sp., Microcystis sp., Osillatoria sp., and Planktothrix sp*. Cyanobacteria densities and toxins were assessed using a multi-tier approach for a screening program using microcystin toxin as a surrogate for other cyanotoxins (e.g., anatoxin, saxitoxin, cylindrospermopsin). The multi-tier approach allowed for near real-time decision making for relaying health alerts as performed by the following procedure. First, rapid microscopic screening of the dominant taxa and their abundance were evaluated to ascertain whether a bloom event was occurring. If a bloom occurrence was identified and human health risk was suspected, semi quantitative immunoassay-based strip tests of microwave-digested samples were used to evaluate a potential hazard. If strip tests exceeded a designated threshold level, enzyme-linked immunosorbent assay (ELISA) testing was used to verify the strip test result for microcystin. The

results of the evaluation would dictate whether any intervention (beach closure or alert) was appropriate. The decision for a beach closure is based on microcystin levels above the World Health Organization recommended limit of 20 μg/L (Chorus and Bartram, 1999). Cyanobacteria levels are fueled by excessive nutrient levels such as phosphorus. Lastly, fifteen samples, transported on ice and processed within 6 hours, were tested for total phosphorus inside (I1) and outside (O1) the exclosure.

A one-way Analysis of Variance (ANOVA) was performed to test the statistical difference for water outside the exclosure versus inside for three constituents (turbidity, *E. coli,* and one of the cyanobacteria genera, *Cylindrospermopsis sp*. We prescribe the outside water (O1) as the dependent value to determine if differences exist compared to other sample site locations. When $p \leq 0.05$, past studies for beach monitoring of *E. coli* and cyanobacteria indicate a significant difference between sites (Englebert et al., 2008; Hernandez et al., 2014).

Land topography of site surveys was conducted using a Real-Time Kinematic-Global Positioning System (Trimble R6) with horizontal and vertical accuracy of 10 and 20 mm. Elevations of land at the Brittingham Beach were aided in the design for selecting an appropriate pump based on lifting head requirements in the water treatment sub-system. Underwater bathymetry of site surveys was conducted using an acoustic sub-bottom profiler with a vertical resolution of 2 mm (Lin et al., 2009). Elevations of underwater lake bed with a horizontal grid spacing of 5 meters within the swimming area were used for specifying locations of the exclosure sub-system and modeling next.

4.2.2.4 Modeling

Computational fluid dynamics (CFD) modeling was used for two purposes including: (1) aid in the design of the inlet and outlet locations inside the exclosure sub-system and (2) determination of sizing of sand filters and evaluation of efficiency of UV disinfection. In the past two decades, CFD modeling has been widely employed to design treatment systems such as UV disinfection (Lyn et al., 1999; Sozzi and Taghipour, 2006; Liu et al., 2007), stirred tanks (Sahu et al., 1999; Kasat et al., 2008), and waste stabilization ponds (Abbas et al., 2006). In this paper, the hydrodynamic Finite Volume Coastal Ocean Model (FVCOM) developed by Chen et al., (2003) was implemented. The hydrodynamic model consists of the continuity equation, momentum equation under hydrostatic pressure assumption, and temperature equation. Details of model description can refer to Reimer and Wu (2016). Flexible unstructured meshes to delineate the horizontal domain can be generated. Fig 4-4 shows an example of horizontal meshes with 0.3 to 1m node spacing for a study case of a water intake inlet at the middle location and an effluent outlet at the shallow location. In the vertical model domain, 20 sigma layers are used to cover the water depths ranging up to 2.2 meters with a mean depth of 1.0 meter. In this study, wind impacts on circulation patterns and velocity magnitudes were negligible due to short fetch distance in the bay and small size of the swimming area (approximately 3% difference with 10 m/s southwest wind compared to no wind). Therefore, wind fields were not considered here. The model was applied to examine nine cases, i.e., the combination of three different water intake (shallow, middle, deep) and three effluent outlet (shallow, middle, deep) locations. The implemented FVCOM model was run to reach steady state conditions to generate hydrodynamic (flow and turbulent) fields for the use of modeling particle motions in the next.

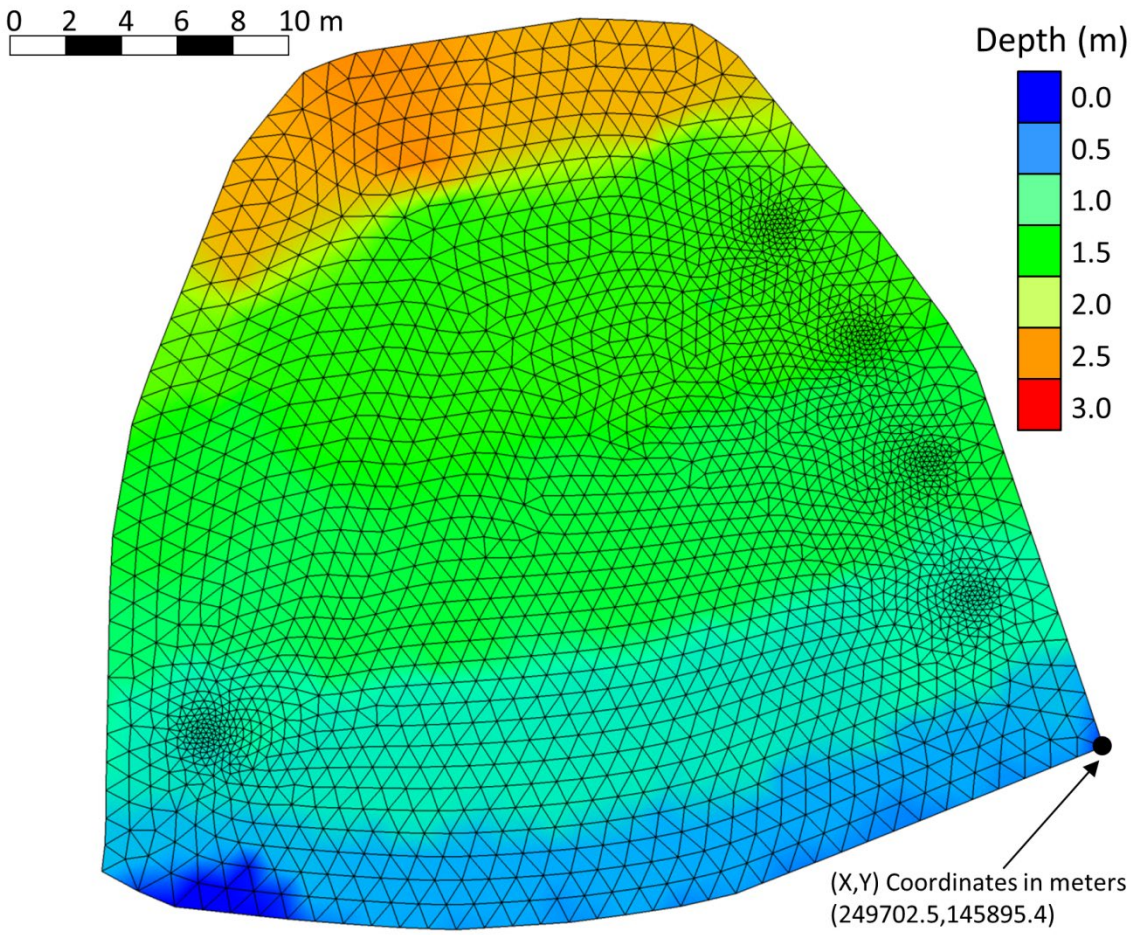

Fig 4-4. An example of unstructured meshes in the hydrodynamic model for the case of inlet at the middle and outlet at the shallow. Spatial resolution for meshes ranges from 0.3 to 1 meter.

A Lagrangian particle tracking model was employed to assess how water flows within the swimming area bounded by the exclosure barrier. Particle tracking models have been widely used to simulate the transport pathways, mixing and exchange of pollutants (Gomez-Gesteira et al., 1999; Perianez, 2004; Cerejo and Dias, 2007; Delpeche-Ellmann and Soomere, 2013). In this study, algae or bacteria are assumed to be passive and neutrally buoyant particles, which undergo flow advection and turbulent mixing processes. Specifically, each particle is moved to new positions by a time step times the flow field obtained from the hydrodynamic model and a random walk model using turbulence mixing estimates. Specifically, the horizontal eddy diffusivity

coefficients, based upon the Smagorinsky parameterization (Liu et al., 2008), are the order of 10-2 m^2/s, which is consistent to turbulent mixing values in a nearshore zone of a small lake with low wind conditions (Lemmin, 1989; Kimura et al., 2016). The vertical eddy diffusivity, based upon the k-ε (turbulence closure scheme Rodi, 1987; Umlauf and Burchard, 2005), are 10^{-3} m^2/s, similar to the numbers for the shallow water and an energetic near surface layer (Rehmann and Dudda, 2000; Bugucki et al., 2005). Particles were initially released using a 1.0 meter uniform, horizontal and vertical spacing, resulting in 1424 initial locations. Monte Carlo simulations of the particle tracking model were performed at least 100 times to calculate two fundamental timescales, i.e. flushing time and residence time. Note that several definitions for both timescales have been employed in the literature. In this study, we employ the definition of flushing time as the amount of time required to exchange the water within the swimming area bounded by the exclosure. Specifically, flushing time is obtained based on a 37% renewal time for a continuous stirred tank reactor (Monsen et al., 2002). Different from flushing time, residence time is the amount of time that a particle initially in the domain of interest resides in domain before leaving through its boundaries (Zimmerman, 1976; Shen and Haas, 2004). Residence time for each water parcel depends on its starting location (Prandle, 1984). As a result, spatial residence time can depict the duration of particles within the swimming area. The model was setup similar to previous calculation of flushing time except that each particle is tagged with its starting location and the time it takes to exit the swimming exclosure is recorded. Through Monte Carlo simulations, the mean time to exit the exclosure for each of the 1,424 coordinate locations was thereby calculated. In short, the two timescales are used to address the two purposes mentioned at the beginning of the section.

4.3 Results

4.3.1 Flushing time

Flushing time is a bulk value that reflects the integral time scale of combined effects of physical transport processes of the water body (Dyer, 1973; Fisher et al., 1979; Geyer et al., 2000; Monsen et al., 2002). In this study, we find that steady values of flushing time are reached after approximately 20 ~ 25 Monte Carlo simulations. Table 4-1 lists the mean flushing time for nine cases consisting of the combination of shallow, middle, and deep water depths for both water intake and effluent outlet locations. Values of flushing time vary over a day, indicating that locations of water intake and effluent outlet play an important role on the efficiency of lake water treatment. For example, the flushing time for the case of deep inlet with deep outlet (flushing time = 1.89 days) and the case of middle inlet and shallow outlet (flushing = 0.67 days) differs up to a factor of three. The flushing time for the cases with the same depths of inlet and outlet is longer in comparison with cases with varying depths of either inlets or outlets. For example, the flushing time for the case with the inlet at the middle depth and the outlet at the middle depth is longer than the one with the shallow/deep inlet location and the outlet at the middle depth; or the one with the inlet at the middle depth and the shallow/deep outlet location. Overall, the results suggest that minimal mixing can occur for the cases of same depth of the inlet and the outlet. Consequently, inlet and outlet locations at different depths are desired to enhance mixing. The two short flushing times are 0.67 and 0.96 days when the outlet is at the shallow location and inlet is at either the middle location, which are chosen to be the design inside the exclosure sub-system.

Table 4-1. Flushing time (in days) for nine simulations comparing inlet and outlet locations.

Inlet / Outlet	Shallow	Middle	Deep
Shallow	1.12	0.67	0.96
Middle	1.39	1.61	1.33
Deep	0.98	1.43	1.89

4.3.2 Spatial residence time

Based upon the modeling described in Section 2.4, Fig 4-5 reveals the spatial distribution for mean residence time for the nine cases with the combination of three different water intake (shallow, middle, deep) and three effluent outlet (shallow, middle, deep) locations. The depth averaged velocity vectors (white arrows) are plotted over the residence time map. Two type of spatial circulation patterns are seen. First, a two-gyre circulation pattern occurs for the three cases with the outlet at the middle, yielding less mixing due to short circuiting. The residence time at the dead zones at the middle water depth can go up to 3 days (see color map in Fig. 5). Second, a one-gyre circulation pattern is seen in all other six cases. Specifically, a clockwise/counter-clockwise gyre pattern occurs for the cases with the outlet at the deep/shallow water. Similar to the two-gyre circulation, the residence time at the dead zone can go up to 3 days. Among all nine cases, the residence time maps for the two cases with the intake at the middle and deep water locations under a shallow effluent outlet exhibit less than 0.5 days for most of the areas. Interestingly, the results are consistent to the two smaller flushing times (0.67 days and 0.96 days), as shown in Table 4-1. From a different perspective, Brittingham Beach has been most used by toddlers and young children. Klenheinz et al. (2006) showed that concentrations of *E. coli* are inversely related to water depth of recreation waters, suggesting that young children confined to shallow depths have higher risk. As a result, we select the inlet in the middle and the outlet in the shallow water as the

pipe configuration that has short residence time in the shallow water and overall lowest flushing time.

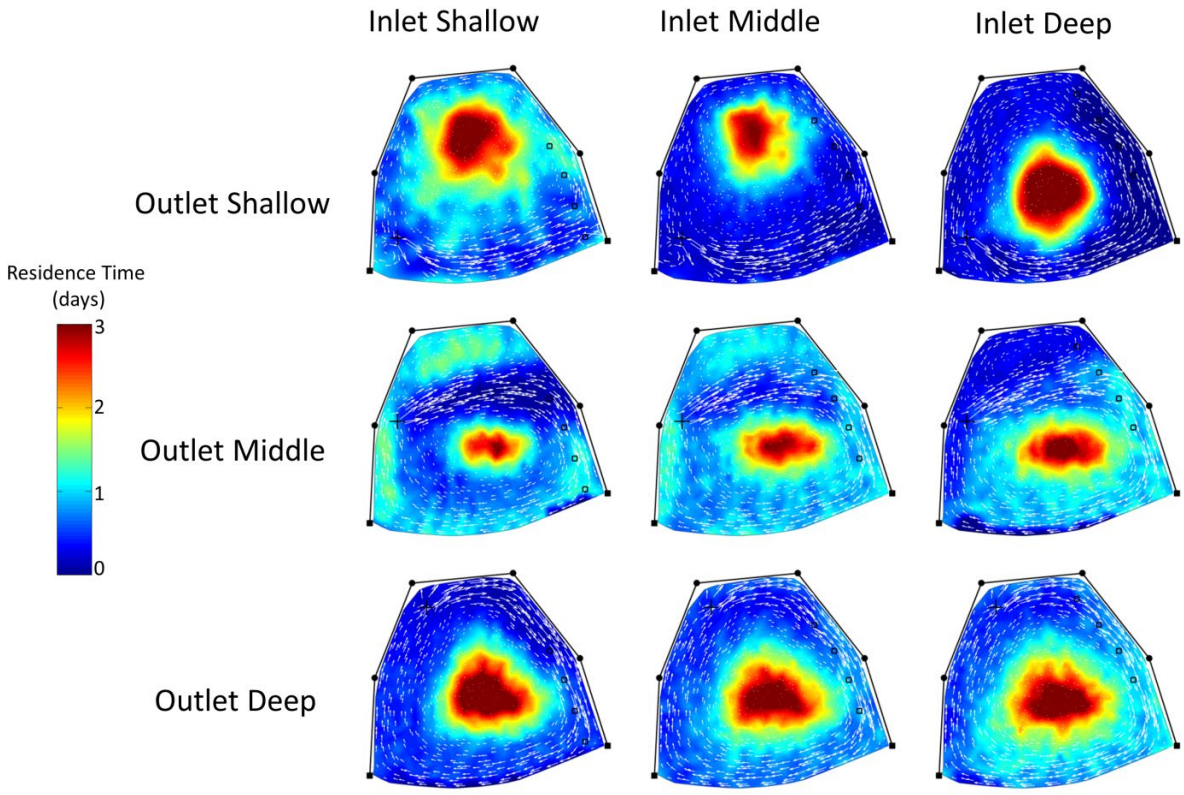

Fig 4-5. The mean residence time map for nine cases with the combination of three different water intake (shallow, middle, deep) and three effluent outlet (shallow, middle, deep) locations.

4.3.3 Turbidity and E. coli

High turbidity is often an indicator of high suspended solids which may be responsible for the transport of viruses and bacteria (Wong et al., 2009). Fig 4-6a shows that turbidity levels inside the exclosure were up to 15 times lower than outside. The lake water was turbid with peak nearing 100 Nephelometric Turbidity Unit (NTU) on August 16. In contrast, the turbidity inside the exclosure was consistently low (less than 5 NTU) during the whole period. Table 4-2 shows that ANOVA tests of turbidity is p=0.000003, indicating that a significant difference is apparent for

water inside (I1) versus outside (O1) the exclosure. Fig 4-6b shows the range of turbidity as a box plot with the central mark as the median, the extent of the box as the 25th and 75th percentiles, the whiskers range to the most extreme data points not considered outliers, and the outliers, individually. A larger span of percentiles is outside (26.38-41.03 NTU) versus inside (2.02-3.59 NTU). Overall, the median turbidity outside is 31.60 NTU versus inside is 2.43 NTU, indicating WETS has successfully reduced turbidity or suspended solids to yield clearer swimming water. Furthermore, the decreased turbidity may increase the natural UV killing of microbes inside the exclosure.

E. coli results inside the exclosure were consistently lower than those outside, as shown in Fig 4-6c. The water outside experienced two peaks in high levels of *E. coli* on August 16 and September 1. On these peak days large rainfalls occured, a slight rise in *E. coli* also occurred inside the exclosure due to runoff into the swimming area; however, *E. coli* levels inside were about 30 times lower than those outside. A beach closure is issued by the local health department, PHMDC, when *E. coli* levels exceed a threshold of 1000 MPN/100mL. *E. coli* values inside the exclosure ranged from non-detectable limits up to 20 MPN/100 mL, significantly less than criteria for issuing a closure. Table 4-2 shows that ANOVA tests of *E. coli* is p=0.059 between inside (I1) and outside (O1) water for all data, which is not significant. If only peak days of elevated *E. coli* levels were used for ANOVA testing, it is found that p=0.012, showing water inside is significantly different than outside. Fig 4-6d shows that the 25th to 75th percentiles of *E. coli* outside is 7.5 to 90 MPN/100 mL and inside is 4.5 to 15 MPN/100 mL, respectively. Overall, the results indicate that WETS reduced *E. coli* levels, an indicator of fecal contamination, providing safer swimming water.

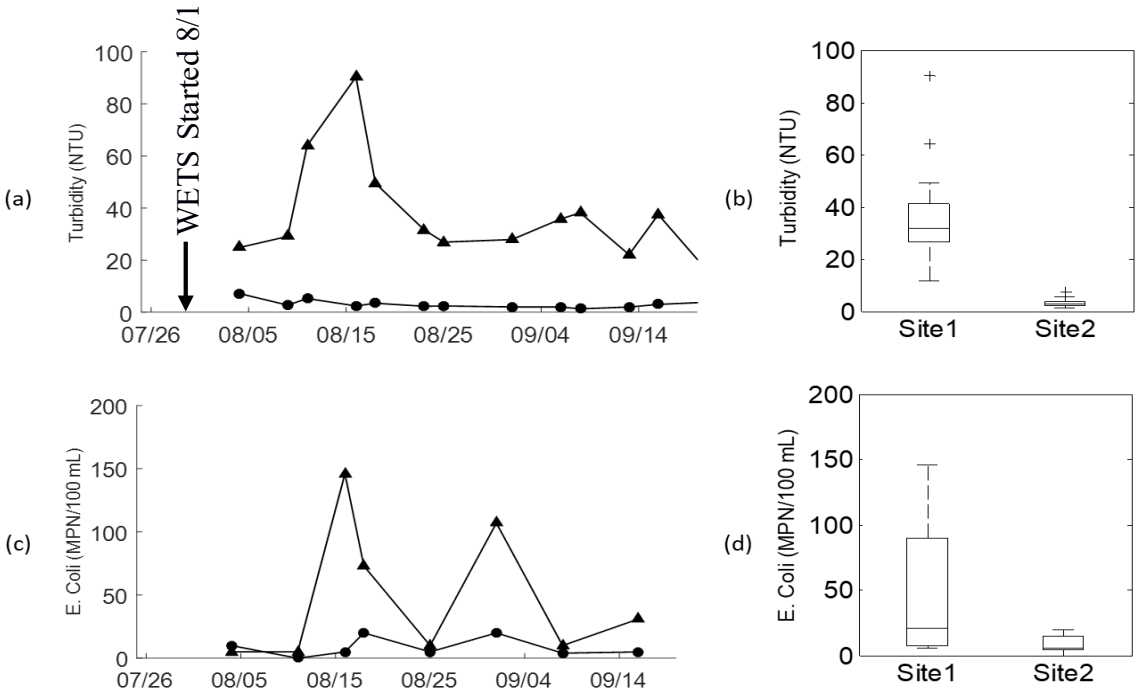

Fig 4-6. Time series of (a) turbidity and (b) box plot at the outside sample site O1 (triangle symbol) and the inside sample site I1 (o symbol). Similarly, time series of (c) *E. coli* and (d) box plot at the outside sample site O1 (triangle symbol) and the inside sample site I1 (o symbol).

Both turbidity and *E. coli* samples were evaluated for how well they were related using the Pearson correlation for water outside versus inside the exclosure. Correlation analysis showed that turbidity and *E. coli* for outside water were moderately, positively correlated (Pearson: 0.545) suggesting turbidity may serve as an indicator for *E. coli*. However, inside the exclosure, a weak and negative correlation (Pearson: 0.073) was found, indicating that the relationship does not hold. Overall, the moderate correlation outside versus weak correlation inside suggests the benefit of the exclosure to minimize wind and waves that stir up bottom sediments and the effectiveness of the treatment system to remove particulates and disinfect *E. coli* in the water column.

Table 4-2. One-way analysis of variance comparing site O1 (outside) to other sampling locations.

Measurement Variables at OI	Source of Variation	P Value
Turbidity	Site I1 (inside)	0.000003
E. coli	Site I1 (inside)	0.059 (all samples) 0.012 (peak days)
***Cylindrospermopsis* sp.**	Site I1 (inside)	0.0001
	Site I2 (inside)	0.0001
	Site O2 (outside)	0.732

4.3.4 Cyanobacteria genera

Cyanobacteria, were found to be the dominant forms among the phytoplankton populations at the study site. Fig 4-7 shows a visual of the phytoplankton content witnessed during the study period. In each photo, three samples are shown from left to right (tap water, water inside exclosure, and water outside exclosure at four different times. Water outside the exclosure was significantly greener in color compared to tap water suggesting that photosynthetic organisms are present. Tap water and inside exclosure water were visually difficult to distinguish implying WETS has reduced cyanobacteria levels. In addition to qualitative data, quantitative analysis was performed.

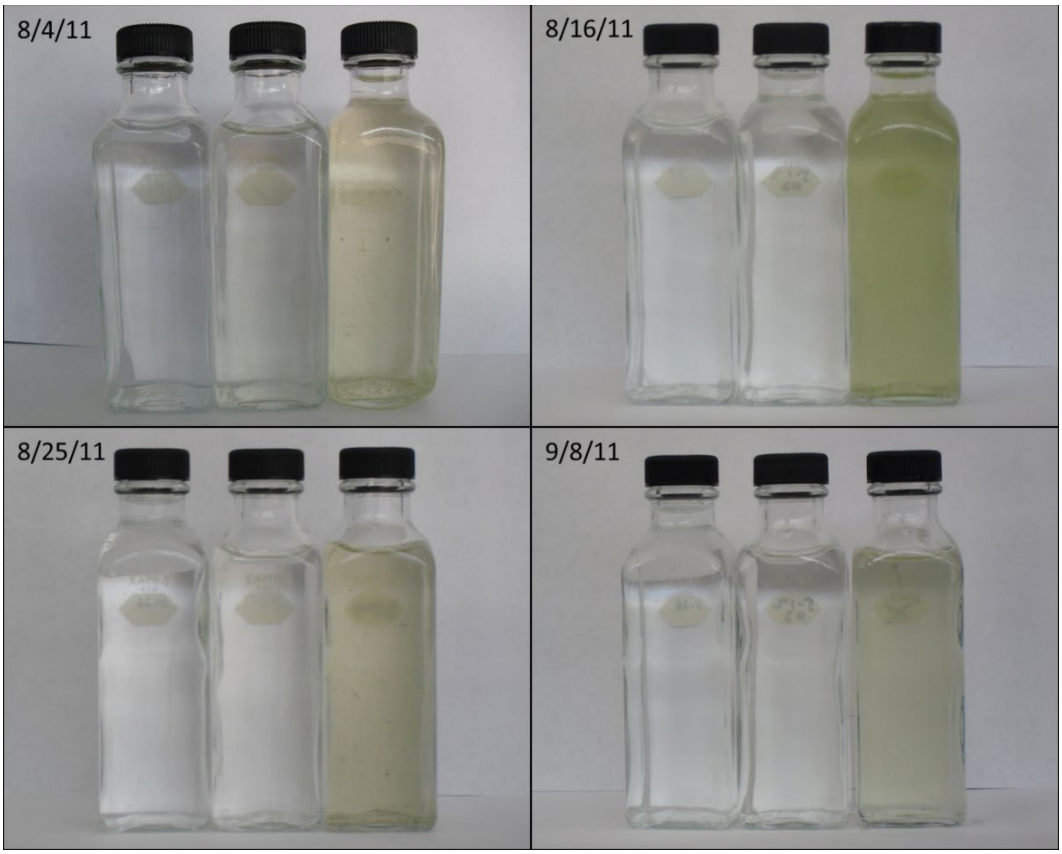

Fig 4-7. Three sample bottles (from left to right) show water clarity of tap water, swimming water inside the exclosure, and lake water outside the exclosure at four different times. The outside lake water is green with peak occurring on 8/16/11, suggesting high cyanobacteria concentration. Inside swimming water remains clear as compared to tap water.

Cylindrospermopsis sp., one of ten cyanobacteria genera tested, are shown in Fig 4-8a comparing outside (O1 and O2) versus inside (I1 and I2) the exclosure. Cylindrospermopsis sp. peaked in quantity around August 16 and September 1 outside of the exclosure. In contrast, a consistent low concentration of Cylindrospermopsis sp. was found inside the exclosure and did not exhibit any response to peaking cyanobacteria levels in the lake. Table 4-2 shows that ANOVA testing for Cylindrospermopsis sp. between outside O1 and O2 is 0.732, indicating that the lake water is at similar cyanobacteria levels. In contrast, ANOVA testing between outside water is significantly different than the inside water ($p=0.0001$). Fig 4-8b shows the median

Cylindrospermopsis sp. values outside are 8000 colonies/mL and inside are 595 colonies/mL or approximately 16 times less concentrated inside. Similar results and conclusions can be drawn for the remaining ten cyanobacteria tested and for brevity are not shown.

Cyanobacteria levels are often fueled by excessive nutrient levels such as phosphorus. Fifteen samples were tested for total phosphorus and the results inside the exclosure were consistently, up to eight times lower than outside the exclosure, reflecting phosphorus content removed during the treatment. Specifically, total phosphorus inside and outside the exclosure ranged from non-detectable to 0.07 mg/l and 0.08 to 0.16 mg/l, respectively. Interestingly, total phosphorus levels inside the swimming area were less than targets (0.075 mg/l) set by the EPA in the development of the Total Maximum Daily Load (TMDL) for the Yahara Lakes (Cadmus Group, 2011). In conclusion, WETS appears to be effective in reducing elevated cyanobacteria concentrations, providing clean and safe swimming water.

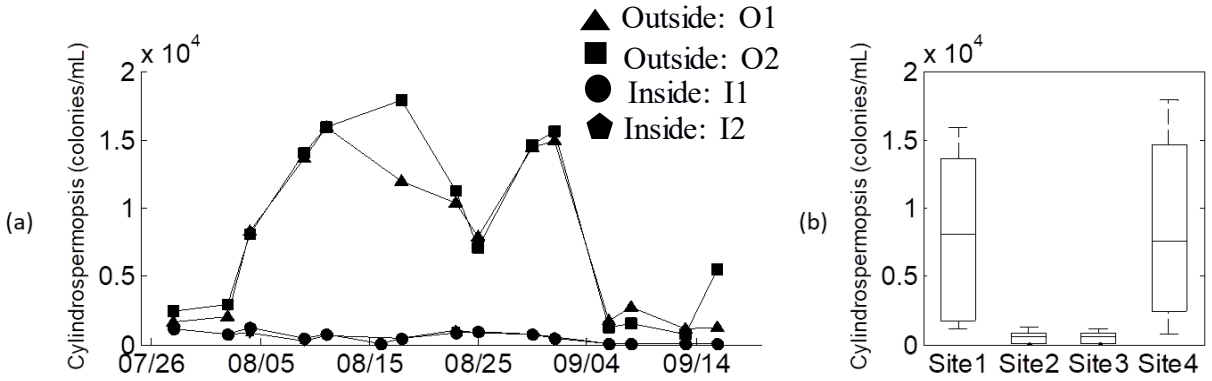

Fig 4-8. Time series of (a) *Cylindrospermopsis* sp. and (b) box plot at the outside sample site O1 (triangle symbol) and site O2 (square symbol) and the inside sample site I1 (solid circle) and site I2 (pentagon symbol).

4.4 Discussion

4.4.1 Beaches in the Yahara River Chain of Lakes

WETS was successfully deployed and implemented at Brittingham Beach, WI, in 2011. Due to strong support and further demand from the communities in the Yahara River Chain of Lakes, WI, WETS was thereby implemented at other beaches including Bernie's Beach in Lake Monona, in 2012, Mendota County Park Beach in Lake Mendota in 2016, and Goodland County Park Beach in Lake Waubesa in 2017 (see Fig. 1a). In comparison with WETS at Brittingham Beach, WETS at other beaches have different configurations of inlet and outlet to further enhance efficiency of water treatment. For example, it is found that two inlets on each side of the swimming area and one outlet pipe at the center inside the excloure can enhance mixing and reduce flushing time. From visual observations, young children are attracted to play with the flowing clean water at the center of beach. Another feature of WETS is the design of polypropylene barriers that can attenuate wave height of a range of up to 0.3 m (one foot). Overall, WETS installed and implemented at all beaches in the Yahara River Chain of Lakes all have delivered water quality improvement, in terms of cyanobacteria and *E. coli* results (not shown here for brevity). To date, no closures at all the WETS beaches have been issued and reported.

4.4.2 Economic costs and socio-economic benefits

WETS is typically deployed for a duration of 3.5 months in the summer, starting a week proceeding Memorial Day and removed a week after Labor Day. The electrical cost to operate WETS equates to an average of $5.91 per day or $579.18 per summer season. Other operational costs include labor to install/remove the exclosure, startup/winterization of the treatment system, and transportation of one portable trailer with the treatment system to be used at other beaches.

The capital costs including pump, strainer, sand filter, UV disinfection, PLC, cooling fan, electrical wiring, PVC pipes, trailer, polypropylene exclosure, and buoys was approximately 25,000 USD. For a larger treatment system, the capital cost for items such as the pump, strainer, sand filter, and polypropylene exclosure are estimated to linearly increase proportional to flow. In this study, WETS is capable of treating swimming water with a flow of 380 l/m. The cost for items such as PLC, cooling fan, electrical wiring, PVC pipes, and trailer would remain similar. In the first month of WETS operation at Brittingham Beach, the pump was shut down for maintenance. During the shutdown 5-day period, we continued to monitor water quality inside the swimming area. Results indicate water quality inside the exclosure remained excellent due to the barrier curtain that was effective in preventing outside lake water from polluting the swimming water, suggesting that continuous water treatment at a single beach is not necessary. Therefore, WETS inside the portable trailer can be moved to other beach sites to optimize the cost and early deployment may be considered to insure beaches are treated before opening. Overall, WETS is a cost-effective system to provide clean and safe swimming water at Brittingham Beach. Furthermore, the WETS project inspired the startup of a food/coffee shop and a rental store for water sport equipment (kayaks, canoes, paddleboards, sailboats, etc.) in 2012 at Brittingham Beach. From social-economic perspective, WETS has offered an incentive to local business development for revitalizing recreational park and provided benefits to the community with increased beach user activities.

4.5 Conclusions

Closures of Brittingham Beach at an inland freshwater lake in Wisconsin were frequently issued due to high levels of cyanobacteria and *E. coli* transported from onshore (resident geese) and offshore. An innovative Water Exclosure Treatment System (WETS) was designed and implemented. WETS consists of an “exclosure” with a five-sided polypropylene barrier that

excludes offshore lake contaminated water from the swimming area. Inside the exclosure, water was pumped to a portable filtration-ultraviolet treatment system. Computational fluid dynamics modeling with a Lagrangian particle-tracking method was employed that provided flushing time to determine sizing of sand filters and evaluation of efficiency of UV disinfection and aid in the design of the inlet and outlet locations for the pump network of the treatment system. It was found that the design of inlet and outlet locations play an important role on efficiency of lake water treatment. Specifically, residence time maps and flushing times range from 1.89 days (deep inlet with deep outlet) to 0.67 days (middle inlet and shallow outlet). Installation of WETS required a crew of two barges and two boats totaling 6 people and 18 person-hours. Water samples were tested two times per week during the study period. Water sampling showed that cyanobacteria and *E. coli* levels were 30 and 16 times lower inside the swimming area, respectively as compared to outside lake water. ANOVA testing reinforced that WETS created an environment that improves water quality significantly different from the outside lake water. After the success of implementing WETS in Brittingham Beach in 2011, WETS was deployed at other three beaches in the Yahara River Chain of Lakes (see Fig. 1) including Bernie's Beach in 2012 to 2017, Mendota County Beach in 2016 to 2017, and Goodland County Beach in 2017. Prior to WETS deployment at Bernie's Beach, Mendota County Beach, and Goodland County Beach, closings averaged 5, 8, and 16 days per year, respectively. Outcomes for other others are similar, in terms of excellent water quality improvement. To date, no closures at the WETS implemented beaches have been issued and reported. WETS provides safe, clean water inside the exclosure for minimizing beach closure, which has proved to promote social-economic benefits.

4.6 Acknowledgements

This study has been funded by the City of Madison, Wisconsin, Dane County Land and Water Resources Department (DCLWRD), and College of Engineering at University of Wisconsin-Madison. Specifically, we thank Mr. Robert Phillips, City Engineer, and Mr. Greg Fries, Principal City Engineer, for their support of the WETS project. We also thank Mr. Kevin Connors, former Director at DCLWRD, for continuously promoting WETS throughout the Yahara River Chain of Lakes. Furthermore, tremendous efforts in installing and removing the exclosure curtains led by Joseph Yaeger, Joseph Taylor, and Jon Ninnemann at DCLWRD are greatly acknowledged. Last but not least, the authors thank staff at PHMDC for their in-kind support to monitor beach water quality for public safety.

4.7 References

Abbas, H., Nasr, R., Seif, H., 2006. Study of waste stabilization pond geometry for the wastewater treatment efficiency. Ecological Engineering 28, 25-34.

Aragones, L., Lopez, I., Palazon, A., Lopez-Ubeda, R., Garcia, C., 2016. Evaluation of the quality of coastal bathing waters in Spain through fecal bacteria *Escherichia coli* and *Enterococcus*. Science of the Total Environment 566-567, 288-297.

Araujo, S., Henriques, I.S., Leandro, S.M., Alves, A., Pereira, A., Correia, A., 2014. Gulls identified as major source of fecal pollution in coastal waters: A microbial source tracking study. Science of the Total Environment 470-471, 84-91.

Ashbullby, K.J., Pahl, S., Webley, P., White, M.P., 2013. The beach as a setting for families' health promotion: a qualitative study with parents and children living in coastal regions in southwest England. Health & Place 23, 138–147.

Badgley, B.D., Ferguson, J., Vanden Heuvel, A., Kleinheinz, G.T., McDermott, C.M., Sandrin, T.R., Kinzelman, J., Junion, E.A., Byappanahalli, M.N., Whitman, R.L., Sadowsky, M.J. 2011. Multi-scale temporal and spatial variation in genotypic composition of *Cladophora*-borne *Escherichia coli* populations in Lake Michigan. Water Research 45, 721-731.

Brownell, M.J., Harwood, V.J., Kurz, R.C., McQuaig, S.M., Lukasik, J., Scott, T.M., 2007. Confirmation of putative stormwater impact on water quality at a Florida beach by microbial source tracking methods and structure of indicator organism populations. Water Research 41, 3747-3757.

Bugucki, D.J., Jones, B.H., Carr, M.E., 2005. Remote measurements of horizontal eddy diffusivity. Journal of Atmospheric and Oceanic Technology 22 (9): 1373-1380.

Cadmus Group, 2011. Total maximum daily loads for total phosphorus and total suspended solids in the Rock River basin. Prepared for U.S. Environmental Protection Agency and Wisconsin Department of Natural Resources.

Carmichael, W.W., Azevedo, S.M., An, J.S., Molica, R.J.R., Jochimsen, E.M., Lau, S., Rinehart, K.L., Shaw, G.R., Eaglesham, G.K., 2001. Human fatalities from cyanobacteria: Chemical and biological evidence for cyanotoxins. Environmental Health Perspectives 109 (7), 663-668.

Cerejo, M., Dias, J.M., 2007. Tidal transport and dispersal of marine toxic microalgae in a shallow, temperate coastal lagoon. Marine Environmental Research 63, 313-340.

Chen, C., Liu, H., and Beardsley, R.C., 2003. An unstructured grid, finite-volume, three-dimensional, primitive equations ocean model: Application to coastal ocean and estuaries. Journal of Atmospheric and Oceanic Technology 20 (1), 159-186.

Chorus, I. and Bartram, J., 1999. Toxic Cyanobacteria in water. World Health Organization, London, 416 pp.

Converse, R.R., Kinzelman, J.L., Sams, E.A., Hudgens, E., Dufour, A.P., Ryu, H., Santo-Domingo, J.W., Kelty, C.A., Shanks, O.C., Siefring, S.D., Haugland, R.A., Wade, T.J., 2015. Dramatic improvements in beach water quality following gull removal. Environmental Science and Technology 46, 10206-10213.

DeFlorio-Barker S., Wade T.J., Jones R.M., Friedman L.S., Wing C., Dorevitch S., 2017. Estimated costs of sporadic gastrointestinal illness associated with surface water recreation: a combined analysis of data from NEEAR and CHEERS studies. Environmental Health Perspectives 125, 215–222.

Delpeche-Ellmann, N.C., Soomere, T., 2013. Investigating the marine protected areas most at risk of current-driven pollution in the Gulf of Finland, the Baltic Sea, using a Lagrangian transport model. Marine Pollution Bulletin 67, 121-129.

Dorfman, M. and Haren, A., 2013. Testing the Waters. 23rd Edition. Report for the Natural Resources Defense Council. http://www.nrdc.org/water/oceans/ttw/titinx.asp

Dufour, A.P., 1984. Bacterial indicators of recreational water quality. Canadian Journal of Public Health 75, 49-56.

Dufour A.P., Cabelli, V.J, 1986. Ambient Water Quality Criteria for Bacteria–1986. U.S. Environmental Protection Agency. EPA-440/5-84-002.

Dwight, R.H., Fernandez, L.M., Baker, D.B., Semenza, J.C., Olson, B.H., 2005. Estimating the economic burden from illnesses associated with recreational coastal water pollution – a case study in Orange County, California. Journal of Environmental Management 76 (2), 95-103.

Dyer, K.R., 1973. Estuaries, a physical introduction. John Wiley and Sons, New York, 109.

Englebert, E.T., McDermott, C., Kleinheinz, G.T., 2008. Effects of the nuisance algae, *Cladophora*, on *Escherichia coli* at recreational beaches in Wisconsin. Science of the Total Environment 404, 10-17.

Falconer, I.R., 1999. An overview of problems caused by toxic blue-green algae (cyanobacteria) in drinking and recreational water. Environmental Toxicology 14, 5-12.

Fisher, H.B., List E.J., Koh, R.C.Y., Imberger, J., Brooks, N.H., 1979. Mixing in inland and coastal waters. Academic Press, London.

Geyer, W.R., Morris, J.T., Pahl, F.G., Jay, D.A., 2000. Interaction between physical processes and ecosystem structure: A comparative approach In Hobbie, J.E., Estuarine science: A synthetic approach to research and practice. Island Press. P 177-206.

Given, S., Pendleton, L.H., Boehm, A.B., 2006. Regional public health cost estimates of contaminated coastal caters: A case study of Gastroenteritis at Southern California beaches. Environmental Science and Technology 40, (16): 4851-4858.

Gomez-Gesteira, M., Montero, P., Prego, R., Taboada, J.J., Leitao, P., Ruiz-Villarreal, M., Neves, R., Perez-Villar, V., 1999. A two-dimensional particle tracking model for pollution dispersion in A Coruna and Vigo Rias (NW Spain). Oceanologica Acta 22 (2), 167-177.

Hernandez, R.J., Hernandez, Y., Jimenez, N.H., Piggot, A.M., Klaus, J.S., Feng, Z., Reniers, A., Solo-Gabriele, H.M., 2014. Effects of full-scale beach renovation on fecal indicator levels in shoreline sand and water. Water Research 48, 579-591.

Houston, J.R., 2008. The economic value of beaches - a 2008 update. Shore & Beach 76 (3), 22–26.

Kasat, G.R., Khapkar, A.R., Ranade, V.V., Pandit, A.B., 2008. CFD simulation of liquid-phase mixing in solid-liquid stirred reactor. Chemical Engineering Science 63, 3877-3885.

Kimura, N., Wu, C.H., Hoopes, J.A., Tai, A., 2016. Diurnal dynamics in a small shallow lake under spatially nonuniform wind and weak stratification. Journal of Hydraulic Engineering ASCE 142(11).

Kinzelman, J., Pond, K., Longmaid, K., Bagley, R., 2004. The effect of two mechanical beach grooming strategies on *Escherichia coli* density in beach sand at a southwestern Lake Michigan beach. Aquatic Ecosystems Health Management 7, 425-432.

Kleinheinz GT., 2003. Microbial contamination of Wisconsin's recreational waters. Wisconsin Academic Science Arts Lett, 90:75–86.

Kleinheinz, G.T., Englebert, E., 2005. Cladophora and the beach: implications for public health. Cladophora Research and Management in the Great Lakes. Great Lakes Water Institute Special Report; No. 2005-01.

Kleinheinz, G.T., McDermott, C.M., Leewis, M.C., Englebert, E.T., 2006. Influence of sampling depth on Escherichia coli concentrations in beach monitoring. Water Research 40:3831-3837.

Lathrop, R.C., Reimer, J.R., Sorsa, K.K., Steinhorst, G.M., Wu, C.H., 2013. Madison's lake beaches - results of a three-year pilot study, Lakeline 33 (3), 31-38.

Lee, C., Marion, J.W., Lee, J., 2013. Development and application of a quantitative PCR assay targeting *Catellicoccus marimammalium* for assessing gull-associated fecal contamination at Lake Erie beaches. Science of the Total Environment 454-455, 1-8.

Lee, C.S., Lee, C., Marion, J., Wang, Q., Saif, L, Lee, J., 2014. Occurrence of human enteric viruses at freshwater beaches during swimming season and its link to water inflow. Science of the Total Environment 472, 757-766.

Lemmin, U., 1989. Dynamics of horizontal turbulent mixing in a nearshore zone of Lake Geneva. Limnology and Oceanography 34 (2), 420-434.

Lin, Y.T., Schuettpelz, C.C., Wu, C.H., and Fratta, D., 2009 A combined acoustic and electromagnetic wave-based techniques for bathymetry and subbottom profiling in shallow waters. Journal of Applied Geophysics. 68 (2), 203-218.

Liu, D., Wu, C.H., Linden, K., Ducoste, J., 2007. Numerical simulation of UV disinfection reactors: evaluation and alternative turbulence models. Applied Mathematical Modelling 31 (9), 1753-1769.

Liu, W.C., Chen, W.B., Kuo, J.T., and Wu, C.H., 2008. Numerical determination of residence time and age in a partially mixed estuary using three-dimensional hydrodynamic model. Continental Shelf Research, 28(8), 1068-1088.

Lowe, S.A., 2008. Case study of a marine filter curtain system for coliform reduction at a public beach. Journal of Environmental Engineering 134 (1), 60-66.

Lyn, D.A., Chiu, K., Blatchley III, E.R., 1999. Numerical modeling of flow and disinfection in UV disinfection channels. Journal of Environmental Engineering ASCE 125, 17-26.

McLellan, S.L, Salmore, A.K., 2003. Evidence for localized bacterial loading as the cause of chronic beach closings in a freshwater marina. Water Research 37, 2700-2708.

Monsen, N.E., Cloern, J.E., Lucas, L.V., Monismith, S.G., 2002. A comment on the use of flushing time, residence time, and age as transport time scales. Limnology and Oceanography 47 (5), 1545-1553.

Patz, J.A., Vavrus, S.J., Uejio, C.K., McLellan, S.L., 2008. Climate change and waterborne disease risk in the Great Lakes Region of the U.S. American Journal of Preventive Medicine 35 (5): 451-458.

Perianez, R., 2004. A particle-tracking model for simulating pollutant dispersion in the Strait of Gibraltar. Marine Pollution Bulletin 49, 613-623.

Prandle, D.A., 1984. A modeling study of the mixing of 137Cs in the sea of the European continental shelf. Philosphical Transaction of the Royal Society of London 310, 407-436.

Pruss, A., 1998. Review of epidemiological studies on health effects from exposure to recreational water. International Journal of Epidemiology 27 (1): 1-9.

Przybyla-Kelly, K., Nevers, M.B., Breitenbach, C., Whitman, R., 2013. Recreational water quality response to a filtering barrier at a Great Lakes beach. Journal of Environmental Management 129, 635-641.

Rabinovici, S.J.M., Bernknopf, R.L., Coursey, D.L., Wein, A.M., Whitman, R.L., 2004. Economic and health risk trade-offs of swim closures at a Lake Michigan beach. Environmental Science and Technology 38 (10), 2737-45.

Rehmann, C.R., Duda, T.F., 2000. Diapycnal diffusivity inferred from scalar microstructure measurements near the New England shelf/slope front. Journal of Physical Oceanography, 30, 1354–1371.

Reimer, J.R., Wu, C.H., 2016. Development and application of a nowcast and forecast system tool for planning and managing a River Chain of Lakes. Water Resources Management, 30: 1375-1393.

Rodi, W. 1987. Examples of calculated methods for flow and mixing in stratified flows. Journal of Geophysical Research, 92, 5305-5328.

Sabino, R., Rodrigues, R., Costa, I., Carneiro, C., Cunha, M., Duarta A., Faria, N., Ferreira, F.C., Gargate, M.J., Julio, C., Martins, M.L., Nevers, M.B., Oleastro, M., Solo-Gabriele H., Verissimo, C., Viegas, C., Whitman, R.L., Brandao, J., 2014. Routine screening of harmful microorganisms in beach sands: Implications to public health. Science of the Total Environment 472, 1062-1069.

Sahu, A.K., Kumar, P., Patwardhan, A.W., Joshi, J.B., 1999. CFD modelling and mixing in stirred tanks. Chemical Engineering Science 54, 2285-2293.

Shen, J., Haas, L., 2004. Calculating age and residence time in the tidal York River using three-dimensional model experiments. Estuarine, Coastal and Shelf Science 61, 449-461.

Sozzi, D.A. and Taghipour, F., 2006. UV reactor performance modeling by Eularian and Lagrangian methods. Environmental Science and Technology 40, 1609-1615.

Speziale, B.J., Dyck, L.A., 1992. Lyngbya infestations: comparative taxonomy of Lyngbya wollei comb. nov. (cyanobacteria). Journal of Phycology 28, 693–706.

Turner, P.C., Gammie, A.J., Hollinrake, K., Codd, G.A., 1990. Pneumonia associated with contact with cyanobacteria. British Medical Journal 300, 1440-1441.

Umlauf, L., Burchard, H., 2005. Second-order turbulence closure models for geophysical boundary layers. A review of recent work. Continental Shelf Research 25 (7-8), 795-827.

USEPA, 2014. National Beach Guidance and Required Performance Criteria for Grants, 2014 Edition. U.S. Environmental Protection Agency. EPA-823-B-14-001.

Wade, T.J., Pai, N., Eisenberg, J.N.S., Colford, J.M., 2003. Do U.S. Environmental Protection Agency water quality guidelines for recreational waters prevent gastrointestinal illness? A systematic review and meta-analysis. Environmental Health Perspectives 111 (8), 1102-1109.

Wheeler, B.W., White, M., Stahl-Timmins, W., Depledge, M.H., 2012. Does living by the coast improve health and wellbeing? Health & Place 18 (5), 1198–1201.

Whitman R.L., Shively D.A., Pawlik H., Nevers M.B., Byappanahalli M.N.. 2003. Occurrence of Escherichia coli and Enterococci in Cladophora (Chlorophyta) in near shore water and beach sand. Applied and Environmental Microbiology 69, 4714–4719.

Wiegand, C., Pflugmacher, C., 2005. Ecotoxicological effects of selected cyanobacterial secondary metabolites a short review. Toxicology and Applied Pharmacology 203, 201-218.

Winfield, M.D. and Groisman, E.A., 2003. Role of nonhost environments in the lifestyles of Salmonella and *Eschericia coli*. Applied and Environmental Microbiology 69, 3687-3694.

WDNR, 2000. Wisconsin beach health frequently asked questions. https://www.wibeaches.us/apex/f?p=181:5:171236131245 20::NO:::

Wong, M., Kumar, L., Jenkins, T.M., Xagoraraki, I., Phanikumar, M.S., Rose, J.B., 2009. Evaluation of public health risks at recreational beaches in Lake Michigan via detection of enteric viruses and a human-specific bacteriological marker. Water Research 43, 1137-1149.

Zimmerman, J.T.F., 1976. Mixing and flushing of tidal embayments in the Western Dutch Wadden Sea, Part I: distribution of salinity and calculation of mixing time scales. Netherlands Journal of Sea Research 10, 149-191.

5. Impacts of Legacy Phosphorus in Streams on Water Quality before and after Dredging

The following is in preparation to be submitted to *Journal of Environmental Management*.

5.1 Introduction

Legacy phosphorus (P), often referred to as accumulated P in agricultural soils, can deteriorate water quality, posing health risks of livestock wildlife, pets, and humans (Turner et al., 1990; Tanner et al., 1995; Chorus and Bartram, 1999; Falconer, 1999; Charmichael et al., 2001). Legacy in surface waters (e.g., lakes and streams) with high P levels can cause eutrophication of freshwater systems resulting in seasonal hypoxia and harmful algal bloom (HAB) which can introduce toxins into drinking-water supplies (Michalak et al., 2013; Sayers et al., 2016) and pose a threat to public health in recreation waters and beaches (Reimer and Wu, 2018). To address issues of P on water quality, the United States Environmental Protection Agency (EPA) established the Total Maximum Daily Load (TMDL) to regulate the maximum amount of P that a water body can receive and meet water quality targets. While P loads under the TMDL can be reduced as point and nonpoint sources of pollution, legacy P in watershed uplands and stream beds can be remobilized or leached as a continuous source to downstream surface waters for years, decades, or even centuries (McDowell et al., 2002). As a result, the time lag between the TMDL reduction in P loads and improvement of downstream surface water quality threaten stream health (Haygarth et al., 2014; Sharpley et al., 2013; Powers et al., 2016). Also, the leaching of legacy P results in delayed water quality improvements following significant economic investments for TMDL reductions on upland sources, resulting in increased public pressure on government and watershed organizations to respond (Sharpley et al., 2013).

Water quality related to legacy P in streams can be influenced by physical, chemical, and biological processes. Water quality may be degraded by physical processes that accumulate legacy P as deposition of particulate or suspended P sediments to stream beds (Owens and Walling, 2002; Ballantine et al., 2009; Rawlins, 2011) with milder slopes and lower overlaying flow velocities (Sharpley et al., 2013) and turbulence (Wood and Armitage 1997). On the other hand, improvement of water quality is found when stream P is dispersed due to erosion of particulate P under high velocities (Dorioz et al., 1989; Drake et al., 2012). Water quality is affected by legacy P through chemical processes like sorption of dissolved P in the water column to bed sediments depending on pH and redox conditions (Reddy et al., 1999; Haggard et al., 2001; Withers and Jarvie, 2008; Stutter et al., 2010). Alternatively, P is diffused due to desorption of dissolved P if the water column P concentrations are lower than P source in stream beds (House and Denison, 2000; Haggard et al., 2005; Hamilton, 2012). Water quality altered by biological processes like microbial activities commonly occurred in shallow stream environments with good light penetration (e.g., pools, eddies) can impact recycling of legacy P in bed sediments. When microbial cells become anaerobic or decompose as a result of enhanced rates of organic matter breakdown, anoxia in the bed sediments and the release of polyphosphate, can degrade water quality due to release of legacy P (Ensign and Doyle, 2005; Hupfer et al., 2007; Withers and Jarvie, 2008). Overall, understanding processes that alter legacy P is important to improve agricultural sustainability and mitigate water quality deterioration.

For several decades, efforts for improving stream water quality have been implemented and the outcome has been compromised due to legacy P (Sharpley et al., 2013). Reduction of nonpoint source pollution from uplands has been successfully addressed by field management practices (e.g., cover crops, no tillage, fertilizer reductions) and watershed management practices

(e.g., converting land use, creating detention ponds, and meandering stream networks). Nevertheless, the intent of reducing load downstream by these practices results in P accumulation, leading to erosion and diffusion of legacy P to the stream later in time as an unintended source. As a result, legacy P may mask or buffer the benefits of upland practices (Meals et al., 2010; Hamilton, 2012; Spears et al., 2012). Several strategies have been successful to remediate P by altering crop rotations (Zhang et al., 2004; Dodd and Mallarino, 2005; Sharpley et al., 2004), protecting streambanks (Meals and Hopkins, 2002), restoring and dredging wetlands (Oldenborg and Steinman, 2019), and adding alum to lakes (Huser et al., 2011). However, no study on remediation of legacy P in stream sediments by dredging has been reported to date, as far as the authors are aware.

The objective of this paper is to investigate the impacts of legacy phosphorus in streams on water quality before and after dredging stream sediments in an agricultural watershed. First, the age of legacy P in stream sediments was evaluated by radionuclide dating testing. Next, P analysis in the field and laboratory was conducted to determine the role of legacy P on water quality impact. Specifically, field mesocosm experiments were carried out to measure P release before and after dredging. Laboratory microcosm testing was carried out to determine rates of P diffusion. Results of water quality response before and after dredging were presented. Achieving TMDL regulations, impacts to hydrologic functions, and enhancements to ecology and recreation are discussed.

5.2 Materials and methods

5.2.1 Study site

The study site is Dorn Creek, located at north of Madison in Dane County, WI (Fig 5-1). The Dorn Creek watershed is 32.6 square kilometers, comprised of 78% agricultural and 16%

wetland land use (Lathrop et al. 1998). The length of Dorn Creek is 6 km, exhibiting three distinct slope characteristics of 0.24% upstream, 0.41% middle, and 0.046% downstream between S1 and S2. A large wetland complex consisting of soil types Houghton muck and Wacousta silt clay loam is located between S1 and S2 on the creek that provide wildlife habitat and spawning for northern pike. The outlet of downstream Dorn Creek connects to Lake Mendota with water level regulated by Tenney Dam, As a result, Dorn Creek is subjected to backwater levels of Lake Mendota that influences release of flow, sediments, and nutrients (Reimer and Wu, 2016).

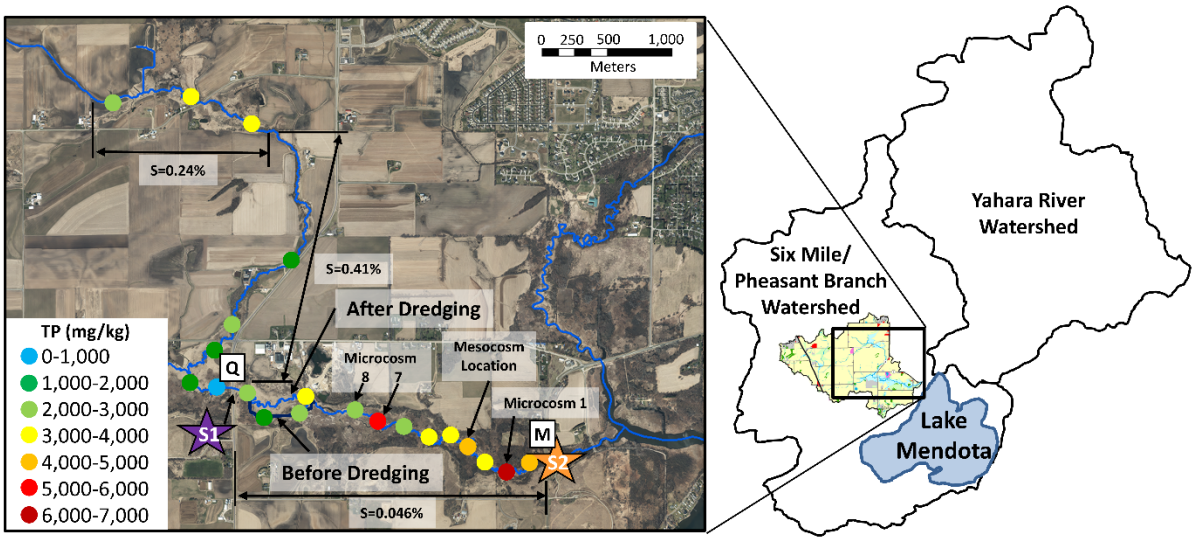

Fig 5-1. The study site is located at Dorn Creek in Dane County, Wisconsin. Circles show sampling location with colors representing P concentrations in stream sediments. Long term gage stations were installed upstream of study site at Highway Q called S1 and downstream at Highway M called S2 to measure water quality and quantity. Three slope (S) locations are shown which represent the average stream bed slope. The locations of microcosm and mesocsom experiments are shown.

Water quality issues in Dorn Creek continue to be of concerns despite many field and watershed practices. The average annual P loading from 1989 to 1998 was 2,097 kg. A TMDL load allocation of 238 kg or a 91% reduction was thereby determined (Cadmus Group, 2011). In 1993, the Mendota Priority Watershed was initiated to install conservation practices to reduce

runoff from barnyards, farm fields, and streambanks (Betz et al., 2000). Most recently in 2016, a Yahara Watershed Improvement Network formed a partnership among Madison Metropolitan Sewerage District, Dane County, area cities, villages, towns, and environmental, farm, and business groups to meet regulatory TMDL requirements of phosphorus loads (MMSD, 2017). Specifically, a four-year pilot project (MMSD 2012) took a collaborative approach to implement cost effective phosphorus controls with over 800 conservation practices (e.g., conservation tillage, waterways, roofs over barnyards). Despite these efforts, Dorn Creek is still on the 303(d) list, referred to as Wisconsin's list of impaired and threatened water list due sediment loading impacting aquatic habitat, E. coli impacting recreation, and high levels of phosphorus.

5.2.2 Field Measurements

5.2.2.1 Sediment sampling

A total of 58 sediment cores with depths ranging from 40.6 to 106.7 cm were acquired underwater near the left bank, thalweg, or right bank. Specifically, 43 sediment cores were obtained at 8 cross sections within the low slope (0.046%) of Dorn Creek located 0.3 to 1.3 km upstream of highway M in March 2015 and December 2015. In March 2018 and September 2019, 15 sediment cores were taken at 13 cross sections to characterize the remaining 6 km of Dorn Creek as shown in Fig 5-1. The procedure for collecting sediment samples is described as follows. A modified piston coring apparatus made of a polycarbonate tube measuring 1.5-m long and 3.8-cm diameter (Fisher et al., 1992; Steinman et al., 2004) was driven into the stream bed sediments by hand until refusal. Retrieval of sediment samples was conducted by placing a rubber stopper at the waterline to create suction to prevent sediment from falling out of the tube. Sediment cores were stored in an upright position during transport. Stratigraphic layers of sediment classification

were identified by pushing a stop plug into the tube to extract the layer samples in heights of 15 cm. The remaining sample was left in the acrylic tube or pushed out to a tray and stored in plastic containers for later laboratory testing.

5.2.2.2 Water sampling

Continuous water samples were taken for total phosphorus and soluble reactive phosphorus (Valderrama, 1981; Hosomi and Sudo, 1986; D'Elia et al., 1997). Specifically, an automated ISCO sampler was installed at highway Q (S1) and highway M (S2) to collect water samples during base flow and rainfall events. From 2013 to 2019, 749 and 677 water samples were collected at S1 and S2, respectively. Sampling intervals ranged from 1 minute to 43 days and averaged 3.6 days. Daily P loads and concentrations were generated using the Graphical Constituent Loading Analysis System (Koltun et al., 2006). In addition, water temperature, DO, pH, and specific conductance at the water surface and near bottom were measured using a YSI 6600 sonde (YSI Incorporated, Yellow Springs, OH).

5.2.2.3 Mesocosms

Three mesocosm experiments were conducted in the field before and after dredging with a 6-day period starting November 14, 2016 at 7:00 a.m. Fig 5-2 shows the mesocosm set up using clear acrylic core tubes that are 1.83 meters long and 14.0 cm diameter driven 0.6 meters deep in the streambed to simulate natural conditions (Zhou et al., 2016) Water inside the mesocosms is prevented from contact with outside surface water (Jerauld et al., 2020) but is in contact with bottom sediments and exposed at the top to the atmosphere (Stephen et al., 2004). To minimize disturbance of bottom sediments when sampling, a peristaltic pump connected to a 12.7 mm

transparent polyvinyl chloride tubing withdrew water from within the top 15 cm of the mesocosm. Before dredging, water samples were collected to verify the mesocosm experiment inside (green) represent the outside natural environment (red) as shown in Fig 5-2. After dredging, water samples were collected from the mesocosms to compare differences between before dredging stream water (light blue) and clean distilled water (blue). TP and SRP of water samples were analyzed in the laboratory.

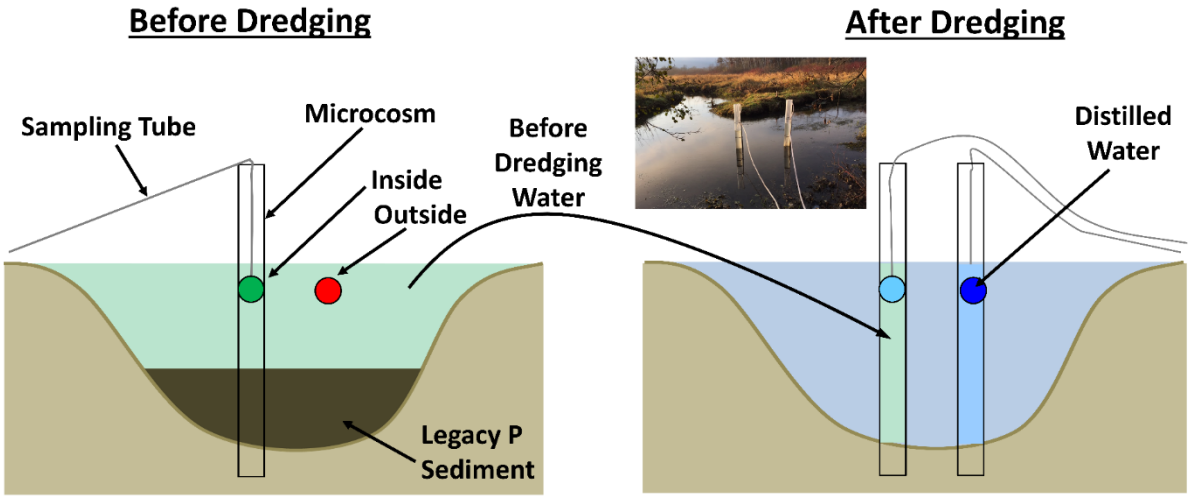

Fig 5-2. Mesocosm experiments were conducted before dredging (left) with water sampling performed inside (green) and outside (red). After dredging (right), mesocosm were installed using water before dredging (light blue) and distilled water (blue).

5.2.3 Laboratory experiments

5.2.3.1 Radionuclides

Radionuclide activities were determined based upon 4 cm spaced slices of the sediment core for Beryllium-7 (Be-7), Cesium-137 (Cs-137), Lead-210 (Pb-210), and Radium-226 (Ra-226) (Abril, 2003; Van Metre et al., 2004). Unsupported or excess Pb-210 was determined by subtracting total Pb-210 from Ra-226 (Appleby and Oldfield, 1992). Procedures for testing samples are similar to previous studies (McMurtry et al., 1995; Van Metre et al., 2004; Evrard et

al., 2010) and briefly summarized as follows. All sediment samples were freeze dried, ground with mortar and pestle, and sealed into polypropylene containers to insure no radon gas leaked out. The sealed containers were allowed to incubate for at least 30 days to allow Radium-226 and Radon-222 to reach secular equilibrium. Afterwards, samples were counted on a low energy high purity germanium planar detector from Canberra (Mirion Technologies) with Genie 2000 data acquisition software until a detection limit of 0.75 pCi/g or less was achieved for the Pb-210 activity. All samples were corrected to the date of sample collection. Quality control samples were counted for a Ra-226, CS-237, Pb-210, K-40 standard and a blank standard (Van Metre et al., 2004).

5.2.3.2 Microcosms

Laboratory microcosm experiments were performed to measure P diffusion from stream sediment samples following the method described in James and Barko (1991). A total of 10 of 43 cores collected in 2015 were used to make 12 microcosms, consisting of various sediment layers (surface, 15 cm, and 30 cm) to relate corresponding P release rates under aerobic and anaerobic conditions. Under aerobic conditions, 10 microcosms were made from 9 cores of stream sediment and 1 blank core without sediment. Under anaerobic conditions, 4 microcosms were made from 3 cores with sediment and 1 core without. P diffusion tests are briefly summarized in the following. The overlying water was drained from each sediment core and replaced with water collected at the site, filtered through a glass fiber (Whatman GF/A). Then the sediment core tubes were sealed with rubber stoppers and placed in a darkened environmental chamber (Psychrotherm) and incubated at 20°C for 10 days. The oxidation-reduction environment was controlled by gently bubbling air (aerobic) or nitrogen (anaerobic) through an air stone placed just above the sediment surface. Water samples were collected daily from the center of each incubation system and

replaced by site water filtered through a glass fiber (Whatman GF/A). The water volumes were measured to adjust SRP for dilution effects. Rates of SRP release from stream sediments (mg/(m2 day) were calculated as the change in SRP in the overlying water divided by time and the area of the sediment core liner.

5.2.4 Sediment age calculation

Sediment ages are calculated to understand stream sediment dynamics (Binford, 1990; Appleby and Oldfield, 1992; Holmes, 1998; Abril, 2003). Potential longevity of sediment dredging was estimated using Cs-137 and unsupported Pb-210. Cs-137 to provide a date marker correlating to the year 1963 due to peak atmospheric testing of nuclear weapons in the United States corresponding to peak Cs-137 activity in undisturbed sediment cores (Holmes, 1998). In this study, two models were used to calculate sediment age. The first model, Constant Initial Concentration (CIC), is based upon the assumption that Pb-210 activity in the uppermost layer of sediment is constant through time (Goldberg, 1963; Robbins, 1978). The second model, Constant Rate of Supply (CRS), assumes a constant flux of Pb-210 to the sediment surface through time (Goldberg, 1963; Robbins, 1978; Appleby and Oldfield, 1992).

5.2.5 Hydraulic dredging

In this study, legacy phosphorus in the stream was removed by hydraulic dredging during 5 months from June 2018 to October 2018. An amphibious hydraulic dredge that floats with its sealed tracks in the shallow stream water would self-propel using a hydraulic direct drive track system on land (Fig 5-3). The dredge was equipped with a wide track system to distribute ground pressure to minimize the impact on wetland land use surrounding Dorn Creek (dark green dashed

line in Fig 5-3). At the upstream, a creek plug was installed at approximately 300 m downstream of highway Q to prevent water back to the 2003 flood-routed path (blue color in Fig 5-3) that short circuited its adjacent wetland complex. Dredging was taken along the original stream to restore to the pre 2003 conditions. The hydraulic dredge was connected to an 8" high density polyethylene pipe (light blue line) that was 4.7 km long with a booster pump to discharge stream sediment into a 3 hectare dewatering basin (red polygon). At the dewatering basin sediment was trapped and effluent water was redirected back to the stream. Polymers were used as necessary to reduce total suspended sediment effluent concentrations to not exceed 40 mg/l above background stream levels. In spring 2019, the dewatering basin was the dredged sediments were capped by topsoil and seeded with prairie. Overall, a total of 18,050 cubic meters of sediments with an average depth of one meter of mucky sediments containing 34,050 kg of legacy phosphorus was removed from the upstream at highway Q to the downstream highway M (see Fig 5-3).

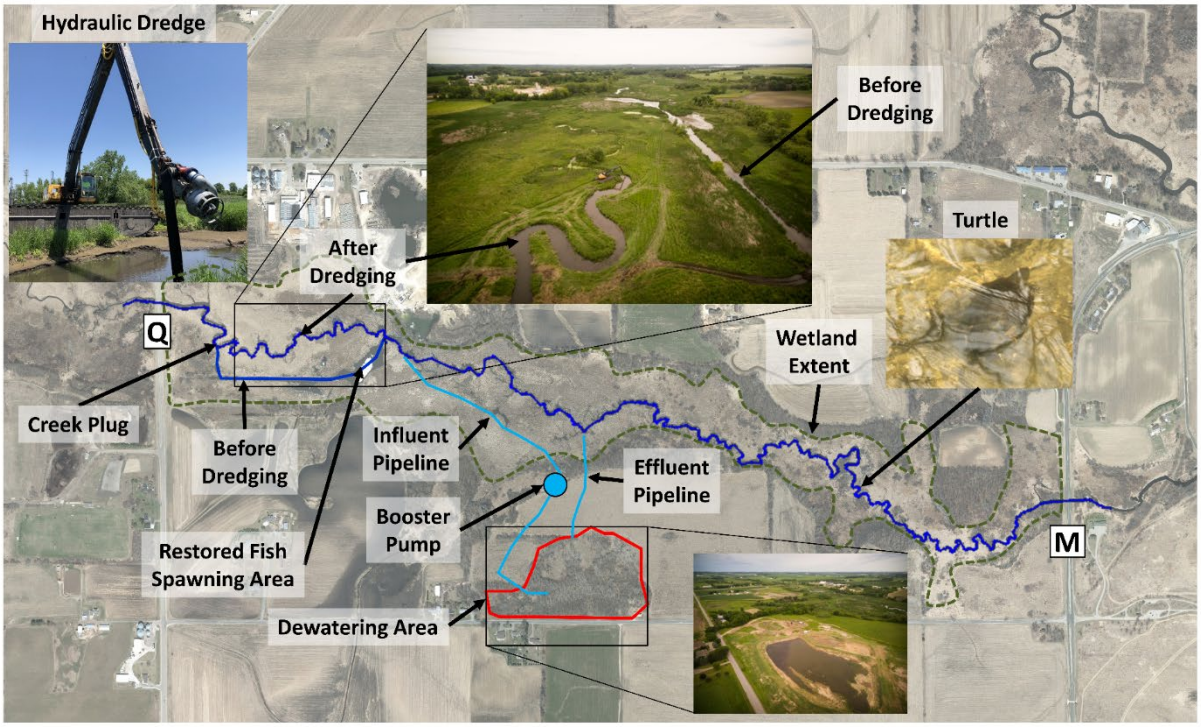

Fig 5-3. Hydraulic dredging schematic performed between Highway Q and M as shown in blue. Hydraulic dredge transports legacy P sediment through influent pipeline (light blue) to dewatering area (red) to trap sediment and clean water is discharged back to stream through effluent pipeline (light blue).

5.3 Results

5.3.1 Legacy P

A spatial map of TP concentrations in the top 5 cm of stream sediments is shown in Fig 5-1. Downstream of highway Q with a bed slope of 0.046%, TP concentrations are significantly higher than that upstream with bed slope of 0.42%. The result is consistent to previous studies that high phosphorus sediments are deposited in the low gradient stream locations (Hoffman et al., 2009; Rogers et al., 2009). In other words, low-slope of downstream Dorn Creek between highway Q and M are most likely the areas that may have legacy P.

Sediment age was calculated to reveal sediment dynamics and confirm the legacy P between highway Q and M. Be-7 was found only within the top 4 cm of each sediment core, indicating age deeper than 4 cm is greater than 1 year. Fig. 5-4a shows a depth profile versus age dating of Pb-210. At a depth of approximately 70 cm, sediment age is 1890. This date matches with the time when Tenney Dam on the downstream of Lake Mendota was built, suggesting that backwater of Lake Mendota may cause sediment deposition in Dorn Creek. At the depth of 50 cm, a dated age based upon Pb-210 is 1963, corresponding well to peak Cs-137 (black dot) at 45 cm, indicating good fit of the Pb-210, CRS model. As depth from 50 cm to near surface, the Pb-210 plot becomes steeper with increasing sediment depths in shorter time periods. Fig 5-4b shows sediment accumulation rates (black line). Starting in 1890 accumulation rates were near 0.1 cm/year and consistently increased to a peak rate of 1.1 cm/year in 1994. Accumulation steadily decreased to more than half to 0.5 cm/year of present day. A change in accumulation rates in 1994 appears one year after the Lake Mendota priority watershed initiatives to implement conservation practices in 1993. The change in accumulation rates suggest that these efforts to control sediment and erosion from upland agriculture sources provided great benefit. Lastly, cumulative mass rates were calculated using accumulation rates and sediment density as shown as the gray line in Fig 5-4b. Starting in the early 1900's the mass rate dramatically increases indicating deposition of heavy grained sediment particles compared to present day small changes of mass rate. Overall, the sediment age dating provides useful insight into the sediment dynamics of Dorn Creek that provides a depositional area accumulating legacy P since 1890.

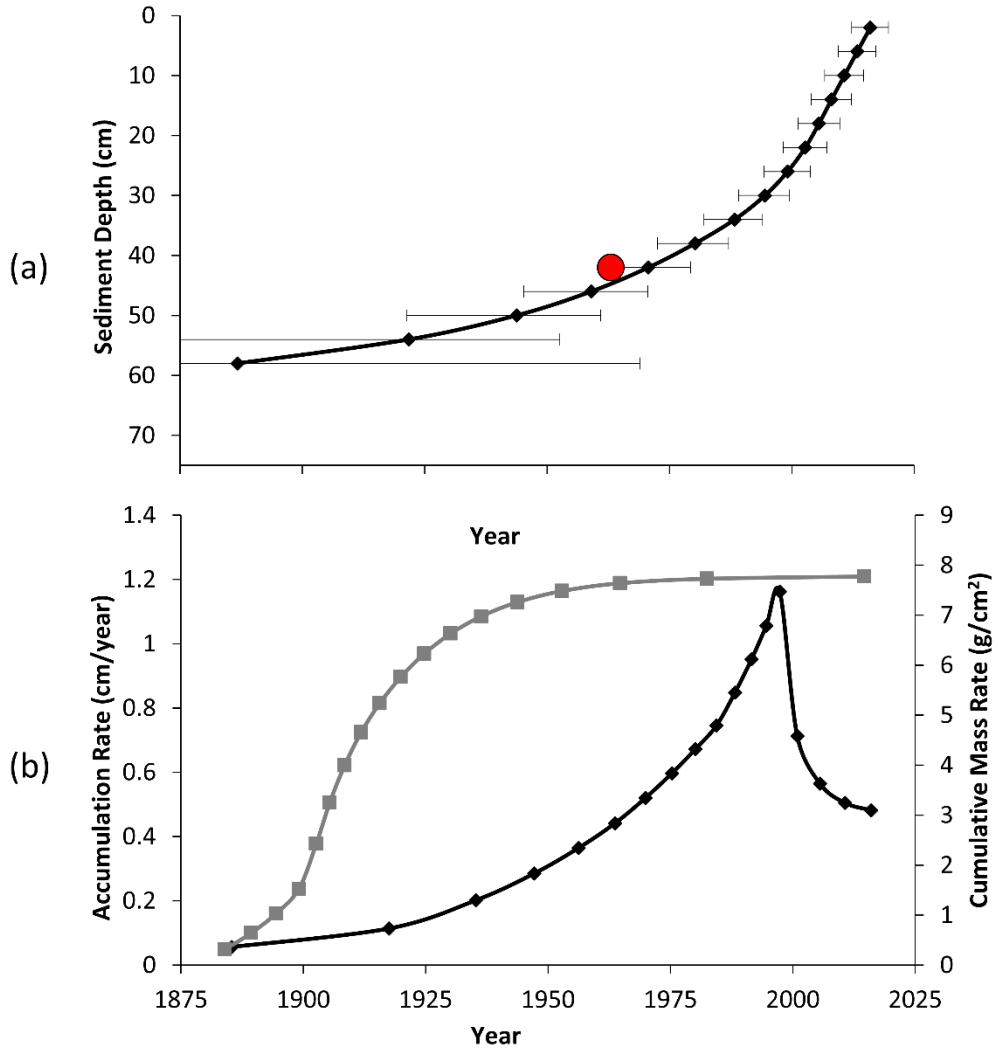

Fig 5-4. (a) Sediment Age calculated from PB-210 (line) and CS-137 peak value (red circle). The error bars represent measurement uncertainty (±1σ). (b) Sediment Accumulation (black) and Cumulative Mass Rate (gray).

5.3.2 Microcosm P diffusion

Microcosm P diffusion to evaluate water quality impacts before dredging is discussed here. Fig 5-5 shows that soluble reactive phosphorus (SRP) released from bottom sediments to stream water (solid lines) and SRP in only stream water (dashed lines) under both aerobic (cyan) and anaerobic (green) conditions. SRP released from both sediment samples (solid lines) at the surface

1(surface) with total P of 4,036 mg/kg and 0.15 m depth 1(0.15) with total P of 815 mg/kg are similar. Negligible differences of SRP 0.076 ~ 0.078 mg/l (see the solid lines), under peak aerobic and anaerobic conditions suggest that phosphorus release is independent of dissolved oxygen content. Spatially, sediment from sites 1 (square), 7 (triangle), and 8 (circle) as shown by location in Fig 5-1 are tested by microcosm experiments, revealing that sediment samples (solid lines) are larger than those in only stream water (dashed lines), confirming release of legacy P in Dorn Creek. SRP release rates from other sites show similar results and are not shown here for brevity.

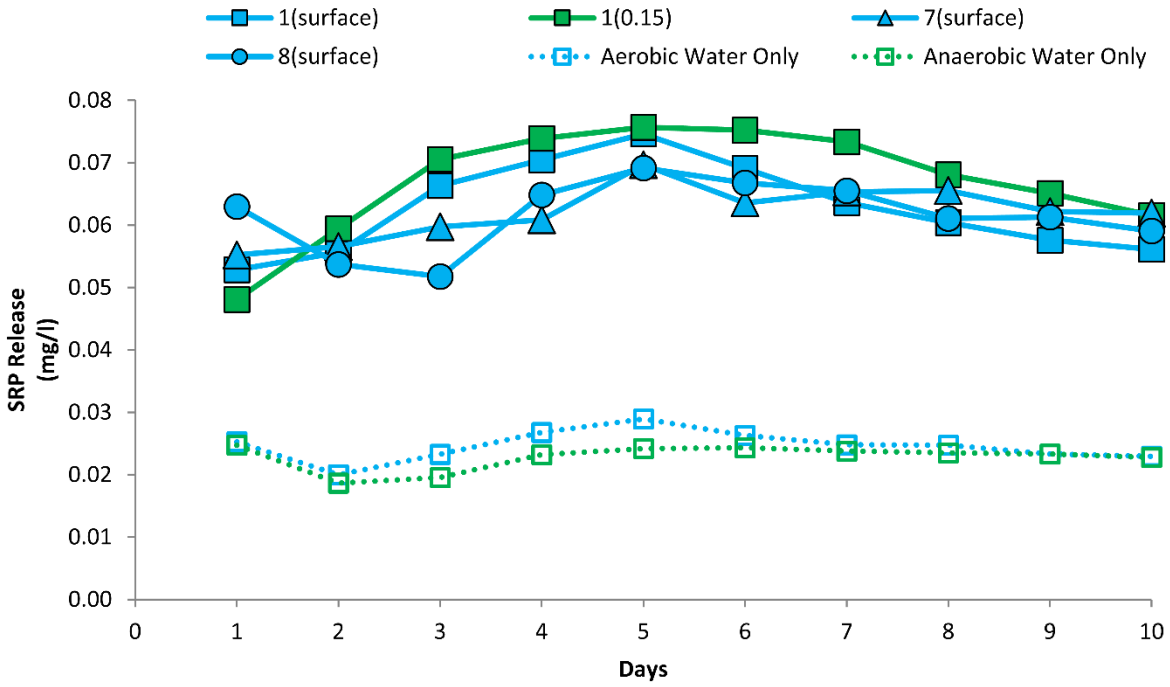

Fig 5-5. Microcosm soluble reactive phosphorus (SRP) release from surface sediments considering aerobic conditions (cyan) at site 1 (square), 7 (triangle), and 8 (circle). SRP release is also shown for subsurface sediment 0.15 m deep under anaerobic conditions (green) at site 1. Microcosms of water only without sediments under aerobic (cyan dashed line) and anaerobic (green dashed line) are shown.

5.3.3 Mesocosm P response

Water quality response before and after dredging based upon field mesocosm experiments are discussed here. For TP measurements in Fig 5-6a, results show that concentrations of ambient stream water (green line) are similar to those of water inside the mesocosm before dredging (red line), indicating the mesocosm testing condition can be representative to the corresponding ambient stream water condition before dredging. After dredging, TP concentrations of stream water inside the mesocosm (light blue line) decline from 0.18 mg/l to 0.06 mg/l (or a 3 times reduction) over a 5-day period, suggesting the effectiveness of dredging legacy P on water quality improvement. Furthermore, concentrations (dark blue line) of the mesocosm with distilled water added to mimic upstream clean water transported through the stream reach dramatically decrease to 0.02 mg/l at day 5, suggesting the negligible residues in the dredged stream beds. Fig 5-6b shows that the SRP concentrations obtained from the mesocosm experiments have similar trends of TPE results except for the 2/3 of the magnitude. It is noted that SRP is a large proportion and important to consider when evaluating and improving water quality due to bioavailability in producing algae.

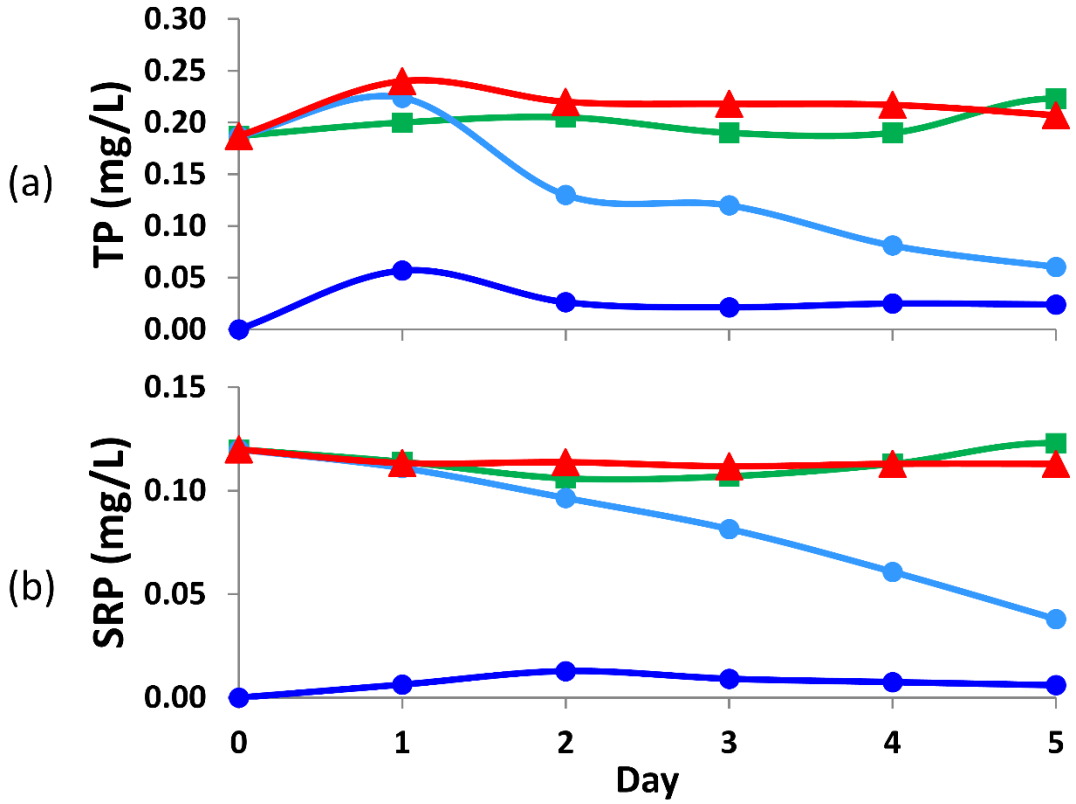

Fig 5-6. (a) Total phosphorus and (b) SRP concentrations comparing outside stream water (green), before dredging in mesocosm (red), after dredging in mesocosm (light blue), and after dredging with stream water replaced by distilled water in mesocosm (dark blue).

5.3.4 Stream water quality response

Water quality response was evaluated by comparing upstream (S1) and downstream (S2) gage station P loads and concentrations from 2013 to 2019. In Fig 5-7a, large variabilities in TP are witnessed, ranging from an annual load of 956 to 7,880 kg. From the seven years evaluated, the top two largest rainfall years are 2018 and 2019 which correspond to the top two largest P load years. In every year except 2019, the downstream (orange) loads are larger than upstream (purple) indicating the study site is releasing P downstream. In 2019, the stream was dredged and loads decreased suggesting the study site area has trapped P, reducing loads delivered downstream.

Specifically, in 2018 approximately 1,500 kg of TP was released followed by 800 kg trapped in 2019 after dredging shown in Fig 5-7b. Lastly, Fig 5-7c shows the median TP concentration calculated by the difference of upstream (S1) and downstream (S2) for three different time periods of annual (red), growing season (green), and spring melt (blue). The annual and growing median concentration difference shows every year except 2019 to be releasing phosphorus. In 2019, reduced P concentrations delivered downstream are witnesses. For the spring melt period, large reductions in P concentrations were greatest in 2019. Overall, water quality improvements are witnessed after dredging (2019) due to trapping of P loading and reduced concentrations delivered downstream.

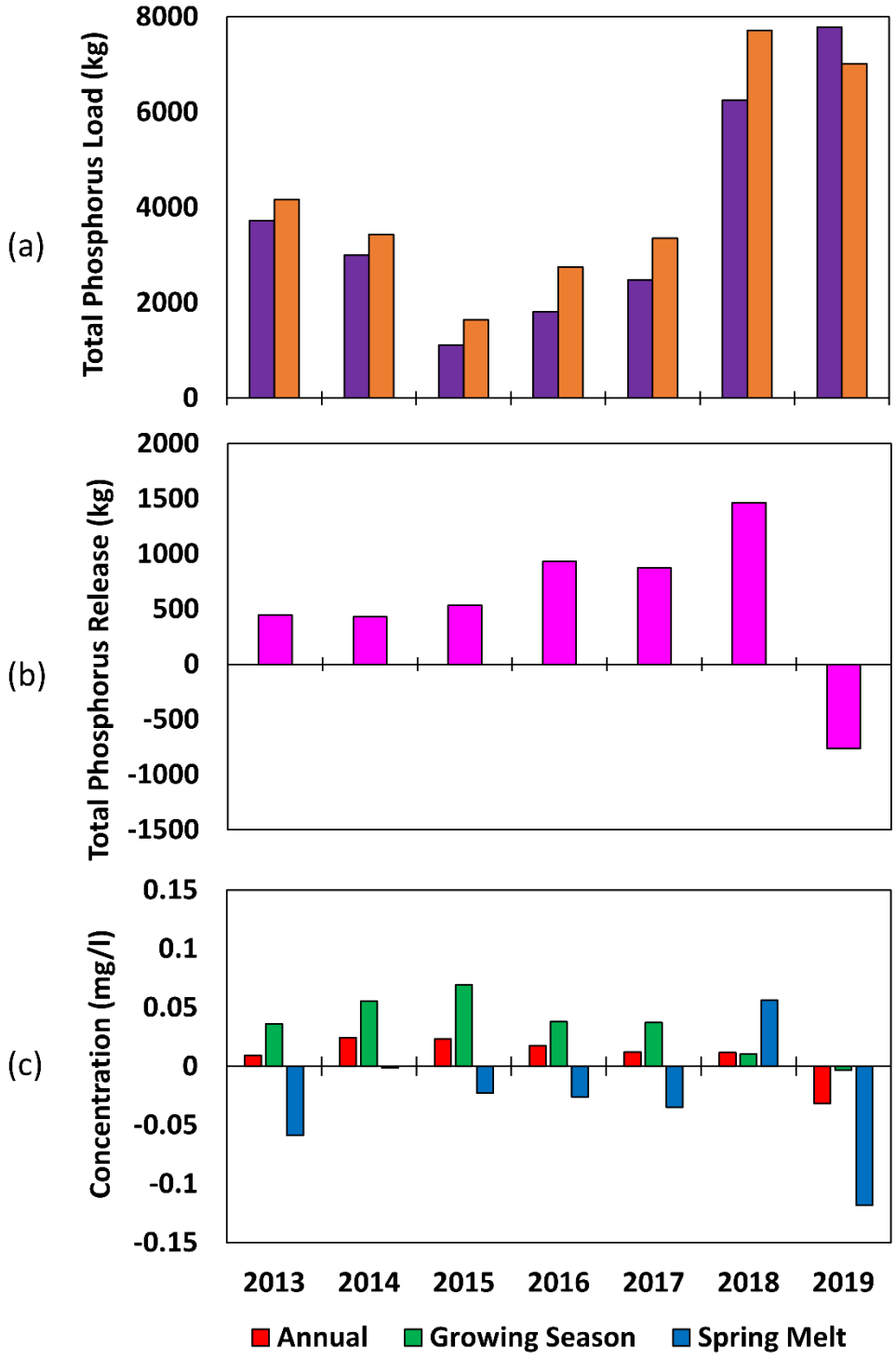

Fig 5-7. (a) Total P Loading from upstream S1 gage (green) and downstream S2 gage (orange). (b) Difference of total P release between downstream and upstream gage stations. (c) SRP median concentrations for annual (red), growing season (green), and spring melt (blue) periods.

5.3.5 Hydrologic Impacts

Hydrologic impacts after dredging were witnessed. Often times, stream dredging is implemented to increase water flow due to sedimentation. In this study, we aim to not only remove legacy P but also restore and enhance hydrologic functions. Fig 5-3 shows that the stream rerouted from a large flood in 2003 and short circuited its adjacent wetland complex before dredging. The dredging was designed to realign the stream to preserve the historical meandering shape, allowing flooded water over the adjacent floodplain and enhance base flows. The comparisons of upstream and downstream hydrographs prior to dredging and after the dredging are shown in Fig 5-8a and Fig 5-8b, respectively. Before dredging, the peak storm flow at the downstream (orange) was larger than upstream (purple). In comparison, after dredging (Fig 5-8b), peak storm flow is less than downstream showing that the sediment removal has attenuated peak storm flows. The annual volume of storm flows was found by integrating the area under the hydrograph after separating base flows from 2013 to 2019. Then a ratio was computed by dividing downstream by upstream volumes. The average storm flow volume ratio is shown in Fig 5-8c by the dark blue bars. Before dredging (2015 to 2017) the storm flow ratio is greater than 2.4 compared to after dredging (2019) the ratio drops in half near 1.2 indicating reduced volume delivered downstream and stored within its adjacent wetland. The flow ratio was repeated for volume of base flow. After dredging, a slight increase in base flow volume is witnessed compared to before suggesting that dredging removed sediment layers preventing groundwater from entering the stream. These results suggest that hydrologic impacts due to dredging affect flood resilience and mitigate flooding by improving hydrologic connectivity between the stream and wetland (Mitsch and Gosselink, 2000).

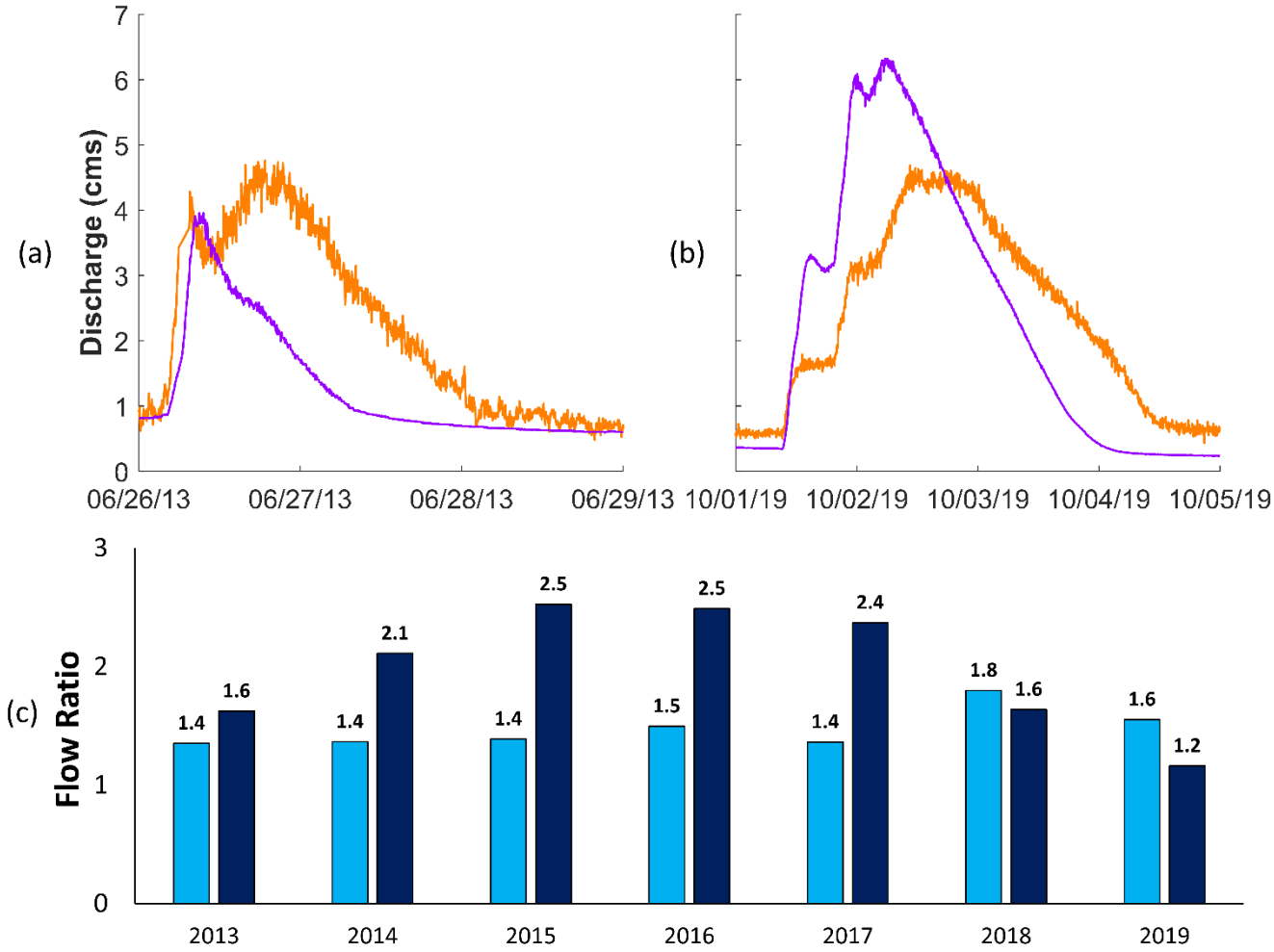

Fig 5-8. Stream discharge at upstream (purple) and downstream (orange) gage stations (a) before and (b) after dredging. Flow Ratio (c) comparing baseflow (light blue) and stormflow (dark blue) changes.

5.4 Discussion

5.4.1 TMDL Targets

Achieving TMDL occurs when the median TP concentration is at or below 0.075 (stream) and 0.10 mg/l (lake) in Dorn Creek and downstream Lake Mendota, respectively, during the growing season (Cadmus Group, 2011). Mesocosm experiments showed TP concentrations at 0.06 mg/l suggesting sediment dredging can be effective for achieving water quality goals. Long term station S2 shows the median concentration in Dorn Creek before dredging was greater than

0.15 mg/l compared to less than 0.07 mg/l after. Therefore, dredging reduced the median concentration and can be effective in achieving TMDL. The median concentration in Dorn Creek coincides during base flow conditions due to more days without rain compared to large loads from storm flows. These large storm P loads are delivered downstream to Lake Mendota which has not achieved its TMDL standard suggesting reducing P load is critical to achieve TMDL for the lake. To reduce large loading a sediment basin constructed along Dorn Creek and upstream of the current stream dredging (highway Q) may be considered. The sediment basin may provide a strategic location to remove and harvest legacy P from traveling downstream and fouling the current dredged area and downstream lake to meet TMDL. Further study is suggested to evaluate pairing dredging to remove legacy P for achieving stream TMDL and creating sediment basins to store P for achieving lake TMDL.

5.4.3 Ecological and recreational enhancements

Several ecological enhancements were witnessed after dredging due to installation of several habitat enhancement features. Some features include exposure of a sandy-gravel stream bed, previously covered by muck sediments, installation of rootwads along the stream banks, and creation of a northern pike spawning area. After dredging, an increase in abundance of turtles (Fig 5-3) and fish were witnessed. To increase fish spawning, the short circuited section of Dorn Creek was left intact as a large open body of water containing tall grasses and aquatic plants with low flow shown be location in Fig 5-3. Northern pike are attracted to this area due to its aquatic vegetation, shallow depths, and thus early warming of water in the spring. As suggested by other studies we intend for stream dredging to improve biodiversity (Ward et al., 2002), filter nutrients

(Fennessy and Cronk, 1997; Reddy et al., 1999), and store carbon (Kayranli et al., 2010). Further study is suggested to quantify these ecological benefits.

Recreational enhancements such as kayaking were witnessed. Prior to dredging, navigation of the stream was challenging and not possible by small water craft without portage around mucky sediments. After dredging, water depths were increased and is possible to paddle by kayak for the complete travel from highway Q to M. As reported by Miles Paddled (https://www.milespaddled.com/2020/01/dorn-creek/), it is a pleasant paddle and will take 2.5 hours to travel by kayak from downstream to upstream and return back. Since Dorn Creek is surrounded by public land, there are great opportunities to access the stream. Improving recreational activities such as stream dredging provides a connection to people and nature for continued interest in restoring and improving water quality.

5.5 Conclusions

In this paper, the impacts of legacy phosphorus in streams on water quality before and after dredging are investigated. Specifically, the presence of legacy P was determined due to the age of stream bed sediments accumulating since 1890. These legacy P sediments diffuse 0.076-0.078 mg/l of SRP into the water column indicating that hypothetically if all sources of TP entering Dorn Creek were eliminated the stream would be above TMDL standards (0.075 mg/l) due to release of legacy P. Therefore stream dredging was performed removing 34,050 kg of legacy P. After dredging, in-field, mesocosm experiments were conducted to reveal effectiveness showing a three times reduction of TP concentration from 0.18 mg/l before to 0.06 mg/l after. To understand the overall water quality response before and after dredging, long term gage station data showed that significant reductions in TP load and concentrations were achieved. Overall, stream dredging has been shown to reduce legacy P and its impact on water quality.

Other positive benefits from stream dredging were witnessed. Hydrologic functions were restored and enhanced by removal of legacy P. Specifically, dredging was designed to realign the stream to preserve the historical meandering shape, allowing flooded water to attenuate and spill over the adjacent floodplain and enhance base flows. Also, ecological benefits were witnessed due to the installation of habitat features (rootwads, sandy-gravel substrates) which increased abundance of fish and wildlife. Recreational benefits such as kayaking can be experienced due to deeper navigational depths from removing accumulated muck sediments. Overall, dredging of legacy P has been shown to provide a valuable management practice to improve water quality and other positive benefits such as restoring hydrologic functions, enhancing ecological services, and improving recreational activities.

5.6 Acknowledgments

This study has been funded by the Dane County Land and Water Resources Department (DCLWRD. Specifically, we thank Mr. Kyle Minks (DCLWRD), Jim Amrhein (Wisconsin DNR), and Mike Sorge (Wisconsin DNR) for their tremendous field work efforts in obtaining sediment cores and water samples for laboratory testing. We also thank Dr. Dave Armstrong, Professor Emeritus at UW-Madison, for his expert advice in applying age dating models. Last but not least, the authors thank staff at Wisconsin State Lab of Hygiene for laboratory analysis including Dr. Patrick Gorsk, Mr. Graham Anderson, and Mr. Gary Krinke.

5.7 References

Abril, J.M. 2003. Difficulties in interpreting fast mixing in the radiometric dating of sediments using 210Pb and 137Cs. Journal of Paleolimnolgy. 30: 407-414.

Appleby P.G., Oldfield F. 1992. Application of lead-210 to sedimentation.studies. In: Ivanovich M, Harmon RS (eds) Uranium series disequilibrium. Clarendon Press, Oxford, pp 731–778.

Ballantine, D.J., Walling, D.E., Collins, A.L., Leeks, G.J.L. 2009. The content and storage of phosphorus in fine-grained channel bed sediment in contrasting lowland agricultural catchments in the UK. Geoderma. 151:141–149.

Betz, C.R. 2000. Nonpoint source control plan for the Lake Mendota priority watershed. The Wisconsin nonpoint source water pollution abatement program. WT-536-00-REV. 253 pp.

Binford, M.W. 1990. Calculation and uncertainty analysis of 210Pb dates for PIRLA project lake sediment cores. Journal of Paleolimnology. 3: 253-267.

Cadmus Group, 2011. Total maximum daily loads for total phosphorus and total suspended solids in the Rock River basin. Prepared for U.S. Environmental Protection Agency and Wisconsin Department of Natural Resources.

Carmichael, W.W., Azevedo, S.M., An, J.S., Molica, R.J.R., Jochimsen, E.M., Lau, S., Rinehart, K.L., Shaw, G.R., Eaglesham, G.K., 2001. Human fatalities from cyanobacteria: Chemical and biological evidence for cyanotoxins. Environmental Health Perspectives 109 (7), 663-668.

Chorus, I. and Bartram, J., 1999. Toxic Cyanobacteria in water. World Health Organization, London, 416 pp.

D'Elia, C.F., Connor, E.E., Kaumeyer, N.L., Keefe, C.W., Wood, K.V., Zimmerman, C.F. 1997. Nutrient analytical services: standard operating procedures. Technical Report Series No. 158-97.

Dodd, J.R., and A.P. Mallarino. 2005. Soil-test phosphorus and crop grain yield responses to long-term phosphorus fertilization for corn–soybean rotations. Soil Science Society America Journal. 69:1118–1128.

Dorioz, J.M., E. Pilleboue, and A. Ferhi. 1989. Phosphorus dynamics in watersheds: Role of trapping processes in sediments. Water Researh. 23:147–158.

Drake, W.M., J.T. Scott, M. Evans-White, B. Haggard, A. Sharpley, and C.W. Rogers. 2012. The effect of periphyton stoichiometry and light on biological phosphorus immobilization and release in streams. Limnology. 13:97–106.

Ensign, S.H., and M.W. Doyle. 2005. In-channel transient storage and associated nutrient retention: Evidence from experimental manipulations. Limnology and Oceanography. 50:1740–1751.

Evrard, O., Nemery, J., Gratiot, N., Duvert, C., Ayrault, S., Lefevre, I., Poulenard, J., Prat, C., Bonte, P., Esteves, M. 2010. Sediment dynamics during the rainy season in tropical highland catchments of central Mexico using fallout radionuclides. Geomorphology. 124, 42-54.

Falconer, I.R., 1999. An overview of problems caused by toxic blue-green algae (cyanobacteria) in drinking and recreational water. Environmental Toxicology 14, 5-12.

Fennessy, M.S., Cronk, J.K., 1997. The effectiveness and restoration potential of riparian ecotones for the management of nonpoint source pollution, particularly nitrate. Critical Reviews in Environmental Science and Technology. 27, 285–317.

Fisher, M.M., Brenner, M., Reddy, K.R., 1992. A simple, inexpensive piston corer for collecting undisturbed sediment/water interface profiles. Journal of Paleolimnology. 7, 157–161.

Goldberg, E. D. 1963. Geochronology with 210Pb. Radioactive Dating. International Atomic Energy Agency. Vienna: 121-131.

Haggard, B.E., E.H. Stanley, and D.E. Storm. 2005. Nutrient retention in a point-source-enriched stream. Journal of North American Benthological Society. 24:29–47.

Haggard, B.E., D.E. Storm, and E.H. Stanley. 2001. Effect of a point source input on stream nutrient retention. Journal of American Water Resources. 37:1291–1299.

Hamilton, S.K. 2012. Biogeochemical time lags may delay responses of streams to ecological restoration. Freshwater Biology. 57:43–57.

Haygarth PM, Jarvie HP, Powers SM, Sharpley AN, Elser JJ, Shen J, Peterson HM, Chan N-I, Howden NJK, Burt T, Worrall F, Zhang F, Liu X. 2014. Sustainable phosphorus management and the need for a long-term perspective: the legacy hypothesis. Environmental Science Technology. 48, 8417–19.

Hoffman, A., Armstrong, D., Lathrop, R., Penn., M. 2009. Characteristics and influence of phosphorus accumulated in the bed sediments of a stream located in an agricultural watershed. Aquatic. Geochemistry. 15:371–389.

Holmes, C.W., 1998, Short-lived isotopic chronometers—A means of measuring decadal sedimentary dynamics: U.S. Geological Survey Fact Sheet 073–98, 2 p.

Hosomi, M., Sudo, R. 1986. Simultaneous determination of total nitrogen and total phosphorus in freshwater samples using persulfate digestion International Journal of Environmental Studies. 27 (3–4). 267-275

House, W.A., and F.H. Denison. 2000. Factors influencing the measurement of equilibrium phosphate concentrations in river sediments. Water Research. 34:1187–1200.

Hupfer, M., S. Gloess, and H.P. Grossart. 2007. Polyphosphate-accumulating microorganisms in aquatic sediments. Aquatic Microbial Ecolology. 47:299–311.

Huser, B., Brezonik, P., Newman, R. 2011. Effects of alum treatment on water quality and sediment in the Minneapolis Chain of Lakes, Minnesota, USA, Lake and Reservoir Management. 27:3, 220-228.

James, W.F., Barko, J.W. 1991. Estimation of phosphorus exchange between littoral and pelagic zones during nighttime convective circulation. Limnology and Oceanography. 36(1), 179-187.

Jerauld, M., Juston, J., DeBusk, T., Ivanoff, D., King, J. 2020. Internal phosphorus loading rate (iPLR) in a low-P stormwater treatment wetland. Ecological Engineering. 156, 105944.

Kayranli, B., Scholz, M., Mustafa, A., Hedmark, Å., 2010. Carbon storage and fluxes within freshwater wetlands: a critical review. Wetlands. 30, 111–124.

Lathrop RC, Carpenter SR, Stow CA, Soranno PA, Panuska JC. 1998. Phosphorus loading reductions needed to control blue-green algal blooms in Lake Mendota. Canadian Journal of Fisheries and Aquatic Sciences. 55:1169–1178.

McDowell, R.W., A.N. Sharpley, and A.T. Chalmers. 2002. Land use and flow regime effects on phosphorus chemical dynamics in the fluvial sediment of the Winooski River, Vermont. Ecological Engineering. 18, 477–487.

McMurtry, G.M., Snidvongs, A., Glenn, C.R. 1995. Modeling Sediment Accumulation and Soil Erosion with 137Cs and 210Pb in the Ala Wai Canal and Central Honolulu Watershed, Hawai'i. Pacific Science. 49, 4: 412-451.

Meals, D.W., Hopkins., R.B. 2002. Phosphorus reductions following riparian restoration in two agricultural watersheds in Vermont, USA. Water Science and Technology. 45:51–60.

Meals, D. W., Dressing, S. A., & Davenport T. E. 2010. Lag time in water quality response to best management practices: A review. Journal of Environmental Quality 39, 85-96.

Michalak, A. M., Anderson, E. J., Beletsky, D., Boland, S., Bosch, N. S., Bridgeman, T. B., et. al. 2013. Record-setting algal bloom in Lake Erie caused by agricultural and meteorological trends consistent with expected future conditions. Proceedings of the National Academy of Sciences USA. 110, 6448-6452.

Mitsch, W.J., Gosselink, J.G., 2000. The value of wetlands: importance of scale and landscape setting. Ecological Economics. 35, 25–33.

Madison Metropolitan Sewerage District (MMSD). 2012. Yahara Watershed improvement network watershed adaptive management pilot project annual report. 16 pp

Madison Metropolitan Sewerage District (MMSD). 2017. Adaptive Management Plan Report. 135 pp.

Oldenborg, K.A., Steinman, A.D. 2019. Impact of sediment dredging on sediment phosphorus flux in a restored riparian wetland. Science of the Total Environment. 650, 1969-1979.

Owens, P. N., & Walling, D. E. 2002. The phosphorus content of fluvial sediment in rural and industrialized river basins. Water Research. 36(3), 685–701.

Powers, S. M., Bruulsema, T. W., Burt, T. P., Chan, N. I., Elser, J. J., Haygarth, P. M., et al. 2016. Long-term accumulation and transport of anthropogenic phosphorus in three river basins. Nature Geoscience. 9(5), 353–356.

Rawlins, B.G. 2011. Controls on the phosphorus content of fine stream bed sediments in agricultural headwater catchments at the landscape-scale. Agriculture, Ecosystems, & Environment. 144:352–363.

Reddy, K.R., R.H. Kadlec, E. Flaig, and P.M. Gale. 1999. Phosphorus retention in streams and wetlands: A review. Critical Reviews in Environmental Science and Technology. 29, 83–146.

Reimer J.R., Wu, C.H. 2016. Development and Application of a Nowcast and Forecast System Tool for Planning and Managing a River Chain of Lakes. Water Resources Management. 30:1375-1393.

Reimer J.R., Wu, C.H. 2018. Water Exclosure Treatment System (WETS): An innovative device for minimizing beach closures. Science of the Total Environment. 625, 809-818.

Robbins, J. A., 1978. Geochemical and geophysical applications of radioactive lead. Biogeochemistry of Lead in the Environment. Elsevier Scientific, Amsterdam. pp. 285-393.

Rogers, J.S., Potter, K.W., Hoffman, A.R., Hoppes, J.A., Wu, C.H., Armstrong, D.E., 2009. Hydrologic and water quality functions of a disturbed wetland in an agricultural setting. Journal of the American Water Resources Association. 45(3):628-640.

Sayers, M., Fahnenstiel, G. L., Shuchman, R. A., & Whitley, M. 2016. Cyanobacteria blooms in three eutrophic basins of the Great Lakes: a comparative analysis using satellite remote sensing. International Journal of Remote Sensing. 37, 4148-4171.

Sharpley, A.N., R.W. McDowell, and P.J.A. Kleinman. 2004. Amounts, forms and solubility of phosphorus in soils receiving manure. Soil Science Society of America Journal. 68:2048–2057.

Sharpley, A., Jarvie, H. P., Buda, A., May, L., Spears, B., Kleinman, P. 2013. Phosphorus legacy: Overcoming the effects of past management practices to mitigate future water quality impairment. Journal of Environmental Quality. 42(5), 1308–1326.

Spears, B.M., L. Carvalho, R. Perkins, A. Kirika, and D.M. Paterson. 2012. Longterm variation and regulation of internal phosphorus loading in Loch Leven. Hydrobiologia. 681:23–33.

Steinman, A.D., Rediske, R., Reddy, K.R. 2004. The reduction of internal phosphorus loading using alum in Spring Lake, Michigan. Journal of Environmental Quality. 33, 2040–2048.

Stephen, D., Balayla, D. M., Be´cares, E., Collings, S. E., Ferna´ndez-Ala´ez, C., Ferna´ndez-Ala´ez, M., Ferriol, C., Garcı´a, P., Goma`, J., Gyllstro¨m, M., Hansson, L. A., Hietala, J., Kairesalo, T., Miracle, M. R., Romo, S., Rueda, J., Sta¨hl Delbanco, A., Svensson, M., Vakkilainen, K., Valentı´n, M., Van de Bund, W. J., Van Donk, E., Vicente, E., Villena, M. J., Moss, B. 2004. Continental-scale patterns of nutrient and fish effects on shallow lakes: introduction to a pan-European mesocosm experiment. Freshwater Biology. 49:1517–1524.

Tanner, C.C., Clayton, J.S. and Upsdell, M.P., 1995. Effect of loading rate and planting on treatment of dairy farm wastewaters in constructed wetlands - I. Removal of oxygen demand, suspended solids and fecal coliforms. Water Resources. 29, 17-26.

Turner, P.C., Gammie, A.J., Hollinrake, K., Codd, G.A., 1990. Pneumonia associated with contact with cyanobacteria. British Medical Journal 300, 1440-1441.

Valderrama, J.C. 1981. The simultaneous analysis of total nitrogen and total phosphorus in natural waters. Marine Chemistry, 10, 109-122.

Van Metre, P.C., Wilson, J.T., Fuller, C.C., Callender, W., Mahler, B.J. 2004. Collection, analysis, and age-dating of sediment cores rrom 56 U.S. lakes and reservoirs sampled by the U.S. Geological Survey, 1992–2001. Scientific Investigations Report 2004-5184.

Ward, J.V., Tockner, K., Arscott, D.B., Claret, C., 2002. Riverine landscape diversity. Freshwater Biology. 47, 517–539.

Withers, P. J. A., & Jarvie, H. P. 2008. Delivery and cycling of phosphorus in rivers: A review. Science of the Total Environment. 400(1–3), 379–395.

Wood P.J., Armitage P.D. 1997. Biological effects of fine sediment in the lotic environment. Environmental Management. 21, 203–217.

Zhang, T.Q., A.F. MacKenzie, B.C. Liang, and C.F. Drury. 2004. Soil test phosphorus and phosphorus fractions with long-term phosphorus addition and depletion. Soil Science Society of America Journal. 68:519–528.

Zhou, J., Qin, B., Casenave, C., Han, X. 2016. Effects of turbulence on alkaline phosphatase activity of phytoplankton and bacterioplankton in Lake Taihu. Hydrobiologia. 765:197-207.

6. Summary and Future Work

6.1 Summary

Generally, water quantity and quality in the Yahara Lakes is becoming more understood (Lathrop et al., 1992; Betz et al., 2005; Carpenter et al., 2006; Lathrop 2007; Motew and Kucharik, 2013; Reimer and Wu, 2016), and specifically there are still unanswered questions in understanding lake level flood risk and remediation approaches to combat the effect of eutrophication. The goal of this dissertation is to address the following: (i) how to assess and provide timely water level information in the Yahara RCL; (ii) what are the flood risks from environmental, social, and economic perspectives in the Yahara RCL; (iii) how to provide safe swimming water conditions that threaten (e.g. algae and E. coli) beaches; (iv) how to assess the impacts of legacy phosphorus in streams on water quality.

In Chapter 2, the state of the art, Integrated Nowcast and Forecast Operation System (INFOS) is developed to provide reliable and timely information for the Yahara RCL. The system infrastructure consist of a web portal to retrieve and display observations that are used to drive models under a high performance computing server. Water level and flow information are obtained from a suite of models that directly simulate the RCL system. It is demonstrated that the INFOS can reliably and effectively model real-time reverse flows due to sustained wind forcings or seiches, and flow choking due to channel constriction. Applications of the developed system are illustrated. Specifically water level planning scenarios provide a quantitative measure for lake management to reduce floods under extreme rainfall events. Overall, the Integrated Nowcast and Forecast Operation System (INFOS) provides reliable and timely water information for the RCL for sharing information to the community, planning for water use and delivery, and management of the Yahara RCL.

In Chapter 3, the sustainability assessment of flood risks from environmental, social, and economic perspectives in a RCL are presented. The flood assessment framework consists of five components including compiling data, modeling, mapping, estimating loss, and risk. Data is compiled from stochastic storm transposition results of RainyDay producing 35 rainfall scenarios. Economic and social impacts are produced from estimates of loss and risk. The results of the economic impacts reveal that the Yahara RCL is susceptible to large loss (in USD) at high return periods and long storm durations but a large risk at low return periods and long durations. The results of social impacts show that the risk of people displaced is of concern at a low return period (10 year) independent of storm duration. Overall, this chapter illustrates that flooding in a RCL can have different economic and social impacts depending on storm duration and return period.

In Chapter 4, an innovative Water Exclosure Treatment System (WETS) is developed and installed to minimize the occurrence of beach closures due to algae and Escherchia coli (E. coli). WETS consists of an "exclosure" sub-system with a five-sided polypropylene, barrier that excludes offshore lake contaminated water from the swimming area. Inside the exclosure, water is pumped to a portable filtration-ultraviolet treatment sub-system. To determine sizing of the treatment system, evaluate efficiency of UV disinfection, and aid in the design of the inlet and outlet locations for the pump system, computational fluid dynamics modeling with a Lagrangian particle-tracking method are employed. Flushing time is determined to range from 0.67 to 1.89 days. Residence time maps reveal inlet and outlet locations play an important role in depicting the duration of particles within the swimming area. Comprehensive water quality sampling conducted and analyzed with ANOVA testing reveal that water quality parameters inside the exclosure are significantly different than those outside. There have been no beach closures issued since

deployment of WETS. Overall, WETS, an innovative Water Exclosure Treatment System, provides safe, clean water inside the exclosure for minimizing beach closure.

In Chapter 5, evaluation of legacy phosphorus in streams on water quality before and after dredging stream sediments are presented. Legacy P sediments in the stream bed was discovered due to age and high concentrations of P. Laboratory microcosm experiments before dredging revealed stream sediments were diffusing soluble reactive phosphorus (SRP) at similar amounts under aerobic and anaerobic conditions, suggesting legacy P is being released regardless of dissolved oxygen content. Field mesocosm experiments after dredging showed that nearly a 3 times reduction (0.18 to 0.06 mg/l) was achieved due to removal of legacy sediments. Furthermore concentrations of the mesocosm with distilled water added to mimic upstream clean water dramatically decrease suggesting negligible residues in the dredged stream bed. Water quality response before and after dredging was evaluated from long term gage station data showing stream dredging reduced legacy P concentration from a source to a sink of upstream P. Overall, this chapter emphasized the important role that legacy P in stream sediments, and how that can affect water quality outcomes and be remediated for the future.

6.2 Recommendations for future work

The Integrated Nowcast and Forecast Operation System (INFOS) would be enhanced to perform hydrologic data assimilation when providing forecasts. This information would provide improved accuracy in lake level predictions. Past research has shown that data assimilation techniques have been used very successfully to improve operational weather forecasts (Daley, 1991) and in oceanography for improving ocean dynamics prediction (Bennett, 1992). However, hydrological data assimilation has a smaller number of case studies demonstrating its utility for use in realtime lake levels. Further study is suggested to determine ideal data assimilation method for the Yahara RCL among several and a few are summarized as follows. First, direct insertion is a simple approach that makes the explicit assumption that the model is wrong and that the observations are correct and then imposed in the model (Houser et al., 1998). Second, statistical correction which for example adjusts the mean and variance of the model states to match those of the observations (Houser et al., 1998). Third, nudging or Newtonian relaxation consists of adding a term to the model equations that causes the solution to be gradually forced towards the observations. (Stauffer and Seaman, 1990). Fourth, Kalman filter minimizes the error or variance of the analysis which can be further extended by ensemble Kalman filter using the Monte Carlo approach rather than a single discrete forecast of variances (Turner et al., 2007). Further study would be recommended to apply data assimilation for hydrologic forecasts to improve reliability in water level predictions.

Flood risk assessment for sustainability in this thesis employed the analytic hierarchy process (AHP) by Saaty (1980) based on current lake level management of the three dams in the Yahara RCL. Future research would expand this study and evaluate alternative management strategies such as dam operations to minimize flood risk from three sustainability perspectives of

environment, social, and economic. This proposed study would provide valuable information regarding science driven lake management of the Yahara RCL such as "ideal" gate operations in times of flooding based on sustainability perspectives. The AHP method in this thesis compares pairs of sustainability criteria and determines how much more important one is than the other according to a predefined scale (Li et al., 2011); however, this presents great difficulties when the number of criteria is large such as alternative management options (Sangiorgio, et al., 2018). Specifically, issues are encountered with the consistency of the judgment matrix (Sangiorgio, et al., 2018). To overcome a drawback, further study is suggested to optimize AHP (Fu, 2008; Malekmohamma de et al., 2011) or consider other alternatives such as optimized ranking (Vaidya and Kumar, 2006; Li et al., 2011), preference ranking (Kangas et al., 2001), and goal-orientated acceptability (Behzadian et al, 2012; Lee et al., 2015) with regards to dam operations. To date, no study on optimizing management of lake levels by dam operations from a sustainability viewpoint in river chains of lakes has been reported in the literature, as far as I am aware.

The Water Exclosure Treatment System (WETS) has shown to be effective in minimizing beach closures during the summer season; however, during the initial install of the system (in May) the system is under a great deal of stress due to extremely dirty lake (swimming) water and can foul the system without human actions. Further study is suggested to develop an environmentally friendly, economically viable, and energy-efficient processes for treating swimming water on onset of startup and when high E. coli and cyanobacteria events are witnessed. During startup, an option is to dose a one-time application of inorganic and synthetic coagulants over the surface water, usually used in water treatment processes which are efficient and cost-effective. However, synthetic coagulants need pH and alkalinity adjustments that may not be present in lake water, generate high volumes of sludge, and their residuals in treated water (like aluminium) are linked

with neurodegenerative diseases such as Alzheimers, and neurotoxic and carcinogenic effects (Rondeu et al., 2000). On the contrary, natural coagulants and adsorbents have increased during last years for treatment of surface waters and are available in abundance, safe to human health, and in general, toxic free (Teixeira et al., 2017). For example, vegetable coconut palm was found to be effective for removal of cyanobacteria and E. coli within the treatment process (Teixeira et al., 2017) but further study is suggested to incorporate other environmentally friendly treatment processes to improve WETS functions.

Legacy P was assessed in Dorn Creek for attaining TMDL target concentration (0.075 mg/l) within the stream during the growing season (Cadmus Group, 2011). As such the median concentration as determined by the TMDL in Dorn Creek coincides during base flow conditions due to more days without rain compared to large loads from storm flows. However, large storm P loads are delivered downstream to Lake Mendota which has not achieved its TMDL standard suggesting reducing P load is critical to achieve TMDL for the lake. Future study would investigate reductions to loading such as construction of a sediment basin along Dorn Creek and upstream of the current stream dredging (highway Q). Sediment detention basins are intended to trap excess sediment that exists within the stream system; however further study is suggested on implementing to overcome potential negative effects. For example, large traps can act as dams and create a discontinuity in sediment and debris flow (Ward and Standford, 1995). Interruption of this flow may affect downstream habitat value, particularly for spawning (Vannote et al., 1980). Segregation of bedload into a coarse fraction (which is trapped) and a fine fraction (which may pass through the trap) may cause downstream scour and incision, potentially leading to alteration in stream-floodplain interaction downstream (Ward et al, 2001). In view of these concerns, further study is suggested to determine the role of sediment basins connected inline to Dorn Creek play in reducing

P loads and legacy P for achieving downstream TMDL goals. Due to current regulation, implementation and study of inline sediment basins would be the first of its kind in Wisconsin.

Future studies could extend current work in each chapter to assess climate change impacts associated with water quantity and quality in the Yahara Lakes. Previous research has shown that physical, biological, and chemical properties of lakes respond to climate changes (Rosenzweig et al., 2007; Adrian et al., 2009). Physically, climate change is expected to have consequences for river regimes, flow velocity, hydraulic characteristics, water levels, and inundation patterns (Brown et al., 2007). In particular, anticipated flood risks are expected to increase in urban areas (Wilby, 2008). Studies could focus on climate change impacts and their associated flood risks of economic, social, and environmental perspectives in urban and suburban areas in the Yahara RCL. Chemically, nutrient loads are expected to increase under climate change (Bouraoui et al., 2002) driven by more intense rainfall resulting in increased loads of suspended solids (Lane et al., 2007) and sediment yields (Wilby et al., 1997). Studies would focus on climate change impacts and how increased sedimentation and nutrient loads may be affect legacy P diffusion from stream beds. Biologically, climate change is expected to increase temperatures resulting in increased growth rates of *E. coli* and algae (Whitehead & Hornberger, 1984), especially cyanobacteria. Studies would focus on improving treatment technologies in WETS to combat increased growth rates of *E. coli* and algae.

6.3 References

Adrian, R., O'Reilly, C. M., Zagarese, H., 2009. Lakes as sentinels of climate change. Limnology Oceanography. 54: 2283–2297.

Behzadian, M., Otaghsara, S. K., Yazdani, M., and Ignatius, J., 2012. A state-of the-art survey of TOPSIS applications, Journal of Expert Systems and Applications. 39, 13051–13069.

Bennett, A.F., 1992. Inverse methods in physical oceanography. Cambridge University Press, 346 pp.

Betz, C.R., Balousek. J., Fries, C., Nowak, P., 2005. Lake Mendota: improving water quality. LakeLine 25:47-52.

Bouraoui, F., Galbiati, L. Bidoglio, G., 2002. Climate change impacts on nutrient loads in the Yorkshire Ouse catchment (UK). Hydrology and Earth System Sciences. 6, 197–209.

Brown, L.E., Hannah, D.M., Milner, A.M., 2007. Vulnerability of alpine stream biodiversity to shrinking glaciers and snowpacks. Global Change Biology. 13(5), 958–966.

Cadmus Group, 2011. Total maximum daily loads for total phosphorus and total suspended solids in the Rock River basin. Prepared for U.S. Environmental Protection Agency and Wisconsin Department of Natural Resources.

Carpenter, S.R., Lathrop, R.C., Nowak, P., Bennett, E.M., Reed, T., Soranno, P.A., 2006. The ongoing experiment: restoration of Lake Mendota and its watershed. Pages 236-256 in J. J. Magnuson, T. K. Kratz, and B. J. Benson, editors. Longterm dynamics of lakes in the landscape: long-term ecological research on north temperate lakes. Oxford University Press, Oxford, UK.

Daley, R., 1991. Atmospheric data analysis. Cambridge University Press, 460 pp.

Houser, P.R., Shuttleworth, W.J., Famiglietti, J.S., Gupta, H.V., Syed, K.H., Goodrich, D.C., 1998. Integration of soil moisture remote sensing and hydrologic modeling using data assimilation. Water Resources Research. 34, 3405-3420.

Kangas, J., Kangas, A., Leskinen, P., and Pykäläinen, J., 2011. MCDM methods in strategic planning of forestry on state-owned lands in Finland: applications and experiences, Journal of Multi-Criteria Decision Analysis. 10, 257–271.

Lane, S.N., Reid, S.C., Tayefi, V., Yu, D., Hardy, R.J., 2007. Interactions between sediment delivery, channel change, climate change and flood risk in a temperate upland environment. Earth Surface Processes and Landforms. 32, 429–446.

Lathrop, R.C., 2007. Perspectives on the eutrophication of the Yahara lakes. Lake and Reservoir Management. 23(4):345-365.

Lathrop, R.C., Nehls, S.B., Brynildson, C.L., Plass, K.R., 1992. The fishery of the Yahara Lakes. Department of Natural Resources Technical Bulletin, No. 181.

Lee, G., Jun, K. S., and Chung, E.S., 2015. Group decision-making approach for flood vulnerability identification using the fuzzy VIKOR method, Natural Hazards and Earth System Science. 15, 863–874.

Li, F., Li, Z.-K., and Yang, C.-B., 2011. Risk Assessment of Levee Engineering Based on Triangular Fuzzy Number and Analytic Network Process and Its Application, in Modeling Risk Management in Sustainable Construction, edited by: Wu, D. D., Springer Verlag, Heidelberg, Berlin, 415–426.

Malekmohammadi, B., Zahraie, B., Kerachian, R., 2011. Ranking solutions of multi-objective reservoir operation optimization models using multi-criteria decision analysis. Expert Systems with Applications 38, 7851-7863.

Motew, M.M., Kucharik, C.J., 2013. Climate-induced changes in biome distribution, NPP, and hydrology in the Upper Midwest U.S.: a case study for potential vegetation. Journal of Geophysical Research: Biogeosciences 118(1):248-264.

Reimer J.R., Wu, C.H., 2016. Development and Application of a Nowcast and Forecast System Tool for Planning and Managing a River Chain of Lakes. Water Resources Management. 30:1375-1393.

Rondeu, V., Commenges, D., Jacqmingadda, H., Dartgues, J.F., 2000. Relation between aluminum concentrations in drinking water and Alzheimer's diseases: an 8 year follow-up study. American Journal of Epidemiology. 152, 59-66.

Rosenzweig, C., Karoly, D.J., Imeson, A., and others. 2007. Assessment of observed changes and responses in natural and managed systems, p. 79–131. In M.L. Parry, O.F. Canziani, J.P. Palutikof, P.J. Van der Linden, and C.E. Hanson [eds.], Climate Change 2007: impacts, adaptation and vulnerability: contribution of Working Group II to the fourth assessment report of the Intergovernmental Panel on Climate Change. Cambridge University Press.

Saaty, T.L., 1980. The Analytic Heirarchy Process. McGraw-Hill, New York.

Sangiorgio, V., Uva, G., Fatiguso, F., 2018. Optimized AHP to Overcome Limits in Weight Calculation: Building Performance Application. Journal of Construction Engineering Management, ASCE. 144(2): 04017101.

Stauffer, D.R., Seaman, N.L., 1990. Use of four-dimensional data assimilation in a limited-area mesoscale model. Part I: Experiments with synoptic-scale data. Monthly Weather Review. 118, 1250-1277.

Teixeira, M.R., Camacho, F.P., Sousa, V.S., Bergmasco, R., 2017. Green technologies for cyanobacteria and natural organic matter water treatment using natural based products. Journal of Cleaner Production. 162, 484-490.

Turner, M.R.J., Walker, J.P., Oke, P.R., 2007. Ensemble Member Generation for Sequential Data Assimilation. Remote Sensing of Environment. 112.

Vaidya, O. S. and Kumar, S., 2006. Analytic hierarchy process: an overview of applications. European Journal of Operational Research. 169, 1–29.

Vannote, R.L., Minshall, G.W., Cummins, K.W., Sedell, J.R., Cushing, C.E., 1980. The river continuum concept. Canadian Journal of Fisheries and Aquatic Sciences 37: 130-137.

Ward, J.V., Standford, J.A., The serial discontinuity concept: Extending the model to floodpla in rivers. 1995. Regulated Rivers: Research and Management. 10: 169-168.

Ward, J.V., Tockner, K., Uehlinger, U., Malard, F., 2001. Understanding natural patterns and processes in river corridors as the basis for effective river restoration. Regulated Rivers Research and Management 17, 311-323.

Whitehead, P.G., Hornberger, G.E., 1984. Modelling algal behaviour in the River Thames. Water Resources. 18, 945–953.

Wilby, R.L., 2008. Constructing climate change scenarios of urban heat island intensity and air quality. Environment & Planning B: Planning and Design 35, 909–919.

Wilby, R.L., Dalgleish, H.Y., Foster, I.D.L., 1997. The impact of weather patterns on contemporary and historic catchment sediment yields. Earth Surface Processes and Landforms 22, 353–363.